How syngas composition affects catalytic steam reforming of tars: an analysis using toluene as model compound

Authors

HuaLun Zhu, Ziyin Chen, Laura Pastor-Perez, Xiangyi Long, Marcos Millan*

Department of Chemical Engineering, Imperial College, London SW7 2AZ

*Corresponding author

Marcos Millan

Mailing address: Department of Chemical Engineering, Imperial College

London SW7 2AZ, UK

Tel.: +44 (0)20 7594 1633

E-mail: marcos.millan@imperial.ac.uk

Abstract

Tar removal by catalytic steam reforming has an important role to play in gasification hot gas treatment. Despite the importance of understanding the influence gas atmosphere has on this reaction, the effect of a full syngas mixture has not been comprehensively investigated. This study aims to bridge that gap by analyzing the effect of each component as well as their combinations on steam reforming of toluene as biomass gasification tar model over a Ni/Al_2O_3 catalyst. It has been found that H_2, CO and CO_2 have minor inhibitory effects, slightly decreasing the initial toluene conversion. On the other hand, while CO and CO_2 do not lead to catalyst deactivation, H_2 and CH_4 deactivate Ni/Al_2O_3 by promoting coke deposition. Only 3 vol.% of CH_4 can significantly increase deactivation, despite being insignificant with toluene or CH_4 separately. The joint presence of CH_4 and H_2 causes further drops in conversion with time on stream.

Keywords

syngas, tar steam reforming, nickel catalyst, carbon deposition, catalyst deactivation.

1. Introduction

Biomass gasification can act as a source of renewable heat and power as well as chemicals. At the core of gasification-based processes is synthesis gas (syngas), a valuable mixture that can provide remarkable versatility in terms of products, including hydrogen, synthetic natural gas, liquid fuels through Fischer-Tropsch synthesis, methanol and others [1-3]. However, one of the major hindrances to technology development is the formation of tar, which consists of a complex mixture of high molecular weight organic material. Tar formed in the biomass gasification process will be present as an impurity in the syngas at high temperatures and could condense or react downstream of the gasifier, affecting power generation, as well as gas separation membranes [4] and catalysts [5], for example decreasing the conversion of methane by steam reforming [6, 7].

Methods studied for tar abatement include optimizing gasifier design and operating parameters to limit their formation [8-10], physical removal (eg. scrubbers, filters) [11], and thermal, plasma or catalytic conversion downstream from the gasifier [12]. Among these technologies, tar catalytic reforming is particularly appealing as the process can take place without cooling the syngas and convert tar into valuable gases, especially H_2, substantially reducing its concentration [1, 13].

Catalytic tar reforming can be applied in either in-situ or ex-situ gasification systems, to remove tar content as part of the treatment to the hot syngas downstream from the gasifier [13, 14]. Systems have been developed that can crack tars while enhancing H_2 production by CO_2 sorption simultaneous to the reforming reaction [15]. Various types of catalyst have been studied, including olivine, dolomite, zeolite, char, metal-based (eg. Fe, Co, Ni, Zn, Pt, Ce, Ru, Rh), and alkali-based (K and Ca) [16-20]. Ni-based catalysts are the most studied for tar removal, likely due to their widespread application in industrial steam reforming of natural gas and other hydrocarbons, representing a lower cost option to noble metals while still providing high activity [14,

21].

The major challenge for Ni-based catalysts is deactivation caused by carbon deposition and sintering [19, 22, 23], which shortens their life cycle [24]. Carbon deposition on the catalyst may encapsulate the active metal particles and prevent the contact between reactants and the metal active sites [12]. Carbon can quickly diffuse into or form on the Ni catalyst surface, cover or block the pores of the active nickel and decrease Ni catalytic activity [25, 26]. Carbonaceous deposits (coke) are found in three forms: polymer, whisker and pyrolytic [27]. Pyrolytic carbon is formed due to the cracking of hydrocarbons which encapsulate the nickel active site [25], and has a significant influence on catalyst deactivation. High temperature (>600 °C) and the acidity of the catalyst promote its formation [12].

The main syngas components are H_2, CO, CO_2 and CH_4. Tar concentrations in the syngas depend on the gasifier type and operating conditions. In moving beds, they can reach relatively high values (~100 g Nm^{-3}) in updraft gasifiers. Downdraft configurations, as they allow cracking to take place in the hot char bed [28, 29], can reach values as low as ~ 1 g Nm^{-3}. Fluidised beds present intermediate values, typically around 15 g Nm^{-3} [30].

Not only is tar quantity but also its composition affected by the gasifier operating conditions. An attempt to rationalize the broad range of chemical species has involved grouping them into primary, secondary and tertiary tars [31, 32]. Primary tars are formed directly from solid biomass and composed of highly oxygenated compounds, like levoglucosan derived from cellulose and methoxyphenols originated in lignin. Secondary (phenols and light olefins) and tertiary tars, consisting largely of monoaromatic and polyaromatic hydrocarbons, are the products of subsequent reactions in the gas phase. Tar composition changes from primary to tertiary as it is exposed to higher temperatures for longer times, losing oxygen functionalities and showing predominance of mono- and polyaromatic hydrocarbons in the process. Thus, updraft gasification tars are richer in primary species while downdraft gasification

tends to produce tertiary tars [33]. An example of this trend is the reported composition of wood gasification tars in a fluidized bed gasifier operating at 940 °C and 5 bar, in which 65 wt.% of the tar was benzene and its derivatives, mostly toluene, styrene and indene, 33 wt.% polyaromatic hydrocarbons and only below 1 wt.% was in molecules containing heteroatoms, mostly as dibenzofurane with a small amount of phenol [34]. This tar distribution is also consistent with the tendency to dealkylation reactions, for example of xylenes, reported in the literature [35] and shows that even relatively short times at such high temperature suffice to remove nearly all heteroatoms in the tar as the freeboard residence time was only 4 s. Reports from fluidized bed gasifiers operating at lower temperatures (up to 850 °C) do not deviate substantially from this trend, reporting concentrations of benzene, toluene and naphthalene as the main components and only 0.7 wt.% of phenol [36].

Work in the literature tends to make use of model compounds to compare the performance of different catalysts and assess their deactivation in catalytic reforming tests. These have included benzene [37], toluene [38], polyaromatic hydrocarbons [39], among others including phenol [40], although it is more typically used as a model compound for the catalytic steam reforming of pyrolysis oils [41, 42]. The use of monoaromatics as model compounds, in particular toluene, has been observed to represent a worst-case scenario for carbon formation on Ni materials in comparison with polyaromatics [37] and real tar samples [43, 44]. This was corroborated by a study showing that lighter tar fractions [45] led to greater carbon formation than heavier ones.

Toluene steam reforming is described by Reaction 1.

$$C_7H_8 + 7H_2O \leftrightarrow 7\,CO + 11\,H_2 \qquad \text{Reaction 1}$$

The water gas shift (WGS) reaction (Reaction 2) will affect the syngas composition as well as steam methane reforming (Reaction 3), which can happen simultaneously if methane is present. Methane addition has also been reported as a way to increase

syngas quality after reforming [46] as Reaction 3 enhances H_2 production.

$$CO + H_2O \leftrightarrow CO_2 + H_2 \qquad \text{Reaction 2}$$

$$CH_4 + H_2O \leftrightarrow CO + 3H_2 \qquad \text{Reaction 3}$$

Other relevant reactions in the presence of CO_2 or CO are toluene dry reforming (Reaction 4) and the reverse Boudouard reaction (Reaction 5).

$$C_7H_8 + 7\,CO_2 \leftrightarrow 14\,CO + 4\,H_2 \qquad \text{Reaction 4}$$

$$2\,CO \leftrightarrow C + CO_2 \qquad \text{Reaction 5}$$

Most past and current research on catalytic steam reforming of tars has the aim of developing new catalyst formulations that can suffer less from deactivation than standard industrial catalysts [13, 45, 46, 47]. Despite the complex reaction system given by Reactions 1-5, novel catalysts are more often than not tested in atmospheres only containing tar (usually a model compound) or other contaminants, such as H_2S [39, 48] and NH_3, and steam [49-51], in some cases with hydrogen added [52]. However, catalyst performance, in particular its activity and tendency to deactivation by carbon deposition, can be very different when all components of the syngas mixture are considered. A previous study has hinted at complex interactions between syngas components, affecting formation of carbon on Ni materials used in solid oxide fuel cell anodes [53], but the influence of syngas composition tends to be overlooked even in comprehensive reviews on this topic [12, 13, 54].

Few research studies have focused on the effect of syngas composition on catalytic tar reforming process, with most of them focusing on varying steam and H_2 concentrations [37, 52]. It is well-known that steam addition increases conversion and decreases carbon deposition on the catalyst. An excess of steam over the reforming stoichiometric amount is necessary to avoid widespread carbon formation and catalyst deactivation. A steam to carbon (S/C) ratio of 1 has been shown to lead to the thermodynamic prediction of no carbon on the catalyst [55], but in practice this

condition resulted in heavy coke formation. S/C ratios of 2 and above have been found suitable to operate the process without significant deactivation in steam/N_2 atmospheres [52, 56]. It has however been reported that S/C ratios of up to 20 keep producing an increase in toluene steam reforming [24].

H_2 has been found to produce a negative impact on the reforming reactions, a feature that may be expected as it is a product from this reversible reaction, with a decrease in tar conversion as well as greater carbon formation as its concentration increases [52]. However, this effect may also be dependent on temperature, as enhancement of benzene and toluene reforming with H_2 partial pressure has been observed in the low temperature treatment of these model compounds between 350-400 °C and S/C ratios from 0 to 1.25 [57].

The effect of CO_2 on tar reforming has been mostly studied as part of dry reforming research both in the presence [58] and absence [-59] of steam. Boudouard reaction was shown effective to lower carbon deposition even at the relatively low temperature of 650 °C and employing a CO_2 to carbon ratio just below one [60]. However, an increase in temperature to 800 °C and in CO_2 to carbon ratio to 4.5 nearly completely removed formation of deposits on various Ni/Palygorskites. In the presence of steam the extent of the Boudouard reaction seems to be small [61]. At lower temperatures, the Sabatier reaction to produce methane competes for the active sites, as observed on a Ni-CeO_2/Al_2O_3 catalyst, and therefore some inhibition of the tar model compound reactions has been observed [57].

A more complex syngas mixture containing CO, H_2, CO_2 and CH_4 was used in a methane steam reforming studies [62, 63] including a comparison at fixed syngas concentrations between Ni and Rh catalysts in the presence of phenanthrene [63]. Similarly, Claude et al. [64] analyzed the behavior of four Ni/γ-Al_2O_3 catalysts with Ni loadings varying between 10 and 50 wt.% in a syngas atmosphere containing relatively fixed amounts of H_2, CO, CO_2 and H_2O at 650 °C. Different scenarios involved injection of toluene only, CH_4 only, and both toluene and CH_4 with a focus to analyze Ni

reduction by toluene under these conditions.

Syngas composition was varied in a study related to air gasification [58], which therefore employed relatively diluted syngas, in which it was found that CO inhibited toluene conversion. It was also established that the reaction takes place mostly through steam rather than dry reforming when both reforming agents are present. Fe-containing silicates including ores and olivine as reference material were investigated as benzene reforming catalysts in a full simulated syngas atmosphere [65]. Variations in the syngas composition affected Fe redox chemistry, with increasing concentrations of reducing agents (H_2 and CO) enhancing benzene conversions at 800 °C while more oxidative atmospheres had the opposite effect.

A recent study [61] focused on the simultaneous reforming of toluene, naphthalene, methane and higher hydrocarbons at S/C ratio of 2 and in a full syngas atmosphere in the context of sorbent enhanced gasification. This is a particular syngas composition, markedly different from a straight gasifier output, as it contains relatively small amounts of CO and CO_2 (9% and 6%, respectively were used in this study), but high H_2 (70%) and CH_4 (13%) contents. It was concluded that there was a competition between hydrocarbons for the Ni active sites that affected the conversion of tars in the presence of non-condensable species and vice-versa.

The objective of this work is to gain an understanding of the influence of reforming gas atmosphere on catalytic steam reforming by performing a systematic study where the effects of major (H_2, CO) and minor (CO_2, CH_4) syngas components and their mixtures of increasing complexity are analyzed. These effects have been investigated using toluene as model compound over a standard Ni/Al_2O_3 catalyst. Toluene is deemed a very suitable model for high-temperature gasification tars and its propensity to carbon formation can be seen as a significant challenge to gasification followed by reforming systems, as discussed above.

2. Experimental

2.1 Catalyst preparation

The Ni/Al_2O_3 catalyst used in the catalytic reforming tests was prepared by the wetness impregnation method, Nickel was impregnated onto an alumina support to produce 20 wt.% of NiO with the alumina support. To this effect $Ni(NO_3)_2{\cdot}6H_2O$ (≥97.0%, Sigma-Aldrich) was dissolved in acetone (≥99.8%, Sigma Aldrich); the support γ- Al_2O_3 (≥98.0% purity, Sasol) was added into the solution stirred for 2 h, then a rotating evaporator at 60 °C under vacuum was used to remove the acetone. The resulting solid was dried overnight at 110 °C and then calcined at 600 °C with a ramping rate of 2 °C·min^{-1} for 4 hours. Finally, it was sieved into particles ranging between 250 and 500 μm. The Ni content is 16.4 wt.% as fully reduced Ni. The catalyst specific surface area measured by BET was 153 m^2 g^{-1}. A full characterization of its textural properties was given in a previous study [56].

2.2 Catalytic toluene steam reforming tests

Toluene steam reforming tests were carried out in a fixed bed reactor used in previous bio-oil reforming studies [66]. A scheme of the system employed, and a detailed drawing of the reactor have been given elsewhere [56]. Briefly, the reactor consists of an Incoloy alloy 625 tube (12 mm i.d., 2 mm thick, 253 mm long), equipped with an inner quartz tube (9 mm i.d., 1 mm thick and 300 mm long) to avoid potential reaction between reactant gas stream and the Incoloy tube walls. Two copper electrodes controlled by a WEST 6100+ digital temperature controller were used to heat up the reactor by Joule effect. Two syringe pumps were installed at the top of the reactor to inject toluene and water into it.

Before each experiment, the reactor was purged with N_2 for 10 min to remove air. The catalyst was reduced under 50 mL·min^{-1} of H_2 at 800 °C for 1 hour. Following catalyst reduction, the carrier gas was switched to the experimental atmosphere gas

composition and allowed 10 min to stabilize. It was made sure the outlet gas pressure remained unchanged during this process as there are five different gas channels and slight pressure changes would affect the accuracy of the gas mixture. The injection of steam and toluene started when the reading of the analyzers stayed stable at desired input readings for at least 5 minutes. The liquid phase reactants were carried by the atmosphere gas and preheated at 200 °C in a bed of 1 g of SiC to vaporize them. Then, the reactant mixture gas entered a 500 mg of Ni/Al_2O_3 catalyst bed, which was held by wire mesh and quartz wool in the middle of the quartz tube. The bed temperature was continuously monitored by a K-type thermocouple.

The product gases passed through two condensers in series to collect any liquid product as well as unreacted toluene and water. Ice and dry ice were used as coolant in the first and second condenser, respectively. The products identified in the gas phase were H_2, CH_4, CO_2 and CO. Two on-line gas analyzers were used to determine product gas compositions: an MGA3000 (ADC, UK) Multi-Gas infrared analyzer for CO_2, CH_4 and CO, followed by a K1550 MLT (Eaton Electric Limited, UK) thermal conductivity H_2 analyzer. The software started to collect gas data (product gas concentrations) when the reactant injection started, and the gas concentrations were recorded continuously for 5 hours.

The reaction gas atmosphere was designed to simulate the syngas composition from biomass gasification processes. The main products include H_2, CO, CO_2 and CH_4. The typical composition ranges of H_2, CO, CO_2 and CH_4 in biomass gasification syngas are 20 – 50 vol%, 20 – 40 vol%, 10 – 30 vol% and 1 – 8 vol% respectively [21, 67, 68]. To investigate the influence of H_2, CO, CO_2 and CH_4 on catalytic toluene steam reforming, their inlet concentrations were fixed at 30, 30, 20 and 3 vol%, respectively, and balanced with N_2. Table 1 shows the detailed reforming atmosphere gas compositions of different toluene catalytic steam reforming tests.

Table 1. Toluene steam reforming atmospheres used in this work (on dry basis). A S/C ratio of 3 was applied in all experiments.

Experimental Condition	Component Concentration (%vol) [Flowrate (mmol h^{-1})]				
	H_2	CO	CO_2	CH_4	N_2
N_2	0	0	0	0	100% [536]
H_2	30% [161]	0	0	0	70% [375]
CO	0	30% [161]	0	0	70% [359]
CO_2	0	0	20% [107]	0	80% [429]
CH_4	0	0	0	3% [16]	97% [520]
H_2 & CO	30% [161]	30% [161]	0	0	40% [214]
H_2 & CH_4	30% [161]	0	0	3% [16]	67% [359]
Full gas mixture	30% [161]	30% [161]	20% [107]	3% [16]	17% [91]

The catalytic reforming test conditions applied in catalytic steam reforming test are shown in Table 2, which were found to be optimal in previous work [56]. S/C ratio is defined as in Equation 1, where *n* is the molar flowrate of each species. This definition takes into account the carbon contents of toluene and methane, and is used throughout this work unless otherwise stated.

$$S/C = \frac{n_{H_2O,in}}{7\, n_{C_7H_8,in} + n_{CH_4,in}} \qquad \text{Eq.1}$$

Table 2. Experimental conditions

Reforming parameters	Value
Temperature	800 °C
S/C ratio	3
GHSV	91800 h^{-1}
Carrier gas flow rate	200 mL min^{-1}
Toluene injection rate	1.38 mL h^{-1} (13 mmol h^{-1})
Toluene concentration	100 g m^{-3}
Catalyst	500 mg Ni/Al_2O_3

The performance of catalysts was evaluated by the toluene conversion ($X_{C_7H_8}$) into gaseous products (based on a carbon balance between the reactor inlet and outlet), according to Equation 2:

$$X_{C_7H_8}(\%) = \frac{(n_{CO,out} - n_{CO,in}) + (n_{CO_2,out} - n_{CO_2,in}) + (n_{CH_4,out} - n_{CH_4,in})}{7\, n_{C_7H_8,in}} * 100 \qquad \text{Eq.2}$$

CO, CO_2 and H_2 yield (*Y*) were defined as in Equations 3 to 5. In the case of H_2, a 100% yield was defined considering the WGS reaction was fully shifted to the right.

$$Y_{CO}(\%) = \frac{(n_{CO,out} - n_{CO,in})}{7\, n_{C_7H_8,in} + n_{CH_4,in}} * 100 \qquad \text{Eq. 3}$$

$$Y_{CO_2}(\%) = \frac{(n_{CO_2,out} - n_{CO_2,in})}{7\, n_{C_7H_8,in} + n_{CH_4,in}} * 100 \qquad \text{Eq. 4}$$

$$Y_{H_2}(\%) = \frac{(n_{H_2,out} - n_{H_2,in})}{18\, n_{C_7H_8,in} + 4\, n_{CH_4,in}} * 100 \qquad \text{Eq. 5}$$

CO_2 selectivity was also calculated to investigate the influence of different gas atmospheres on CO/CO_2 selectivity and assess the extent of WGS reaction. As methane had a total conversion in all the experiments, CO_2 selectivity is defined by the equation below where each term is in moles:

$$S_{CO_2}(\%) = \frac{(n_{CO_2,out} - n_{CO_2,in})}{(n_{CO_2,out} - n_{CO_2,in}) + (n_{CO,out} - n_{CO,in})} * 100 \qquad \text{Eq. 6}$$

The experimental error in toluene conversion, gas selectivity and yield is ± 2%.

Thermogravimetric analysis (TGA) was conducted to investigate the coke deposition on the spent catalyst using a Pyris 1 thermogravimetric analyzer from PerkinElmer. The samples were heated from room temperature to 900 °C at 10 °C·min^{-1} in air according to a procedure described elsewhere [69]. The derivative of the weight loss with time was calculated and normalized to compare regions of carbon burnout.

2.3 Thermodynamic equilibrium simulation

ASPEN V8.4 software was used to study the thermodynamic equilibrium of the toluene reforming reactions under different reaction atmospheres, using an ideal base property method and a RGIBBS reactor (based on Gibbs free energy minimization) to identify reforming products and yields. Material flows, reaction conditions (reforming temperature, pressure) are identical to those from the corresponding experiments.

3. Results and discussion

3.1 Influence of single syngas component atmosphere

A first group of experiments was conducted to understand the influence of single gas atmospheres on toluene steam reforming over a Ni/Al_2O_3 catalyst at the conditions

shown in Table 2. A baseline is provided by experiments with an inert atmosphere (100% N_2). Figure 1 presents toluene conversion and product gas yields for H_2, CO and CO_2 as a function of time on stream during reforming test for each of the single syngas component atmospheres (balanced in N_2) with a S/C ratio of 3. It was observed (Figure 1a) that toluene reforming in a N_2 atmosphere led to steady gas yields and a conversion of nearly 95% over the 5-hour experiment. This experiment is used as the baseline to determine the effect of the presence of each syngas component and their mixtures. The effect of these gases can be related to inhibition of the reforming reaction and/or catalyst deactivation. Inhibition is observed as a drop in the initial activity of the fresh catalyst (at the very beginning of a run) when a given syngas component is introduced respect to that obtained in N_2. Catalyst deactivation is reflected by a decrease in toluene conversion with time on stream within a run.

During the 5-hour test in 30% H_2 atmosphere, shown in Figure 1b, the carbon conversion from toluene to gas steadily decreased from 94% to 88%, as CO yield was reduced from 67% to 62%, while a steady yield of 26 – 28 % was observed for CO_2 throughout the test. H_2 yield declined slightly from 59% to 55%. These trends point to a certain deactivation of the catalyst taking place as a consequence of the presence of H_2 in the gas.

On the other hand, no significant deactivation was observed in CO or CO_2 atmospheres. The toluene conversion into gas products observed in a 30% CO atmosphere (Figure 1c) showed no significant change in 5 hours, and CO, CO_2 yield remained stable at ~33% and ~58%, respectively, throughout the experiment. The input of CO in the carrier gas shifted the WGS reaction to produce more H_2 and CO_2, and H_2 yield stayed above 75% in the 5-hour test. In 20% CO_2, shown in Figure 1d, the overall conversion of toluene stayed higher than 90% during the 5 hours, while CO_2 yield ranged from 17% to 19% and CO yield ranged from 71% to 76%. H_2 yield also remained stable at ~58%.

Two different conditions were tested with a 3% CH_4 concentration to gain a better understanding on the behavior of the system with toluene and methane mixtures. In one of them, the molar ratio between steam and carbon in toluene was 3 (carbon in CH_4 was not considered in the calculation, which is equivalent to S/C ratio of 2.55). In this case, the overall conversion from toluene to gases decreased from 90% to 79% after 5 hours, and H_2 yield declined from 58% to 49% (Figure 1e). CO and CO_2 yields decreased from 65% and 25% to 56% and 22%, respectively. CH_4 conversion stayed at 100% throughout the test.

In another experiment the steam feeding rate was increased to keep the S/C ratio at 3, as per the definition in Equation 1 (considering all carbon in toluene and CH_4). The product yield and total gas conversion trends are presented in Figure 1f. The toluene conversion into gases in first hour achieved 93% as a result of the increasing of S/C ratio from 2.55 to 3. Then the overall conversion decreased with time smoothly, and finally dropped to 79% during the fifth hour. H_2, CO and CO_2 yields decreased from 72%, 59% and 36% to 64%, 52% and 31%, respectively. H_2 yield also increased with the increasing of S/C ratio. Despite the initial increase in toluene conversion, the degree of deactivation in 5 hours was not significantly affected by the increase in S/C ratio with final yield values being very close for the two conditions.

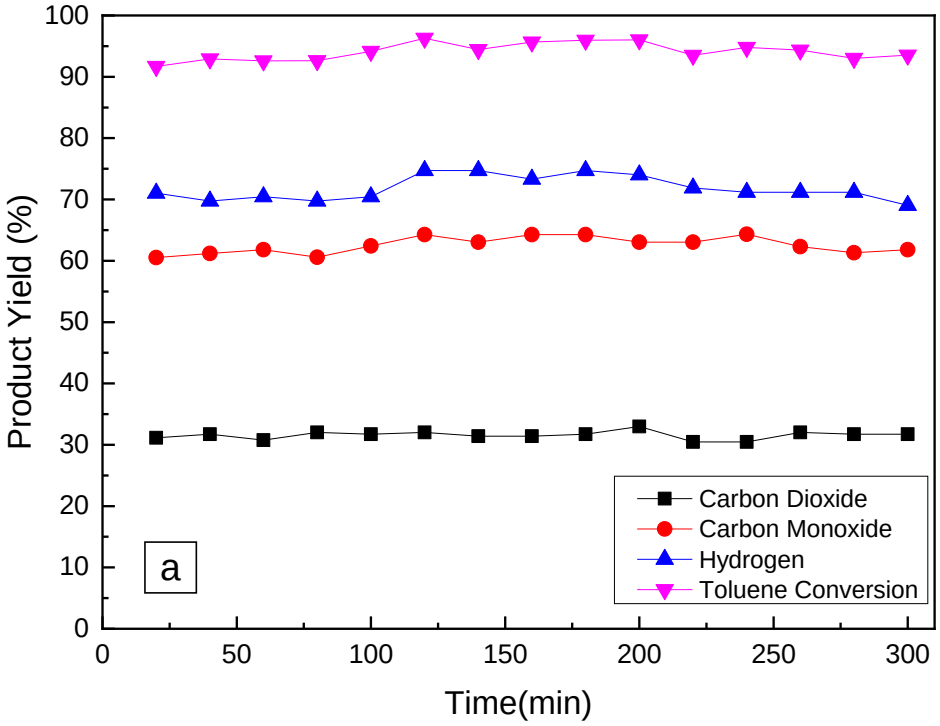
Product Yield (%)
Time(min)
Carbon Dioxide
Carbon Monoxide
Hydrogen
Toluene Conversion
a

335

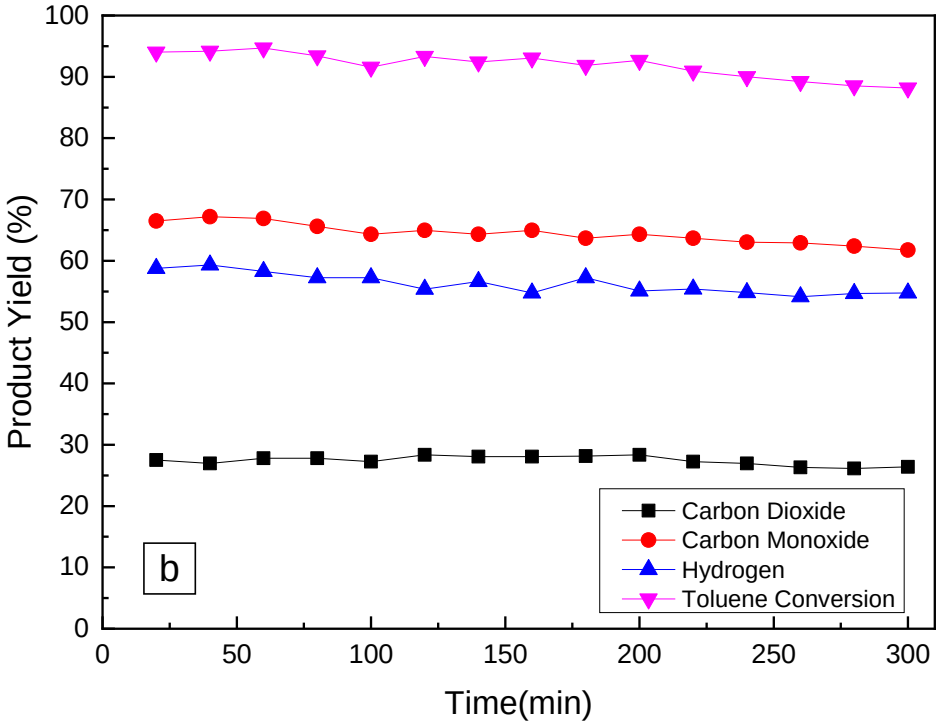
Product Yield (%)
Time(min)
Carbon Dioxide
Carbon Monoxide
Hydrogen
Toluene Conversion
b

336

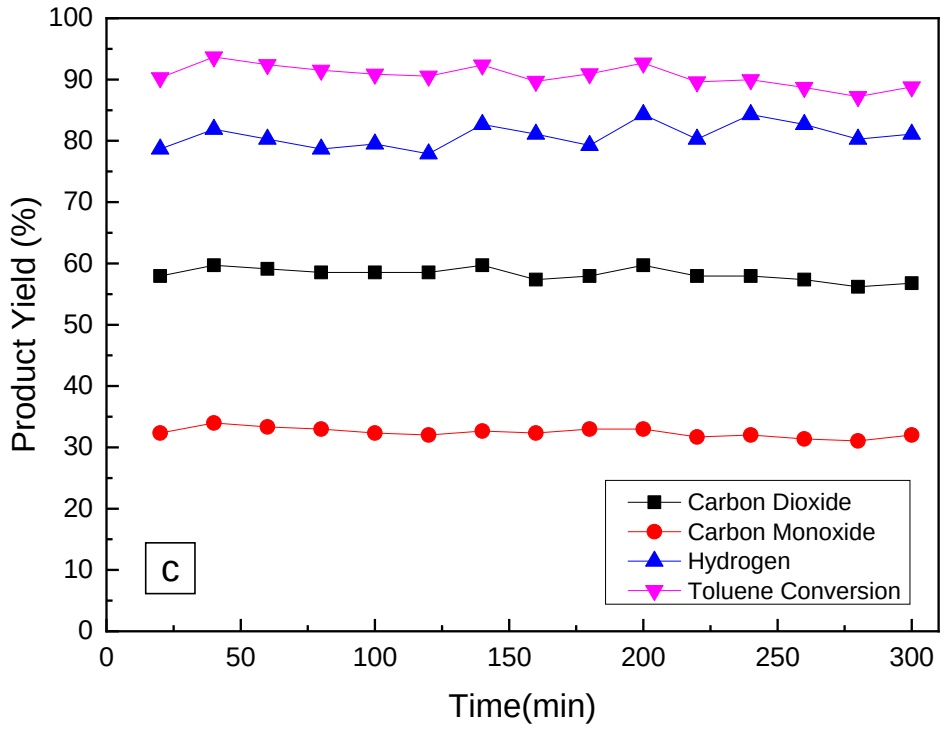
Product Yield (%)
Time(min)
Carbon Dioxide
Carbon Monoxide
Hydrogen
Toluene Conversion
c

337

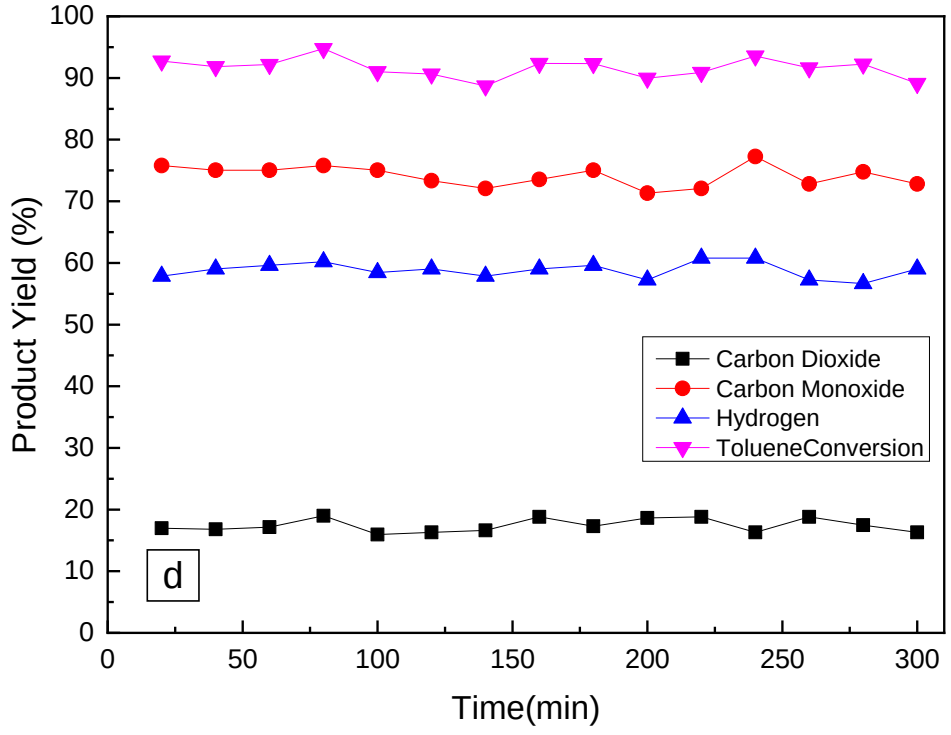
Product Yield (%)
Time(min)
Carbon Dioxide
Carbon Monoxide
Hydrogen
ToluneConversion
d

338

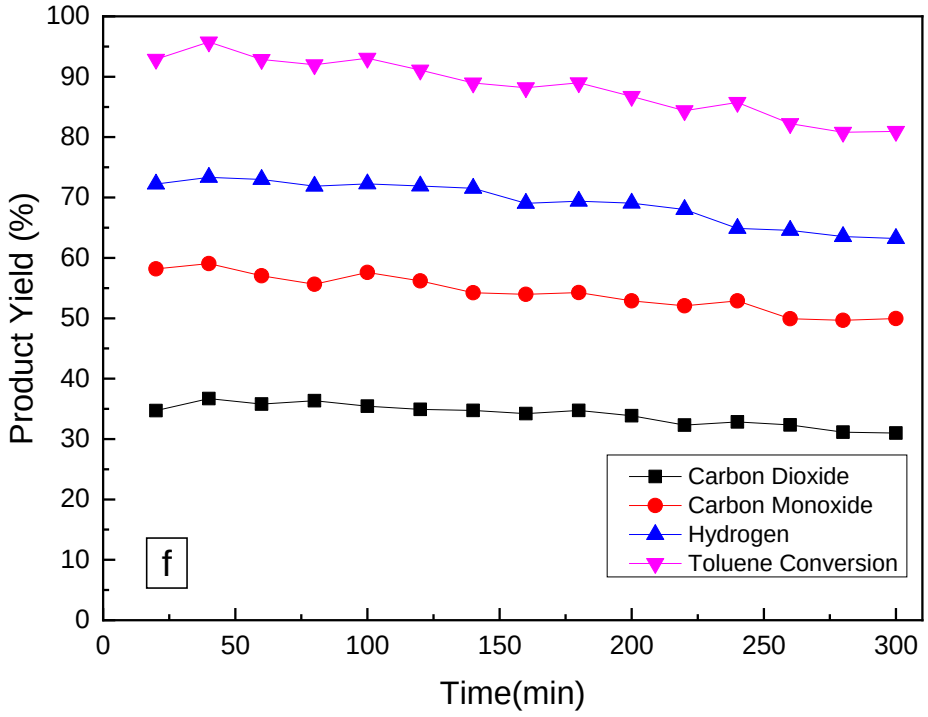

339

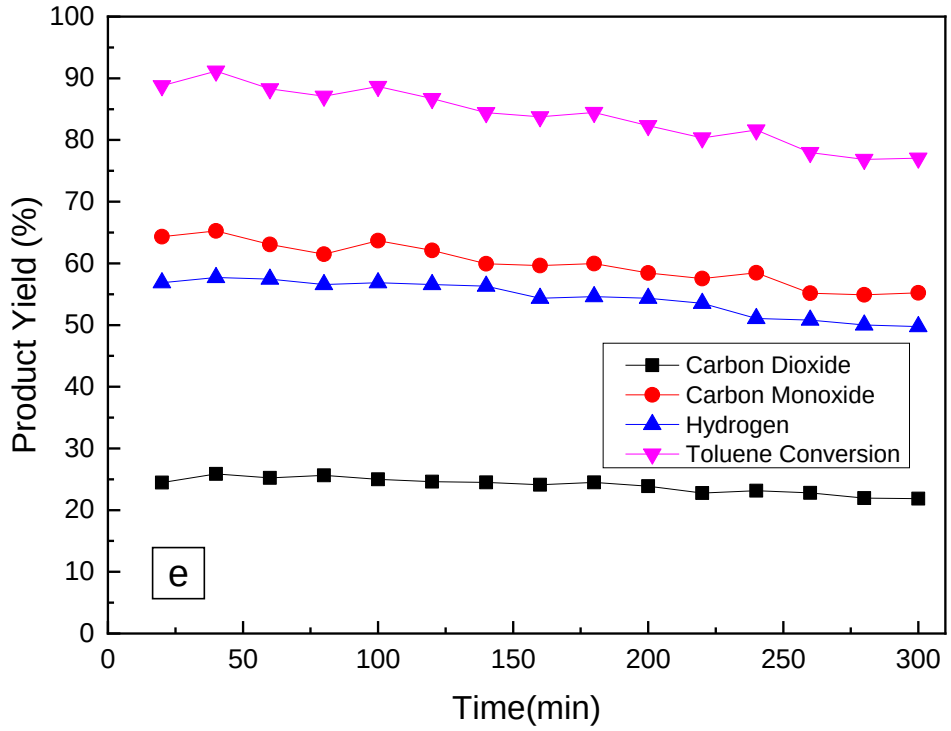

340

341 **Figure 1. Gas product yield and toluene conversion as a function of time on stream in**
342 **steam reforming tests carried out in (a) 100% N_2; (b) 30%H_2; (c) 30% CO; (d) 20% CO_2;**
343 **(e) 3% CH_4 with $S/C_{Toluene}$: 3 (only C in toluene considered); (f) 3% CH_4. All atmospheres**
344 **balanced in N_2. All experiments performed with a bed of Ni/Al_2O_3 catalyst at 800 °C and**

GHSV: 91,800 h^{-1}. S/C 3 for all runs except for (e) as indicated.

Figure 2 summarizes the CO and CO_2 yield and toluene conversion into C-containing gases under different gas atmospheres at the first and fifth hours of the catalytic tests and compares these values with equilibrium results. The equilibrium calculation showed that all these atmospheres reach 100% toluene conversion into gas, and CH_4 yield stayed lower than 0.01% in all the equilibrium results. The experimental results showed that toluene conversion to gas under 100% N_2, 30% CO in N_2, 20% CO_2 in N_2 atmosphere stayed over 90% throughout the 5-hour catalytic reforming tests, with very limited decreases in toluene conversion (< 2.5%) due to deactivation observed in these three atmospheres.

100% N_2 atmosphere presented the highest toluene conversion in the whole 5 hours on stream, while 30% CO in N_2, 20% CO_2 in N_2 and 30% H_2 in N_2 atmospheres showed lower toluene conversions in the 5-hour experiments. In particular, in the case of CO_2, it can be inferred that no significant extent of dry reforming was observed as toluene conversion did not exceed that obtained by steam reforming alone. This indicates that relatively high contents (>20%) of gasification syngas components (CO, H_2, CO_2) can slightly inhibit the reforming reaction of toluene. The use of CH_4 did not show any obvious inhibition effects, presenting a similar initial toluene conversion to the 100% N_2 atmosphere. However, catalyst deactivation in the presence of CH_4 and toluene was large even though 3% CH_4 on its own (also included in Figure 2) did not deactivate the catalyst to any observable extent. The experiment carried out with CH_4 but no toluene presented nearly complete carbon conversion. It led to the formation of 0.112 g of coke per g of catalyst, which represents around only 2.35% of the CH_4 injected. CH_4 was mostly steam reformed into CO, CO_2 and H_2, which is consistent with the fact that these experiments have been carried out a temperature much lower than the onset of CH_4 pyrolysis, which is the main route to ethane, ethylene and carbon formation [70].

The injection of H_2, CO, CO_2 had a significant influence on gas product distribution both in experiments and equilibrium simulations. Equilibrium results confirmed that the WGS reaction played an important role in CO/CO_2 selectivity and H_2 production. It can be observed in Figure 2 that CO_2 yield was typically lower than equilibrium calculations except for the CO_2 atmosphere experiment. The presence of CO in the carrier gas favored the WGS reaction and more CO_2 was produced than in the N_2 atmosphere. On the other hand, feeding CO_2 would largely increase CO yield to ~75%, pushing the reverse WGS reaction. The experimental CH_4 yield in all tests was 0%. The absence of CH_4 under all atmospheres indicated that CH_4 had a total conversion over Ni/Al_2O_3 catalyst even when the deactivation of toluene reforming took place. The CH_4 atmosphere test experienced the largest decrement in toluene conversion during an experiment as it dropped from ~94% to 81% in 5 hours, as well as in CO and CO_2 yields, followed by H_2 atmosphere test. Considering that CH_4 only had a concentration of 3 vol% in carrier gas, it is clear that CH_4 plays a key role in reforming catalyst deactivation among syngas components.

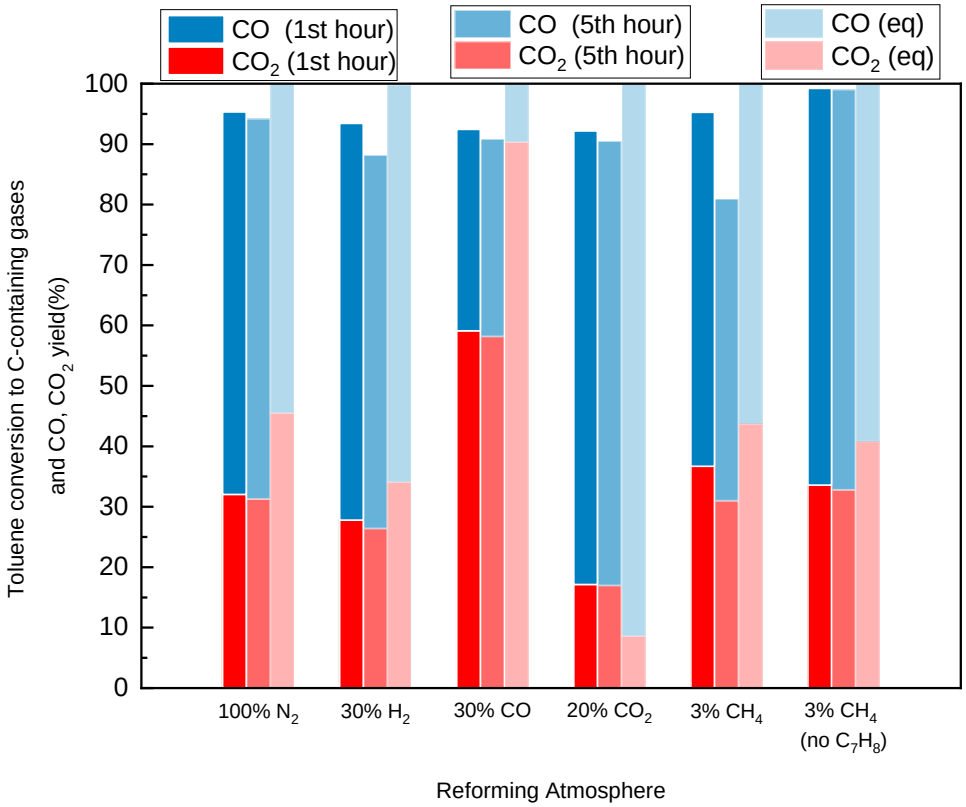

387

388 **Figure 2. Toluene conversion to C-containing gases and CO/CO_2 yield at different single**
389 **gas atmospheres (S/C ratio: 3, GHSV:91800 h^{-1}, reforming temperature 800 °C, all the**
390 **gas atmospheres balanced with N_2). Methane conversion is shown for the experiment**
391 **containing CH_4 but no toluene.**

392 Table 3 shows the gas product yields including CO, CO_2 and H_2 as mol/mol toluene at
393 the first hour and the fifth hour under different atmospheres and compares with the
394 respective equilibrium values. CO/CO_2 product ratios at different atmospheres also
395 changed towards the equilibrium results. Experimental CO_2 selectivity under most
396 atmospheres was lower than equilibrium predicted, indicating that toluene was
397 reformed to CO first, which then underwent WGS reaction in the excess of steam to
398 produce CO_2. The only exception was the 20% CO_2 atmosphere, which shifted the
399 equilibrium towards a low CO_2 yield and made reverse WGSR predominant.

400 As a consequence of the WGS reaction equilibrium, the injection of CO promoted the

401 production of H_2, while CO_2 inhibited H_2 yield. The addition of H_2 also reduced H_2 yield
402 respect to the blank experiment in N_2 atmosphere but it was not enough to change the
403 predominant direction of the WGS reaction. 3% CH_4 in N_2 atmosphere test achieved
404 the highest H_2 at 16.5 mol/mol toluene during the first hour due to the additional H_2
405 production. This run showed the highest decrement (by 16%) at the fifth hour.
406 Meanwhile, H_2 yield of 30% H_2 in N_2 atmosphere test dropped by 7% from 11.2 to 10.4
407 mol/mol toluene in the 5-hour test. The ratio of CO/CO_2 stayed almost the same after
408 5-hour test in all the experiments, suggesting that both reforming and WGS reaction
409 functions were deactivated to the same extent.

410 **Table 3. Product yields for the gaseous products in the different reforming atmosphere**
411 **(S/C ratio 3 GHSV:91800 h^{-1}, reforming temperature 800 °C, N_2: 100%N_2, H_2: 30% H_2 in**
412 **N_2, CO: 30% CO in N_2, CO_2: 20% CO_2 in N_2, CH_4: 3% CH_4 in N_2).**

Reforming Atmosphere	CO_2 (mol/mol toluene)	CO (mol/mol toluene)	H_2 (mol/mol toluene)	CO_2 selectivity
N_2 (1st hour)	2.2	4.5	13.0	33%
N_2 (5th hour)	2.2	4.4	13.0	33%
N_2 (Equilibrium)	(3.2)	(3.8)	(14.3)	(46%)
H_2 (1st hour)	1.9	4.6	11.2	29%
H_2 (5th hour)	1.8	4.3	10.4	30%
H_2 (Equilibrium)	(2.4)	(4.6)	(13.3)	(34%)
CO (1st hour)	4.1	2.3	14.7	64%

CO (5th hour)	4.0	2.3	14.5	63%
CO (Equilibrium)	(6.3)	(0.7)	(17.3)	(90%)
CO_2 (1st hour)	1.2	5.3	10.7	18%
CO_2 (5th hour)	1.2	5.1	10.6	19%
CO_2 (Equilibrium)	(0.6)	(6.4)	(11.6)	(9%)
CH_4 (1st hour)	3.0	4.8	16.5	38%
CH_4 (5th hour)	2.5	4.1	13.8	38%
CH_4 (Equilibrium)	(3.5)	(4.6)	(18.0)	(43%)

Table 4 shows the carbon conversion from toluene to coke and the fraction of coke on the catalyst under different reforming atmospheres determined by thermogravimetric analysis on the spent catalysts. In the CH_4 only (no C_7H_8) test, 2.35% of CH_4 was converted into carbon deposits on the catalyst surface. The conversion to carbon deposits of 100% N_2, 30% CO in N_2 and 20% CO_2 in N_2 atmosphere was very close, which indicates that CO and CO_2 contents have very limited influence on carbon deposition on the catalyst, which remained stable during the tests. The presence of 30% H_2 increased the coke weight, which matched the slight deactivation observed in toluene conversion to C-containing gases and the drop in H_2 product yield. The

presence of H_2 might prevent coke reaction with steam, and shift the equilibrium towards more coke, an observation also made in the literature [52]. The mixed toluene-CH_4 atmosphere test led to the highest coke content and ratio, much higher than could be expected from the simple addition of effects observed with toluene and CH_4 separately. Catalyst deactivation was calculated from the H_2 yields (Y_{H_2}) initially and after 5 hours on stream (Equation 7).

$$Cat.Deac. = \frac{[Y_{H_2}]_{t=0} - [Y_{H_2}]_{t=5h}}{[Y_{H_2}]_{t=0}} \qquad \text{Eq. 7}$$

A reasonable correlation between amount of coke on the catalyst and catalyst deactivation was observed, where the latter does not take place significantly at coke to catalyst ratios below a threshold of around 20 wt.% but increases markedly above that value.

Table 4. Toluene conversion to coke, fraction of coke deposited on the catalyst and catalyst deactivation at different reforming atmospheres (800 °C, S/C:3, GHSV:91800 h^{-1}, 5-hour test. N_2: 100%N_2, H_2: 30% H_2 in N_2, CO: 30% CO in N_2, CO_2: 20% CO_2 in N_2, CH_4: 3% CH_4 in N_2).

Reforming Atmosphere	N_2	H_2	CO	CO_2	CH_4	CH_4 (no C_7H_8)
Coke/C in toluene	0.68%	0.90%	0.61%	0.64%	1.54%	-
Coke/Catalyst (g_C/g_{cat})	0.184	0.245	0.165	0.173	0.417	0.112
Catalyst Deactivation (%)	0	7	1	1	16	0

3.2 Influence of multi-gas atmospheres on toluene steam reforming

While previous tests focused on the influence of single gas in N_2, this section presents the impact of syngas component mixtures on toluene steam reforming. First, a mixture of 30% H_2 and 30% CO balance N_2 is presented, followed by 3% CH_4 and 30% H_2 in N_2 and finally a full syngas mixture consisting of 3% CH_4, 30% H_2, 30% CO and 20% CO_2 in N_2, typical of a gasifier under normal operation conditions [48, 49]

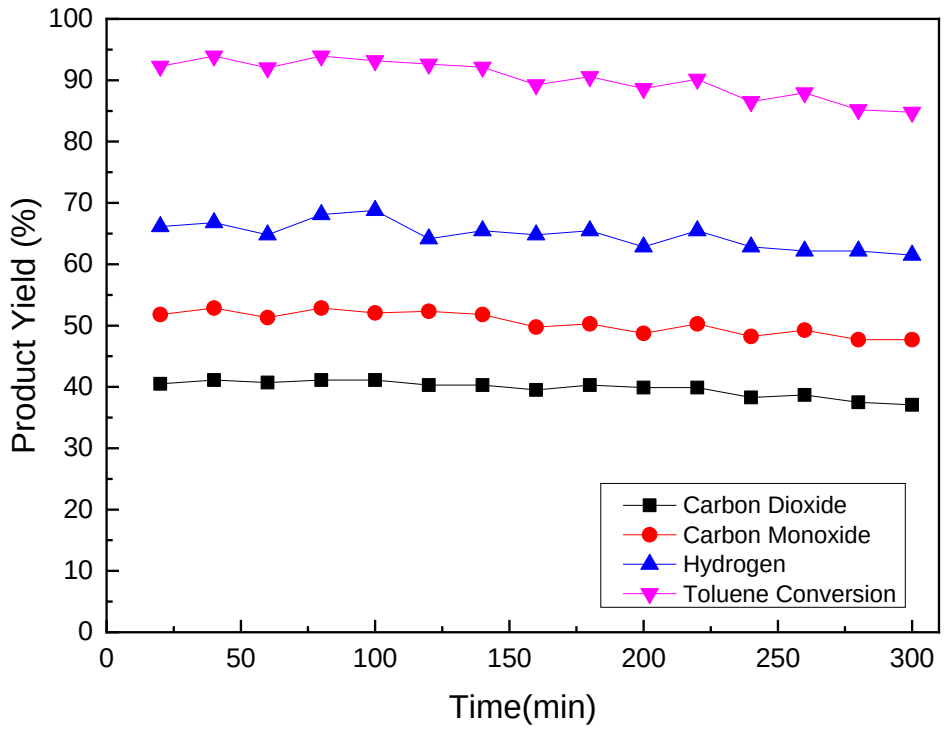

Figure 3. Product yield trend and conversion of toluene steam reforming test in 30% H_2 and 30% CO balanced N_2 atmosphere (5-hour test, Ni/Al_2O_3 catalyst, 800 °C, S/C ratio 3, GHSV: 91800 h^{-1}).

Figure 3 shows the gas product yield and conversion of toluene steam reforming 5-hour test in 30% H_2 and 30% CO balanced N_2 atmosphere. Product yields of CO and H_2 were very stable in the first 2.5 hours, and then started to drop slowly until the end of the tests. The overall conversion from toluene to gases also decreased below

90% at 160 mins to reach a final value of 84%, lower than achieved in CO and H_2 separately. Table 5 shows CO_2, CO and H_2 yields (in mol/mol toluene) declined by ~10% in the 5-hour test, but selectivity towards CO_2 was not affected by catalyst deactivation as discussed above.

Table 5. Product yields for the gaseous products in 30% H_2 and 30% CO balanced N_2 atmospheres (5-hour test, Ni/Al_2O_3 catalyst, 800 °C, S/C ratio 3, GHSV: 91800 h^{-1})

Atmosphere	CO_2 (mol/mol toluene)	CO (mol/mol toluene)	H_2 (mol/mol toluene)	CO_2 selectivity
H_2 & CO (1st hour)	2.8	3.7	11.9	43%
H_2 & CO (5th hour)	2.6	3.3	11.1	44%
(Equilibrium)	(4.3)	(2.7)	(15.3)	(61%)

Figure 4 summarizes toluene conversion to C-containing gases and CO, CO_2 yields at H_2, CO and mixture gas atmosphere. CO content in the carrier gas had no obvious effect on catalyst deactivation in multi-gas mixture atmosphere. Instead, the decrease in toluene conversion was led by the presence of H_2, as the overall toluene conversion showed similar trends in 30% H_2 in N_2 and 30% CO, 30%H_2 in N_2 atmosphere tests. The equilibrium and experimental results both showed that CO had more significant influence on the selectivity of product CO/CO_2 than H_2. When equal concentrations of CO and H_2 were introduced to the reaction system, the equilibrium shifted to produce more CO_2 when comparing to inert N_2 atmosphere and the experimental results followed this behavior.

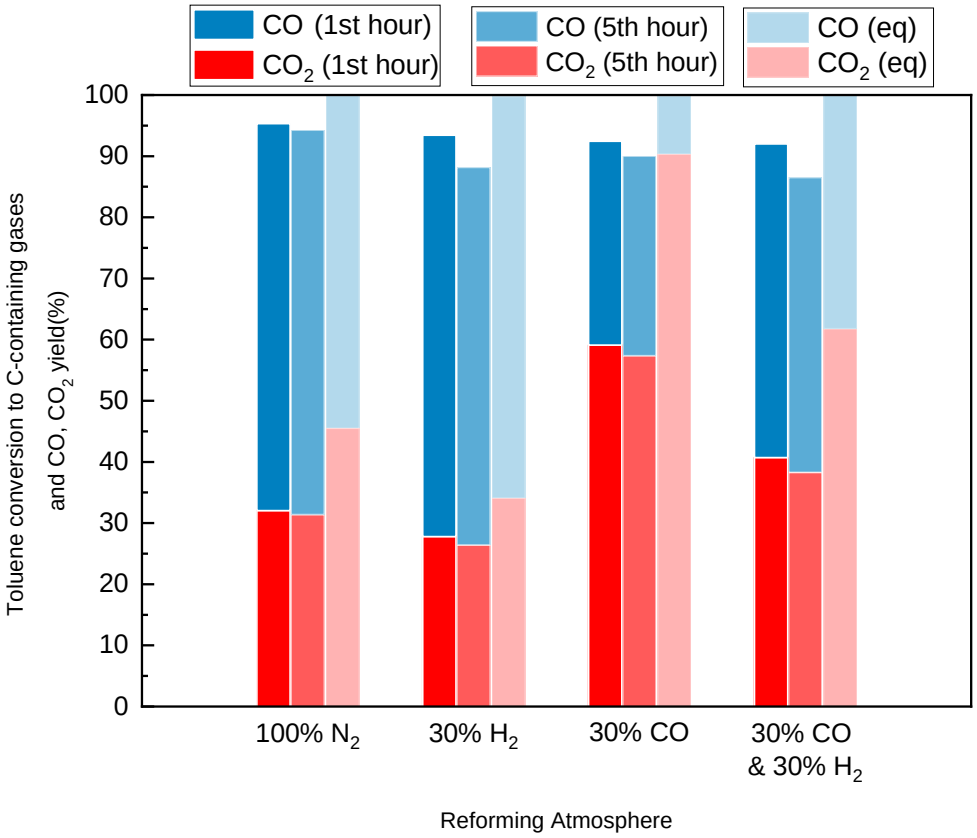

469

470 **Figure 4. Toluene conversion to C-containing gases and CO, CO_2 yields at H_2, CO and**
471 **mixture gas atmospheres (S/C ratio 3 GHSV:91800 h^{-1}, reforming temperature 800 °C,**
472 **all the gas atmosphere balanced with N_2).**

473 The results presented so far showed that CH_4 and H_2 atmosphere had relatively more
474 influence on toluene conversion and carbon deposition than CO and CO_2. Next, the
475 impact of CH_4 and H_2 mixture atmosphere on toluene steam reforming is discussed.
476 To compare with the previous results, the reforming gas atmosphere was designed as
477 3% CH_4 and 30% H_2 in N_2 with a S/C ratio of 3, including CH_4.

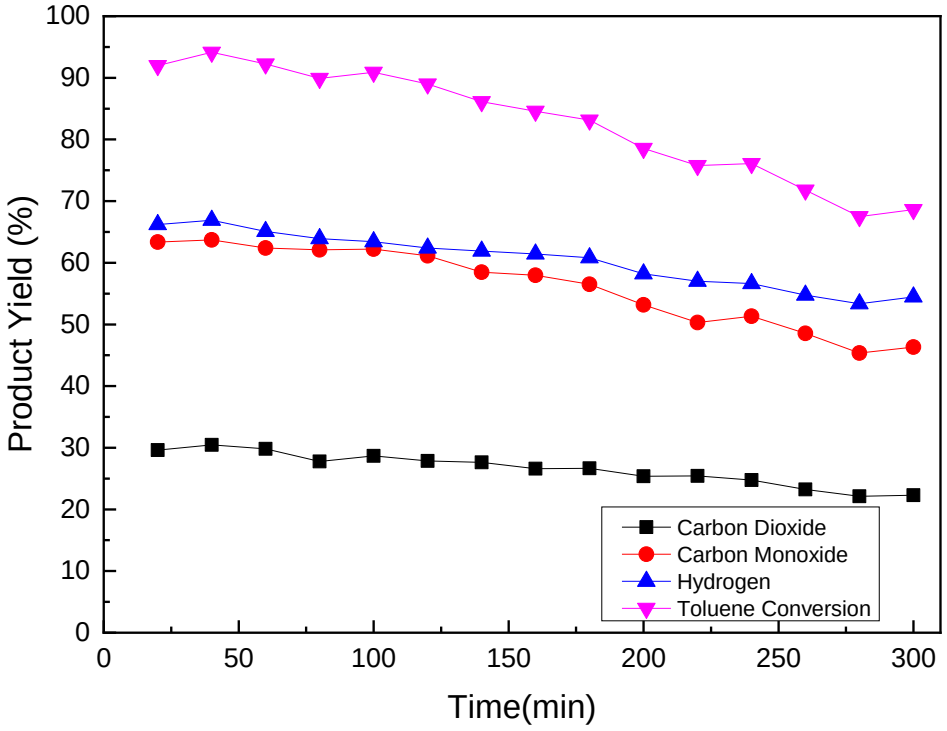

478

479 **Figure 5. Product yield trend and toluene conversion of steam reforming test in 3% CH_4**

480 **and 30% H_2 balanced N_2 atmosphere (5-hour test, Ni/Al_2O_3 catalyst, 800 °C, S/C ratio 3,**

481 **GHSV: 91800 h^{-1})**

482

Table 6. Product yields for the gaseous products in 3% CH_4 and 30% H_2 balanced N_2 atmosphere (5-hour test, Ni/Al_2O_3 catalyst, 800 °C, S/C ratio 3, GHSV: 91800 h^{-1})

Atmosphere	CO_2 (mol/mol toluene)	CO (mol/mol toluene)	H_2 (mol/mol toluene)	CO_2 selectivity
H_2 & CH_4(1st hour)	2.5	5.2	15.1	32%
H_2 & CH_4 (5th hour)	1.8	3.8	10.9	32%
(Equilibrium)	(2.8)	(5.3)	(17.1)	35%

Figure 5 shows the gas product yield and toluene conversion into gases in 3% CH_4 and 30% H_2 balanced N_2 atmosphere. The toluene conversion and CO, CO_2 and H_2 yield started to decrease after 100 min and declined steadily until the end of the test. The conversion of toluene dropped markedly from 93% to 69%, while the CO, H_2 and CO_2 yields decreased from 64%, 66% and 29% to 46%, 54% and 22%, respectively. The CH_4 and H_2 combined atmosphere showed a more significant decrement in gas production from toluene steam reforming respect to the two gases separately.

Table 6 presents CO, CO_2 and H_2 production during the first and fifth hours on stream and compares them with equilibrium results. H_2 production yield decreased by 28%, from 15.1 to 10.9 mol/mol toluene, which was larger than expected based on the behavior of the individual gases. According to Table 4, the decreases in H_2 yield in 30% H_2 in N_2 atmosphere and 3% CH_4 in N_2 atmosphere were 7% and 16%, respectively. The presence of CH_4 and H_2 can deactivate the Ni/Al_2O_3 catalyst much more rapidly than CH_4 or H_2 single gas atmosphere (Figure 6).

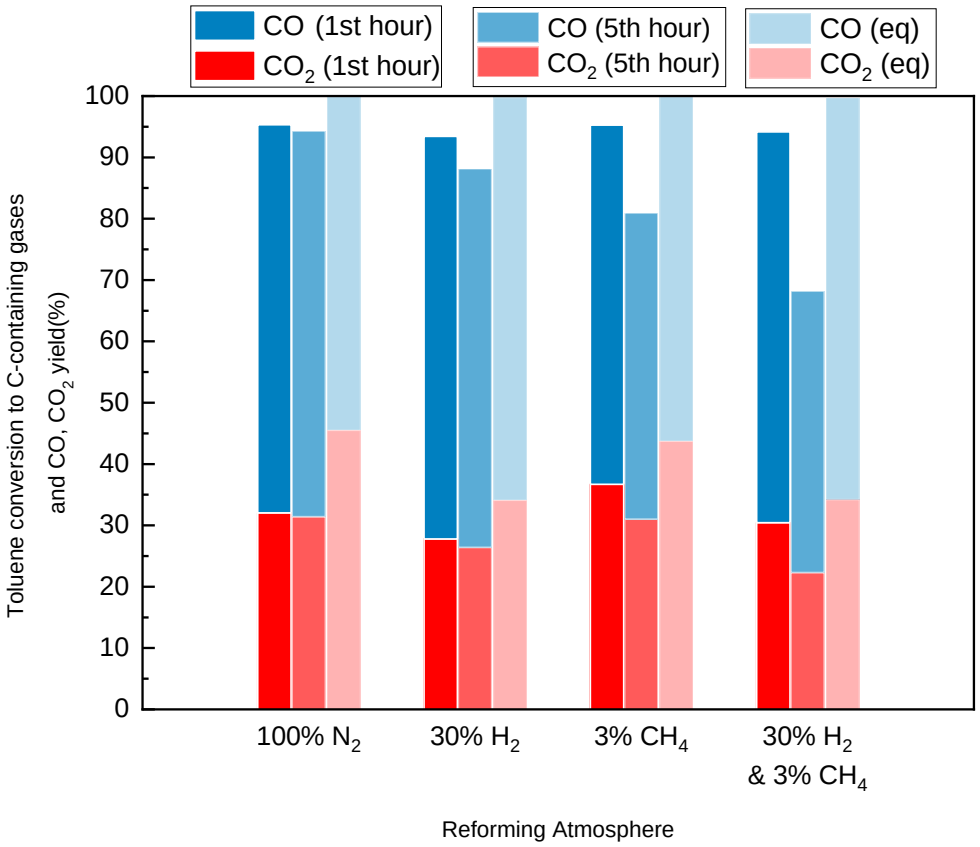

499

500 **Figure 6. Toluene conversion to C-containing gases and CO, CO_2 yield at H_2, CH_4 and**
501 **mixture gas atmosphere (S/C ratio 3, GHSV:91800 h^{-1}, reforming temperature 800 °C, all**
502 **the gas atmosphere balanced with N_2).**

503 Finally, a full gas mixture composed of 3% CH_4, 30% H_2, 30% CO and 20% CO_2 in N_2
504 was chosen to simulate a typical biomass gasification syngas. Figure 7.7 shows the
505 gas product yield and toluene conversion in this simulated gasification atmosphere.
506 Toluene conversion and gas yields started to decline slightly in the second hour, and
507 then decreased significantly in the rest 3 hours. The conversion of toluene dropped
508 from 92% to 66% in the 5-hour test. The trend was similar to the test in 3% CH_4 and
509 30% H_2 atmosphere, which indicated that CO and CO_2 had limited influence on the
510 deactivation of the catalyst.

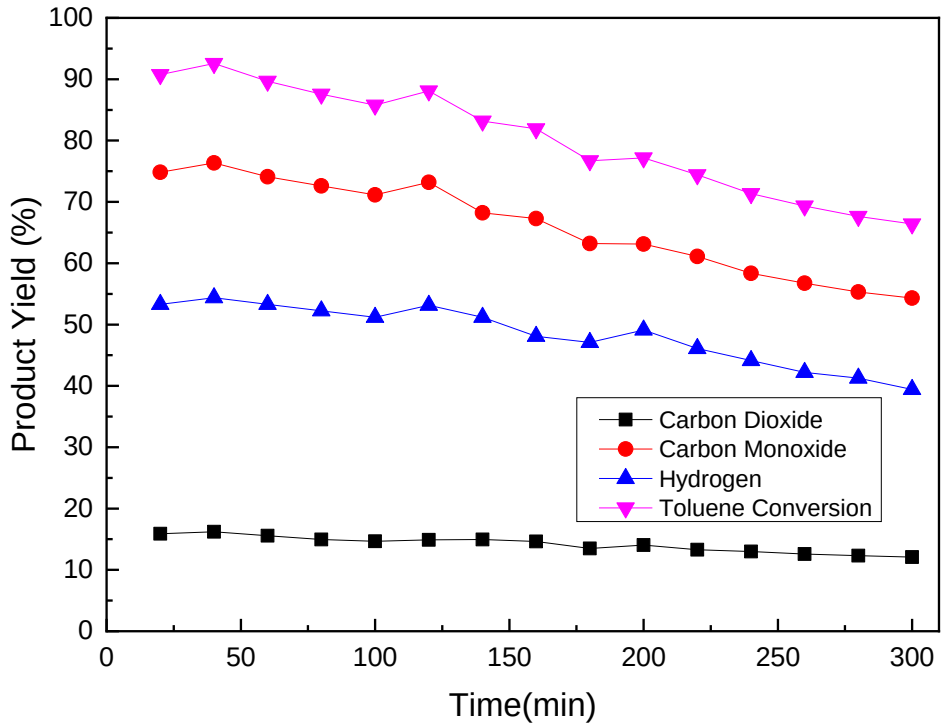

511

512 **Figure 7. Product yield trend and conversion of toluene steam reforming test in 3% CH_4,**
513 **30% H_2, 30% CO and 20% CO_2 balanced N_2 atmosphere (Ni/Al_2O_3 catalyst, 800 °C, S/C**
514 **ratio 3, GHSV: 91800 h^{-1})**

515 Table 7 and Figure 8 summarize the toluene conversion to C-containing gases and
516 CO, CO_2 yields in all the CH_4–containing atmospheres and compares with the
517 experiments in the N_2 atmosphere. Although the concentration of CH_4 in carrier gas
518 was fixed at 3 vol%, which was much lower than the concentration of CO, CO_2 and H_2,
519 CH_4 was the main reason for catalyst deactivation. The injected H_2 could largely
520 decrease the toluene conversion to gases with the presence of a small amount of CH_4.

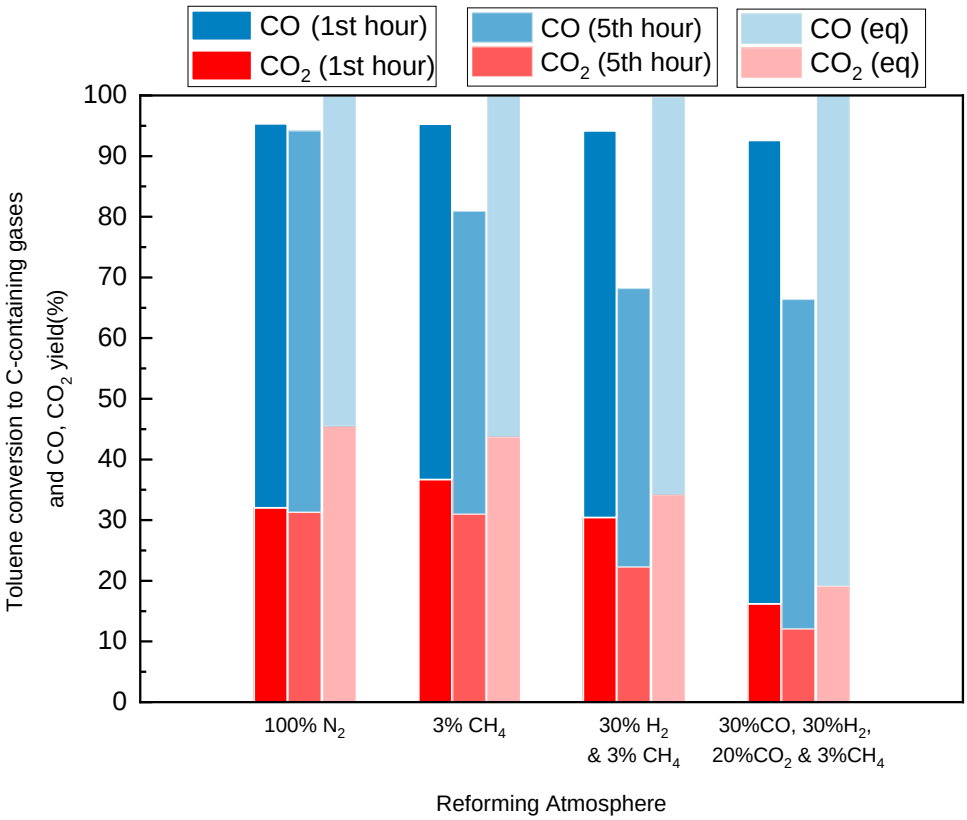

521

522 **Figure 8. Toluene conversion to C-containing gases and CO, CO_2 yield at CO, CO_2, H_2,**

523 **CH_4 and mixture gas atmosphere (S/C ratio 3 GHSV:91800 h^{-1}, reforming temperature**

524 **800 °C, all the gas atmosphere balanced with N_2).**

525

Table 7. Product yields for the gaseous products in 3% CH_4, 30% H_2, 30% CO and 20%CO_2 balanced N_2 atmosphere (5-hour test, Ni/Al_2O_3 catalyst, 800 °C, S/C ratio 3, GHSV: 91800 h^{-1})

Atmosphere	CO_2 (mol/mol toluene)	CO (mol/mol toluene)	H_2 (mol/mol toluene)	CO_2 selectivity
Full gas (1st hour)	1.3	6.2	12.0	17%
Full gas (5th hour)	1.0	4.8	8.7	17%
(Equilibrium)	(1.6)	(6.5)	(15.5)	(20%)

As shown in Table 8, coke formation was favored by the complex gas atmosphere, in particular when a mixture containing H_2 and CH_4 was applied. The amount of coke over the Ni/Al_2O_3 catalyst when 3% CH_4 and 30% H_2 balanced N_2 were employed as well as with the full syngas atmosphere was much larger than observed in any single-gas composition. On the other hand, under 30% H_2 and 30% CO balanced N_2, the coke formation was nearly identical to that observed under H_2 only, reinforcing the role of CH_4 as a trigger in toluene conversion to coke. CO and CO_2 were observed to have no influence on coke formation, with the difference between the full syngas with the CH_4 and H_2 atmosphere being around 1%. The large coke formation in the atmospheres containing H_2 and CH_4 markedly deactivated the Ni/Al_2O_3 catalyst in the first 5 hours on stream (Table 8).

Table 8. Toluene conversion to coke, fraction of coke deposited on the catalyst and catalyst deactivation at different reforming atmosphere (800 °C, S/C:3, GHSV:91800 h^{-1}, 5-hour test. CO & H_2 in N_2: 30% H_2 and 30% CO balanced N_2, CH_4 & H_2 in N_2: 3% CH_4 and 30% H_2 balanced N_2, Full gas mixtures: 3% CH_4, 30% H_2, 30% CO and 20%CO_2 balanced N_2).

Reforming Atmosphere	CO & H_2 in N_2	CH_4 & H_2 in N_2	Full gas mixture
Coke/C in toluene	0.88%	2.53%	2.49%
Coke/Catalyst (g_C/g_{cat})	0.238	0.684	0.676
Catalyst Deactivation (%)	7	28	27

3.3 Discussion of potential pathways for influence of syngas composition on the balance between syngas and carbon formation

A further insight on the type of carbon formed on the catalyst was obtained by analyzing the derivative thermogravimetric profiles obtained during temperature programmed oxidation (DTG-TPO) of the spent catalysts. These are shown in Figure 9, where each profile was normalized to the maximum peak to facilitate comparison. No low-temperature DTG-TPO peak corresponding to gum carbon formation are observed in any of the spent catalysts. This is expected given the high temperature of the reforming experiments, well above the range (typically reported as up to 450 °C [12]) in which gum formation is favored. Two DTG-TPO peaks are visible in most of the spent catalysts, the one at lower temperature corresponding to pyrolytic carbon and the other related to whisker structures. The threshold between both has been estimated to be around 650 °C in the literature [46, 71], which is consistent with the temperature of the shoulder observed in these DTG-TPO curves. It can be seen that

pyrolytic carbon is predominant in all atmospheres, although there is still a significant contribution from whisker carbon.

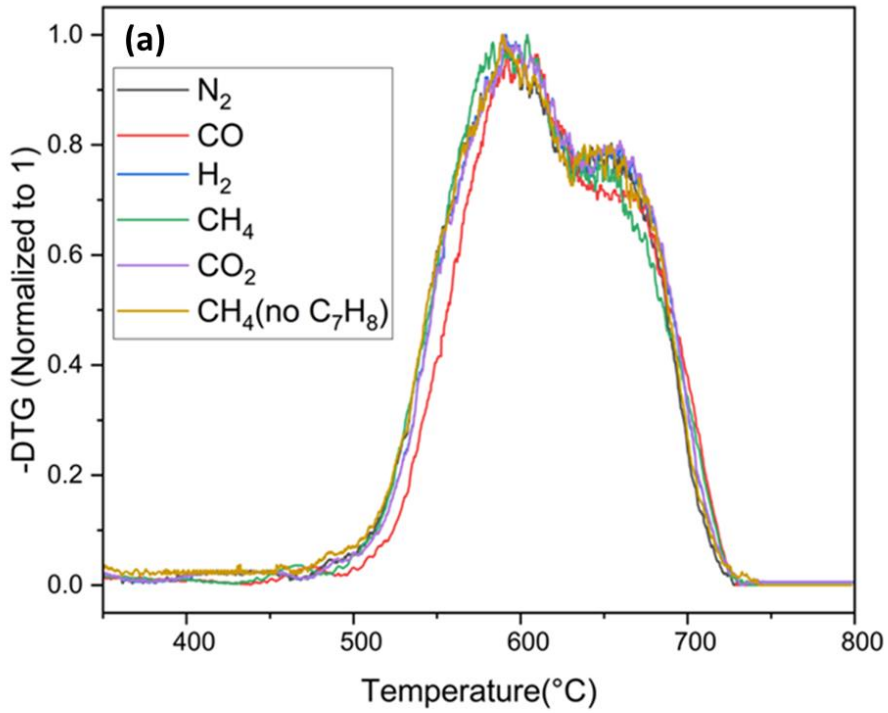

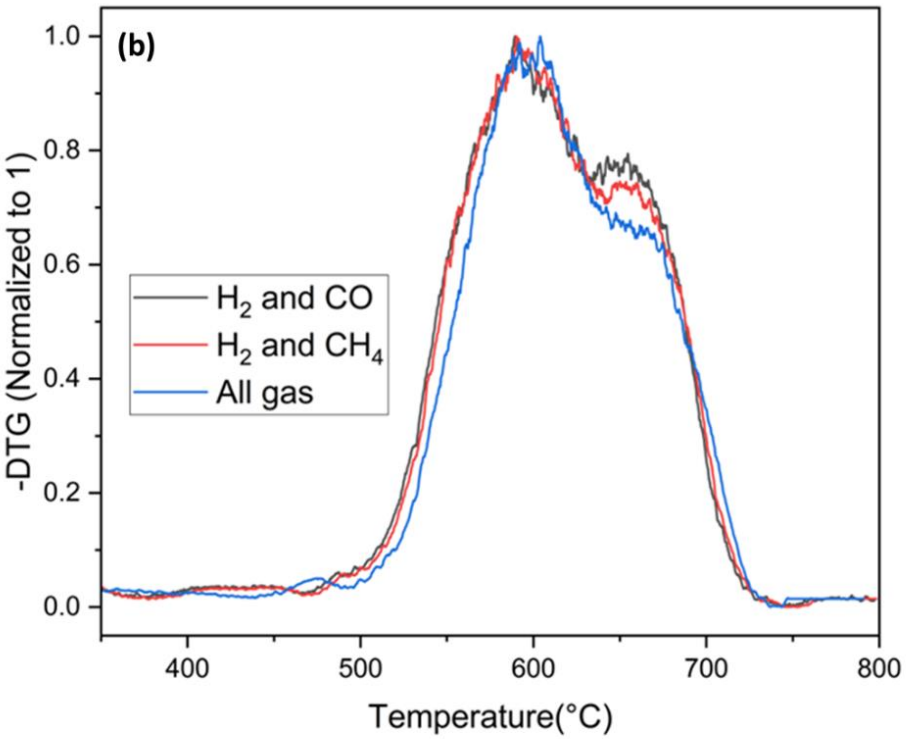

564

565 **Figure 9. DTG-TPO analysis for the spent catalysts at different reforming atmospheres**
566 **(800 °C, S/C:3, GHSV:91800 h^{-1}, 5-hour test). (a) N_2: 100%N_2, H_2: 30% H_2 in N_2, CO: 30%**
567 **CO in N_2, CO_2: 30% CO_2 in N_2, CH_4: 3% CH_4 in N_2 with and without toluene). (b) CO & H_2**
568 **in N_2: 30% H_2 and 30% CO balanced N_2, CH_4 & H_2 in N_2: 3% CH_4 and 30% H_2 balanced N_2,**
569 **All gas mixture: 3% CH_4, 30% H_2, 30% CO and 20%CO_2 balanced N_2. Each trace has**
570 **been normalized.**

571 As differences in carbon formation between different atmospheres appear to be
572 quantitative rather than qualitative, an attempt can be made to rationalize them based
573 on a common reaction pathway. The simplified steam reforming reaction scheme
574 shown in Figure 10 has been proposed [72]. Following adsorption on the catalyst the
575 hydrocarbons undergo hydrocracking to produce adsorbed C and H. These carbon
576 species can then either react with adsorbed OH from the dissociation of water, to
577 produce CO, which can be desorbed into the gas phase or further react to CO_2 with
578 adsorbed OH, or associate with other adsorbed C to form carbon deposits. The latter
579 may involve migration through the Ni particle in the case of whisker carbon. Adsorbed

H species can recombine and undergo desorption to produce H_2 in the gas phase. This scheme can be linked to the observations in this work to explain the effect of syngas components.

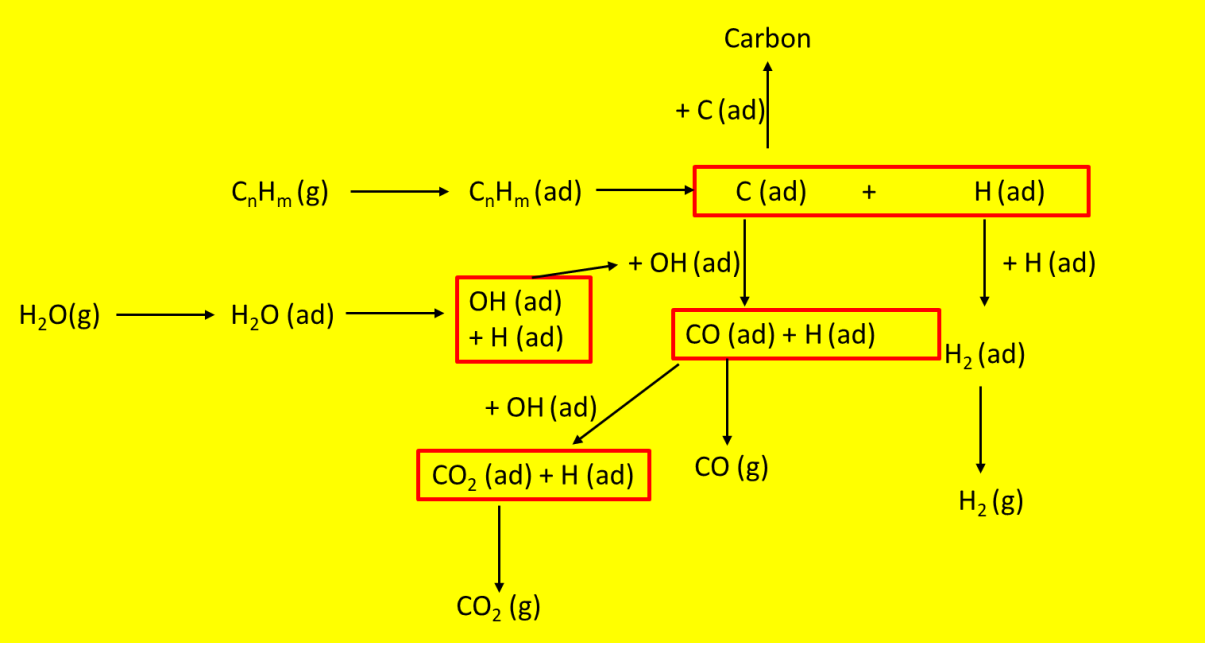

Figure 10. Simplified scheme for the steam reforming reaction of hydrocarbons on a Ni catalyst based on [72].

Taking the experiment in N_2 as the baseline, it was observed that H_2 led to inhibition and a moderate increase in carbon formation. Higher partial pressures of H_2 would tend to counteract the dissociation of the hydrocarbon on the catalyst active site and therefore cause the inhibition detected in the experiments. At the same time, the higher hydrogen pressure would decrease the concentration of surface OH, favoring the competing pathway towards carbon formation.

CO and CO_2 led to very slight inhibition and a decrease in carbon formation. Both could be the result of competition with toluene for adsorption on the catalyst, the very first step on the scheme. As the potential for carbon formation of both gases is low, in the case of CO because the high temperature does not favor reverse Boudouard reaction (Reaction 5), a small substitution of toluene by CO and CO_2 would lead to

slightly lower carbon formation as well as diminished toluene conversion. On the other hand, CH_4 leads to more adsorbed carbon (C(ad)) on the catalyst through hydrocracking, enhancing the potential for carbon formation.

A more detailed reaction mechanism specific for toluene steam reforming has been developed in a study [5] using density functional theory combined with in-situ infrared measurements. It showed that the preferential hydrocracking mechanism would involve full dehydrogenation of the methyl group first to produce a radical C_6H_5-$C^{\cdot}$ adsorbed on the catalyst. This structure subsequently losses an aromatic H atom from one of the β C atoms, which then leads to ring opening by cleavage of the aryl carbon bond resulting in a seven-carbon linear chain. Subsequent C-C dissociation leads to shorter chains with three- and four-carbon linear structures being the more energetically favorable. These structures undergo oxidation with O produced from steam dissociation and subsequent C-H bond scissions to finally produce CO and CO_2 through aldehyde intermediates. Again, the availability of extra H would tend to reverse the C-H bond scissions, causing a degree of inhibition while hindering conversion of the linear structures into aldehydes and increasing the chances of repolymerization to carbon. In this scheme it is also clear that extra carbon species originated in CH_4 would potentiate the pathways leading to carbon formation over the formation of the aldehyde intermediate.

4. Conclusions

This analysis of the effect of reforming gas atmosphere on the catalytic steam reforming of tar using a conventional Ni/Al_2O_3 catalyst shows how the conversion of toluene is markedly affected by the presence of some syngas components, even at constant steam to carbon ratio and despite full equilibrium conversion being expected in all cases. While only slight inhibition and no significant deactivation can be concluded from the presence of CO and CO_2, H_2 and CH_4 have been found to have a

significant adverse effect on the reforming of toluene in terms of catalyst deactivation. H_2 also showed a mild inhibitory effect, which interestingly was not observed when CH_4 only was used, albeit this may be due to the low concentration employed. Strong interactions between gas components were observed, with the joint presence of toluene and CH_4 leading to greater carbon formation, which could not have been predicted from separate steam reforming experiments with each of them. Moreover, the simultaneous exposure of the toluene reforming system to H_2 and CH_4 causes a marked deactivation of the catalyst by carbon deposition with each gas potentiating the negative effects of the other. In view of these results, the importance of testing tar reforming catalysts with full syngas compositions to avoid misleading, typically too optimistic, outcomes cannot be overemphasized.

References

1. Tan, R.S., et al., *Catalytic steam reforming of tar for enhancing hydrogen production from biomass gasification: a review.* Frontiers in Energy, 2020: 1-25.
2. Xiao, Y., et al., *Biomass steam gasification for hydrogen-rich gas production in a decoupled dual loop gasification system.* Fuel Processing Technology, 2017. **165**: 54-61.
3. Ruiz, J.A., et al., *Biomass gasification for electricity generation: Review of current technology barriers.* Renewable and Sustainable Energy Reviews, 2013. **18**: 174-183.
4. Deonarine, B., et al., *Ultra-microporous membrane separation using toluene to simulate tar-containing gases.* Fuel Processing Technology, 2017. **161**: 259-264.
5. Ashok, J., et al., *Recent progress in the development of catalysts for steam reforming of biomass tar model reaction.* Fuel Processing Technology, 2020. **199**: 106252.
6. Dagle, V.L., et al., *Steam reforming of hydrocarbons from biomass-derived syngas over MgAl2O4-supported transition metals and bimetallic IrNi catalysts.* Applied Catalysis B: Environmental, 2016. **184**: 142-152.
7. Nunnally, T., et al., *Gliding arc plasma oxidative steam reforming of a simulated syngas containing naphthalene and toluene.* International Journal of Hydrogen Energy, 2014. **39**(23): 11976-11989.

8. Long, X., et al., *Emission of species of environmental and process concern during simulated oxy-fuel gasification.* Fuel, 2021. **299**: 120886.
9. Fidalgo, B., D. Van Niekerk, and M. Millan, *The effect of syngas on tar quality and quantity in pyrolysis of a typical South African inertinite-rich coal.* Fuel, 2014. **134**: 90-96.
10. Berrueco, C., et al., *Evolution of tar in coal pyrolysis in conditions relevant to moving bed gasification.* Energy & Fuels, 2014. **28**(8): 4870-4876.
11. Rabou, L.P., et al., *Tar in biomass producer gas, the Energy research Centre of the Netherlands (ECN) experience: an enduring challenge.* Energy & fuels, 2009. **23**(12): 6189-6198.
12. Gao, N., et al., *Modified nickel-based catalysts for improved steam reforming of biomass tar: A critical review.* Renewable and Sustainable Energy Reviews, 2021. **145**: 111023.
13. Guan, G., et al., *Catalytic steam reforming of biomass tar: Prospects and challenges.* Renewable and sustainable energy reviews, 2016. **58**: 450-461.
14. Li, C. and K. Suzuki, *Tar property, analysis, reforming mechanism and model for biomass gasification—An overview.* Renewable and Sustainable Energy Reviews, 2009. **13**(3): 594-604.
15. Wang, Y., Zaki Memon, M., Ali Seelro, M., Fu, W., Gao, Y., Dong, Y., Ji G., *A review of CO_2 sorbents for promoting hydrogen production in the sorption-enhanced steam reforming process.* International Journal of Hydrogen Energy, **46** (2021), 23358-23379.
16. Yoon, S.J., Y.K. Kim, and J.G. Lee, *Catalytic oxidation of biomass tar over platinum and ruthenium catalysts.* Industrial & engineering chemistry research, 2011. **50**(4): 2445-2451.
17. Li, D., et al., *Production of renewable hydrogen by steam reforming of tar from biomass pyrolysis over supported Co catalysts.* International Journal of hydrogen energy, 2013. **38**(9): 3572-3581.
18. Chianese, S., et al., *Hydrogen from the high temperature water gas shift reaction with an industrial Fe/Cr catalyst using biomass gasification tar rich synthesis gas.* Fuel Processing Technology, 2015. **132**: 39-48.
19. Zuber, C., et al., *Investigation of sulfidation and regeneration of a ZnO-adsorbent used in a biomass tar removal process based on catalytic steam reforming.* Fuel, 2015. **153**: 143-153.
20. Li, W.-P., et al., *Interaction of Ce-char catalyst and partial oxidation on changes in biomass syngas composition.* Journal of Renewable and Sustainable Energy, 2019. **11**(2): 023101.
21. Shen, Y. and K. Yoshikawa, *Recent progresses in catalytic tar elimination during biomass gasification or pyrolysis—A review.* Renewable and Sustainable Energy Reviews, 2013. **21**: 371-392.
22. Miyazawa, T., et al., *Catalytic properties of Rh/CeO2/SiO2 for synthesis gas production from biomass by catalytic partial oxidation of tar.* Science and

technology of Advanced Materials, 2005. **6**(6): 604-614.
23. Heo, D.H., et al., *The effect of addition of Ca, K and Mn over Ni-based catalyst on steam reforming of toluene as model tar compound.* Catalysis Today, 2016. **265**: 95-102.
24. Park, S.Y., et al., *Deactivation characteristics of Ni and Ru catalysts in tar steam reforming.* Renewable Energy, 2017. **105**: 76-83.
25. Baker, E.G. and L.K. Mudge, *Mechanisms of catalytic biomass gasification.* Journal of analytical and applied pyrolysis, 1984. **6**(3): 285-297.
26. Uchida, H. and M.R. Harada, *Hydrogen Energy Engineering Applications and Products*, in *Science and Engineering of Hydrogen-Based Energy Technologies*. 2019, Elsevier. p. 201-220.
27. Sehested, J., *Four challenges for nickel steam-reforming catalysts.* Catalysis Today, 2006. **111**(1-2): 103-110.
28. Dabai, F., et al., *Tar formation and destruction in a fixed-bed reactor simulating downdraft gasification: equipment development and characterization of tar-cracking products.* Energy & fuels, 2010. **24**(8): 4560-4570.
29. Dabai, F., et al., *Tar formation and destruction in a fixed bed reactor simulating downdraft gasification: effect of reaction conditions on tar cracking products.* Energy & fuels, 2014. **28**(3): 1970-1982.
30. Rios, M.L.V., et al., *Reduction of tar generated during biomass gasification: A review.* Biomass and bioenergy, 2018. **108**: 345-370.
31. Evans, R.J., Milne, T.A., *Molecular characterization of the pyrolysis of biomass. 1. Fundamentals.* Energy & Fuels 1987, **1**(2), 123-137.
32. Evans, R.J., Milne, T.A., *Molecular characterization of the pyrolysis of biomass. 2. Applications.* Energy & Fuels 1987, **1**(4), 311-319.
33. Milne, T.A., Evans, R.J., Abatzoglou, N., *Biomass gasifier "tars": their nature, formation, and conversion.* NREL/TP-570-25357; National Renewable Energy Lab (US DoE): 1998, available at https://www.nrel.gov/docs/fy99osti/25357.pdf. Accessed 18 August 2022.
34. Simell, P., Kurkela, E., Ståhlberg, P., *Formation and catalytic decomposition of tars from fludized-bed gasification.* in Bridgwater, A.V., editor. Advances in thermochemical biomass conversion Vol. 1, Chapman and Hall 1993, p 265-279.
35. Sarioglan, A., *Tar removal on dolomite and steam reforming catalyst: benzene, toluene and xylene reforming.* International Journal of Hydrogen Energy, **37** (2012), 8133-8142.
36. Di Carlo, A., Borello, D., Sisinni, M., Savuto, E., Venturini, P., Bocci, E., Kuramoto, K., R*eforming of tar contained in a raw fuel gas from biomass gasification using nickel-mayenite catalyst.* International Journal of Hydrogen Energy, **40** (2015), 9088-9095.
37. Mermelstein, J., M. Millan, and N. Brandon, *The impact of carbon formation on Ni–YSZ anodes from biomass gasification model tars operating in dry*

conditions. Chemical Engineering Science, 2009. **64**(3): 492-500.
38. Tian, Y., et al., *The influence of shell thickness on coke resistance of core-shell catalyst in CO2 catalytic reforming of biomass tar.* International Journal of Hydrogen Energy, 2022. **47**(29): 13838-13849.
39. Taira, K., K. Nakao, and K. Suzuki, *Steam reforming of 1-methylnaphthalene over pure CeO2 under model coke oven gas conditions containing high H2S concentrations.* International Journal of Hydrogen Energy, 2020. **45**(58): 33248-33259.
40. Geis, M., et al., *Coupling SOFCs to biomass gasification-The influence of phenol on cell degradation in simulated bio-syngas. Part I: Electrochemical analysis.* International journal of hydrogen energy, 2018. **43**(45): 20417-20427.
41. Wang, S., et al., *Catalytic steam reforming of bio-oil model compunds for hydrogen production over coal ash supported Ni catalyst.* International journal of hydrogen energy 39 (2014) 2018-2025,
42. Wang, S., et al., *Hydrogen production via catalytic reforming of the bio-oil model compunds: acetic acid, phenol and hydroxyacetone.* International journal of hydrogen energy 39 (2014) 18675-18687
43. Long, X., et al., *Towards integrated gasification and fuel cell operation with carbon capture: Impact of fuel gas on anode materials.* Fuel, 2022. **318**: 123561.
42. Lorente, E., M. Millan, and N. Brandon, *Use of gasification syngas in SOFC: Impact of real tar on anode materials.* International Journal of Hydrogen Energy, 2012. **37**(8): 7271-7278.
43. Lorente, E., et al., *Effect of tar fractions from coal gasification on nickel–yttria stabilized zirconia and nickel–gadolinium doped ceria solid oxide fuel cell anode materials.* Journal of Power Sources, 2013. **242**: 824-831.
44. Shen, Y., Liu, Y., Yu, H., *Enhancement of the quality of syngas from catalytic steam gasification of biomass by the addition of methane/model biogas.* International Journal of Hydrogen Energy, **43** (2018), 20428-20437.
45. Zhang, Z. et al., *Preparation, modification and development of Ni-based catalysts for caatalytic reforming of tar produced from biomass gasification*. Renewable and Sustainable Energy Reviews, 94, 2018, 1086-1109,
46. Wangen, E.S., Osatiashtiani, A., Blekkan, E.A., *Reforming of syngas from biomass gasification: deactivation by tar and potassium species*. Topics in Catalysis 2011, *54* (13-15) , 960-966.
47. Wang, L. et al. *Catalytic performance and characterization of Ni–Co catalysts for the steam reforming of biomass tar to synthesis gas*. Fuel 112 (2013) 654-661
48. Boldrin, P., M. Millan-Agorio, and N.P. Brandon, *Effect of sulfur-and tar-contaminated syngas on solid oxide fuel cell anode materials.* Energy & Fuels, 2015. **29**(1): 442-446.
49. Huang, C.W., et al., *Optimal Fe/Ni/Ca -Al catalyst for tar model steam reforming*

by using the Taguchi method. International Journal of Energy Research, 2022. **46**(6): 7799-7815.
50. Gao, X., et al., *Steam reforming of toluene as model compound of biomass tar over Ni–Co/La2O3 nano-catalysts: Synergy of Ni and Co.* International Journal of Hydrogen Energy, 2021. **46**(60): 30926-30936.
51. Yahya, H.S.M., T. Abbas, and N.A.S. Amin, *Optimization of hydrogen production via toluene steam reforming over Ni–Co supported modified-activated carbon using ANN coupled GA and RSM.* International Journal of Hydrogen Energy, 2021. **46**(48): 24632-24651.
52. Cao, J.-P., et al., *Effect of atmosphere on carbon deposition of Ni/Al2O3 and Ni-loaded on lignite char during reforming of toluene as a biomass tar model compound.* Fuel, 2018. **217**: 515-521.
53. Mermelstein, J., M. Millan, and N. Brandon, *The interaction of biomass gasification syngas components with tar in a solid oxide fuel cell and operational conditions to mitigate carbon deposition on nickel-gadolinium doped ceria anodes.* Journal of power sources, 2011. **196**(11): 5027-5034.
54. Ren, J., Cao, J-P., Yang, F-L., Liu, Y-L., Tang W., Zhao X-Y., *Understandings of catalyst deactivation and regeneration during biomass tar reforming: A crucial review*. ACS Sustainable Chemistry & Engineering 2021, 9, 17186-17206.
55. Mermelstein, J., Brandon, N.P., Millan, M., *The impact of steam on the interaction between biomass gasification tars and nickel based Solid Oxide Fuel Cell anode materials.* Energy & Fuels, 2009, 23, 10, 5042-5048.
56. Zhu, H.L., Pastor-Pérez, L., Millan, M., *Catalytic Steam Reforming of Toluene: Understanding the Influence of the Main Reaction Parameters over a Reference Catalyst.* Energies, 2020. **13**(4): 813.
57. Namioka et al. *Low-temperature trace light-tar reforming in biomass syngas by atmospheric hydrogenation and hydrogenolysis.* Fuel Processing Technology 181 (2018) 304-310.
58. Simell, P.A., Hepola, J.O., Krause, A.O.I., *Effects of gasification gas components on tar and ammonia decomposition over hot gas cleanup catalysts.* Fuel 1997, 76(12), 1117 - 1127.
59. Kong, M., et al., *Influence of supports on catalytic behaviour of nickel catalysts in carbon dioxide refrorming of toluene as a model compound of tar from biomass gasification.* Bioresource Technology 102 (2), 2011, 2004-2008
60. Chen et al., *CO_2 reforming of toluene as model compound of biomass tar on Ni/Palygorskite*. Fuel 107 (2013) 699-705.

61. Kertthong, T., et al., *Influence of gas atmosphere and role of tar on catalytic reforming of methane and tar model compounds: Special focus on syngas produced by sorption enhanced gasification*. Fuel 317 (2022) 123502.
62. Pinto F. et al., *Methane reforming of syngas produced by co-gasification of coal and wastes. Effect of catalysts and of experimental conditions.* Fuel 90 (4), 2011,

1645-1654.
63. Laprune, D., *Effects of H_2S and phenanthrene on the activity of Ni and Rh-based catalysts for the reforming of a simulated biomass-derived producer gas.*Applied Catalysis B: Environmental 221, 2018, 206-214.
64. Claude. V., et al., *Ni-doped γ-Al_2O_3 as secondary catalyst for bio-syngas purification: influence of Ni loading, catalyst preparation and gas composition on catalytic activity*. Materials Today Chemistry 13, 2019, 98-109.
65. Sarvaramini, A., Larachi, F., *Catalytic oxygenless steam cracking of syngas-containing benzene model tar compound over natural Fe-bearing silicate minerals*. Fuel 97 (2012) 741-750.
66. Bizkarra, K., et al., *Nickel based monometallic and bimetallic catalysts for synthetic and real bio-oil steam reforming.* International Journal of Hydrogen Energy, 2018. **43**(26): 11706-11718.
67. Abu El-Rub, Z., E.A. Bramer, and G. Brem, *Review of catalysts for tar elimination in biomass gasification processes.* Industrial & engineering chemistry research, 2004. **43**(22): 6911-6919.
68. Sutton, D., B. Kelleher, and J.R.H. Ross, *Review of literature on catalysts for biomass gasification.* Fuel Processing Technology, 2001. **73**(3): 155-173.
69. Puron, H., et al., *Hydroprocessing of Maya vacuum residue using a NiMo catalyst supported on Cr-doped alumina.* Fuel, 2020. **263**: 116717.
70. Hiblot, H., Ziegler-Devin, I., Fournet, R., Glaude, P.A., *Steam reforming of methane in a synthesis gas from biomass gasification*. International Journal of Hydrogen Energy, **41** (2016), 18329-18338.
71. Ashok, J., Kawi, S., *Nickel-Iron Alloy Supported over Iron-Alumina Catalysts for Steam Reforming of Biomass Tar Model Compound.* ACS Catalysis 2014, 4, 289-301.
72. Rostrup-Nielsen, J., Christiansen, L.J., *Concepts in Syngas Manufacture*. Catalytic Science Series Vol. 10, Imperial College Press, 2011.

How syngas composition affects catalytic steam reforming of tars: an analysis using toluene as model compound

Authors

HuaLun Zhu, Ziyin Chen, Laura Pastor-Perez, Xiangyi Long, Marcos Millan*

Department of Chemical Engineering, Imperial College, London SW7 2AZ

*Corresponding author

Marcos Millan

Mailing address: Department of Chemical Engineering, Imperial College

London SW7 2AZ, UK

Tel.: +44 (0)20 7594 1633

E-mail: marcos.millan@imperial.ac.uk

Abstract

Tar removal by catalytic steam reforming has an important role to play in gasification systems as part of the treatment to the hot product gas from the gasifier. Despite the importance of understanding the influence gas atmosphere has on this reaction, the effect of a full synthesis gas mixture has not been comprehensively investigated. This study aims to bridge that gap by analyzing the effect of each single synthesis gas component, including H_2, CO, CO_2 and CH_4, as well as their combinations on steam reforming of toluene as a biomass gasification tar model over a Ni/Al_2O_3 catalyst. It has been found that H_2, CO and CO_2 have minor inhibitory effects, slightly decreasing the initial toluene conversion. On the other hand, while CO and CO_2 do not lead to catalyst deactivation, H_2 and CH_4 deactivate the Ni/Al_2O_3 by promoting coke deposition. A small amount (3%) of CH_4 can significantly increase coke deposition, despite deactivation been insignificant with toluene or CH_4 used separately, and the joint presence of CH_4 and H_2 causes further drops in toluene conversion with time on stream.

Keywords

syngas, tar steam reforming, nickel catalyst, carbon deposition, catalyst deactivation.

1. Introduction

Biomass gasification can act as a source of renewable heat and power as well as chemicals. At the core of gasification-based processes is synthesis gas (syngas), a valuable product that can provide remarkable versatility in terms of products, including hydrogen, synthetic natural gas, liquid fuels through Fischer-Tropsch synthesis, methanol and others [1-3]. However, one of the major hindrances to technology development is the formation of tar, which consists of a complex mixture of high molecular weight organic material. Tar formed in the biomass gasification process will be present as an impurity in the syngas at high temperatures and could condense or react downstream of the gasifier, affecting power generation, as well as gas separation membranes [4] and catalysts [5], for example decreasing the conversion of methane by steam reforming [6, 7].

Methods studied for tar abatement include optimizing gasifier design and operating parameters to limit their formation [8-10], physical removal (eg. scrubbers, filters) [11], and thermal, plasma or catalytic conversion downstream from the gasifier [12]. Among these technologies, tar catalytic reforming is particularly appealing as the process can take place without cooling the syngas and convert tar into valuable gases, especially H_2, substantially reducing its concentration in the syngas [1, 13].

Catalytic tar reforming can be applied in either in-situ or ex-situ gasification systems, to remove tar content in the gasification gas, as part of the treatment to the hot product gas from the gasifier [13, 14]. Various types of catalyst have been studied, including olivine, dolomite, zeolite, char, metal-based (eg. Fe, Co, Ni, Zn, Pt, Ce, Ru, Rh), Alkali-based (K and Ca) [15-19]. Nickel-based catalysts are the most common catalyst for tar removal, mainly due to their low cost, high catalytic activity and easy regeneration [14, 20].

The major challenge for Ni-based catalysts is deactivation caused by carbon deposition and sintering [18, 21, 22], which shortens their life cycle [23]. Carbon deposition on the catalyst may encapsulate the active metal particles and prevent the contact between reactants and the metal active sites [12]. Carbon can quickly diffuse

into or form on the Ni catalyst surface, cover or block the pores of the active nickel and decrease Ni catalytic activity [24, 25]. The carbonaceous deposit (coke) can be in three forms: polymer, whisker and pyrolytic [26]. The pyrolytic carbon is formed due to the cracking of hydrocarbons which encapsulate the nickel active site [24], and has a significant influence on catalyst deactivation, high temperature (>600 °C) and the acidity of the catalyst could promote its formation [12].

The main syngas components are H_2, CO, CO_2 and CH_4. Tar concentrations in the syngas depend on the gasifier type and operating conditions. In moving beds, they can reach relatively high values (~100 g Nm^{-3}) in updraft gasifiers. Downdraft configurations, as they allow cracking to take place in the hot char bed [27, 28], can reach values as low as ~ 1 g Nm^{-3}. Fluidised beds present intermediate values, typically around 15 g Nm^{-3} [29]. Work in the literature tends to make use of model compounds to compare the performance of different catalysts and assess their deactivation in catalytic reforming tests. These have included benzene [30], toluene [31], phenol [32], polyaromatic hydrocarbons [33], among others. The use of monoaromatics as model compounds, in particular toluene, has been observed to represent a worst-case scenario for carbon formation on Ni materials in comparison with polyaromatics [30] and real tar samples [34, 35]. This was corroborated by a study showing that lighter tar fractions [36] led to greater carbon formation than heavier ones.

Toluene steam reforming is described by Reaction 1.

$$C_7H_8 + 7H_2O \leftrightarrow 7\,CO + 11\,H_2 \qquad \text{Reaction 1}$$

The water gas shift (WGS) reaction (Reaction 2) will affect the syngas composition as well as steam methane reforming (Reaction 3), which can happen simultaneously if methane is present.

$$CO + H_2O \leftrightarrow CO_2 + H_2 \qquad \text{Reaction 2}$$

$$CH_4 + H_2O \leftrightarrow CO + 3H_2 \qquad \text{Reaction 3}$$

Other relevant reactions in the presence of CO_2 or CO are toluene dry reforming (Reaction 4) and the reverse Boudouard reaction (Reaction 5).

$$C_7H_8 + 7\,CO_2 \leftrightarrow 14\,CO + 4\,H_2 \qquad \text{Reaction 4}$$

$$2\,CO \leftrightarrow C + CO_2 \qquad \text{Reaction 5}$$

Despite this complex reaction system, catalytic steam reforming of tar is typically studied in atmospheres only containing tar (usually a model compound) or other contaminants, such as H_2S [33, 37], and NH_3, and steam [38-40], in some cases with hydrogen added [41]. Few research studies have focused on the effect of syngas composition on catalytic tar reforming process, and those that did have tended to focus on varying steam and H_2 concentrations [30, 41]. A previous study has hinted at complex interactions between syngas components, affecting formation of carbon on Ni materials [42].

The objective of this work is to gain an understanding of the influence of reforming gas atmosphere on catalytic steam reforming by performing a systematic study where the effect of each gas (H_2, CO, CO_2 and CH_4) and their mixtures is analyzed. These effects have been investigated using toluene as model compound over a standard Ni/Al_2O_3 catalyst. Toluene was deemed a very suitable model due to its propensity to carbon formation as discussed above.

2. Experimental

2.1 Catalyst preparation

The Ni/Al_2O_3 catalyst used in the catalytic reforming tests was prepared by the wetness impregnation method, Nickel was impregnated onto an alumina support to produce 20 wt.% of NiO with the alumina support. To this effect $Ni(NO_3)_2{\cdot}6H_2O$ (≥97.0%, Sigma-Aldrich) was dissolved in acetone (≥99.8%, Sigma Aldrich); the support γ- Al_2O_3 (≥98.0% purity, Sasol) was added into the solution stirred for 2 h, then a rotating evaporator at 60 °C under vacuum was used to remove the acetone. The

resulting solid was dried overnight at 110 °C and then calcined at 600 °C with a ramping rate of 2 °C·min^{-1} for 4 hours. Finally, it was sieved into particles ranging between 250 and 500 μm. The obtained catalyst sample was labelled Ni/Al_2O_3. The reduced Ni content is 16.4 wt.% (assuming 100% reduction).

2.2 Catalytic toluene steam reforming tests

Toluene steam reforming tests were carried out in a fixed bed reactor used in previous bio-oil reforming studies [43]. A scheme of the system employed, and a detailed drawing of the reactor have been given elsewhere [44]. Briefly, the reactor consists of an Incoloy alloy 625 tube (12 mm i.d., 2 mm thick, 253 mm long), equipped with an inner quartz tube (9 mm i.d., 1 mm thick and 300 mm long) to avoid potential reaction between reactant gas stream and the Incoloy tube walls. Two copper electrodes controlled by a WEST 6100+ digital temperature controller were used to heat up the reactor by Joule effect. Two syringe pumps were installed at the top of the reactor to inject toluene and water into the reactor.

Before each experiment, the reactor was purged with N_2 for 10 min to remove air. The catalyst was reduced under 50 mL·min^{-1} of H_2 at 800 °C for 1 hour. After activating the catalyst, the carrier gas was then switched to the experimental atmosphere gas composition and allowed 10 min to stabilize. It was made sure the outlet gas pressure remained unchanged during this process as there are five different gas channels and slight pressure changes would affect the accuracy of the gas mixture. The injection of steam and toluene started when the reading of the analyzers stayed stable at desired input readings for at least 5 minutes. The liquid phase reactants were carried by the atmosphere gas and preheated at 200 °C in a bed of 1 g of SiC to vaporize them. Then, the reactant mixture gas entered a 500 mg of Ni/Al_2O_3 catalyst bed, which was held by wire mesh and quartz wool in the middle of the quartz tube. The bed temperature was continuously monitored by a K-type thermocouple.

The product gases passed through two condensers in series to collect any liquid product as well as unreacted toluene and water. Ice and dry ice were used as coolant

in the first and second condenser, respectively. The products identified in the gas phase were H_2, CH_4, CO_2 and CO. Two on-line gas analyzers were used to determine product gas compositions: an MGA3000 Multi-Gas infrared analyzer for CO_2, CH_4 and CO, followed by a K1550 thermal conductivity H_2 analyzer. The software started to collect gas data (product gas concentrations) when the reactant injection started, the gas concentration was recorded continuously for 5 hours.

The reaction gas atmosphere was designed to simulate the gas composition from biomass gasification processes. The main products include H_2, CO, CO_2 and CH_4. The typical composition ranges of H_2, CO, CO_2 and CH_4 in biomass gasification gas products are 20 – 50 vol%, 20 – 40 vol%, 10 – 30 vol% and 1 – 8 vol% respectively [20, 45, 46].To investigate the influence of H_2, CO, CO_2 and CH_4 on catalytic toluene steam reforming, their inlet concentrations were fixed at 30, 30, 20 and 3 vol%, respectively, and balanced with N_2.

Table 1 shows the detailed reforming atmosphere gas compositions of different toluene catalytic steam reforming tests.

Table 1. Toluene steam reforming atmospheres used in this work (on dry basis). A S:C ratio of 3 was applied in all experiments.

Component Concentration (%vol) [Flowrate (mmol h^{-1})]				
H_2	CO	CO_2	CH_4	N_2
0	0	0	0	100% [536]
30% [161]	0	0	0	70% [375]
0	30% [161]	0	0	70% [359]
0	0	20% [107]	0	80% [429]
0	0	0	3% [16]	97% [520]
30% [161]	30% [161]	0	0	40% [214]
30% [161]	0	0	3% [16]	67% [359]
30% [161]	30% [161]	20% [107]	3% [16]	17% [91]

The catalytic reforming test conditions applied in catalytic steam reforming test are shown in Table 2, which were found to be optimal in previous work [44]. Steam to Carbon (S/C) ratio is defined as in Equation 1, where *n* is the molar flowrate of each species. This definition takes into account the carbon contents of toluene and methane, and is used throughout this work unless otherwise stated.

$$S/C = \frac{n_{H_2O,in}}{7\, n_{C_7H_8,in} + n_{CH_4,in}} \qquad \text{Eq.1}$$

Table 2. Experimental conditions

Reforming parameters	Value
Temperature	800 °C
S/C ratio	3
GHSV	91800 h^{-1}
Carrier gas flow rate	200 mL min^{-1}
Toluene injection rate	1.38 mL h^{-1} (13 mmol h^{-1})
Catalyst	500 mg Ni/Al_2O_3

The performance of catalysts was evaluated by the toluene conversion ($X_{C_7H_8}$) into gaseous products (based on a carbon balance between the reactor inlet and outlet), according to Equation 2:

$$X_{C_7H_8}(\%) = \frac{(n_{CO,out} - n_{CO,in}) + (n_{CO_2,out} - n_{CO_2,in}) + (n_{CH_4,out} - n_{CH_4,in})}{7\, n_{C_7H_8,in}} * 100 \qquad \text{Eq.2}$$

CO, CO_2 and H_2 yield (*Y*) were defined as in Equations 3 to 5. In the case of H_2, a 100% yield was defined considering the WGS reaction was fully shifted to the right.

$$Y_{CO}(\%) = \frac{(n_{CO,out} - n_{CO,in})}{7\, n_{C_7H_8,in} + n_{CH_4,in}} * 100 \qquad \text{Eq. 3}$$

$$Y_{CO_2}(\%) = \frac{(n_{CO_2,out} - n_{CO_2,in})}{7\, n_{C_7H_8,in} + n_{CH_4,in}} * 100 \qquad \text{Eq. 4}$$

$$Y_{H_2}(\%) = \frac{(n_{H_2,out} - n_{H_2,in})}{18\, n_{C_7H_8,in} + 4\, n_{CH_4,in}} * 100 \qquad \text{Eq. 5}$$

CO_2 selectivity was also calculated to investigate the influence of different gas atmospheres on CO/CO_2 selectivity and assess the extent of WGS reaction. As methane had a total conversion in all the experiments, CO_2 selectivity is defined by the equation below where each term is in moles:

$$S_{CO_2}(\%) = \frac{(n_{CO_2,out} - n_{CO_2,in})}{(n_{CO_2,out} - n_{CO_2,in}) + (n_{CO,out} - n_{CO,in})} * 100 \qquad \text{Eq. 6}$$

The experimental error in toluene conversion, gas selectivity and yield is ± 2%.

Thermogravimetric analysis (TGA) was conducted to investigate the coke deposition on the spent catalyst using a Pyris 1 thermogravimetric analyzer from PerkinElmer. The samples were heated from room temperature to 900 °C at 10 °C·min^{-1} in air according to a procedure described elsewhere [47].

2.3 Thermodynamic equilibrium simulation

ASPEN V8.4 software was used to study the thermodynamic equilibrium of the toluene reforming reactions under different reaction atmospheres, using an ideal base property method, a RGIBBS reactor (based on Gibbs free energy minimization) to identify reforming products and yields. Material flows, reaction conditions (reforming temperature, pressure) are identical to those from the corresponding experiments.

3. Results and discussion

3.1 Influence of single syngas component atmosphere

A first group of experiments was conducted to understand the influence of single gas atmospheres on toluene steam reforming over a Ni/Al_2O_3 catalyst at the conditions shown in Table 2. A baseline is provided by experiments with an inert atmosphere (100% N_2). **Error! Reference source not found.**1 presents toluene conversion and product gas yields for H_2, CO and CO_2 as a function of time on stream during reforming test

for each of the single syngas component atmospheres (balanced in N_2) with a steam to carbon ratio of 3. It was observed (Figure 1a) that toluene reforming in a N_2 atmosphere led to steady gas yields and a conversion of nearly 95% over the 5-hour experiment.

During the 5-hour test in 30% H_2 atmosphere, shown in Figure 3, the carbon conversion from toluene to gas steadily decreased from 94% to 88%, as CO yield was reduced from 67% to 62%, while a steady yield of 26 – 28 % was observed for CO_2 throughout the test. H_2 yield declined slightly from 59% to 55%. These trends point to a certain deactivation of the catalyst taking place as a consequence of the presence of H_2 in the gas.

On the other hand, no significant deactivation was observed in CO or CO_2 atmospheres. The toluene conversion into gas products observed in a 30% CO atmosphere (Figure 1c) showed no significant change in 5 hours, and CO, CO_2 yield remained stable at ~33% and ~58%, respectively, throughout the experiment. The input of CO in the carrier gas shifted the WGS reaction to produce more H_2 and CO_2, and H_2 yield stayed above 75% in the 5-hour test. In 20% CO_2, shown **Error! Reference source not found.** the overall conversion of toluene stayed higher than 90% during the 5 hours, while CO_2 yield ranged from 17% to 19% and CO yield ranged from 71% to 76%. H_2 yield also remained stable at ~58%.

Two different conditions were tested with a 3% CH_4 concentration to gain a better understanding on the behavior of the system with toluene and methane mixtures. In one of them, the molar ratio between steam and carbon in toluene was 3 (carbon in CH_4 was not considered in the calculation, which is equivalent to S/C ratio of 2.55). In this case, the overall conversion from toluene to gases decreased from 90% to 79% after 5 hours, and H_2 yield declined from 58% to 49% (Figure 1e). CO and CO_2 yields decreased from 65% and 25% to 56% and 22%, respectively. CH_4 conversion stayed 100% throughout the test. An experiment carried out with CH_4 without toluene led to the formation of 0.112 g of coke per g of catalyst, which represents around 2.4% of the

CH_4 injected. Therefore, CH_4 was mostly steam reformed into CO, CO_2 and H_2.

In another experiment the steam feeding rate was increased to keep the S/C ratio at 3, as per the definition in Equation 1. The product yield and total gas conversion trends are presented in Figure 1f. The toluene conversion into gases in first hour achieved 93% as a result of the increasing of S/C ratio from 2.55 to 3. Then the overall conversion decreased with time smoothly, and finally dropped to 79% during the fifth hour. H_2, CO and CO_2 yields decreased from 72%, 59% and 36% to 64%, 52% and 31%, respectively. H_2 yield also increased with the increasing of S/C ratio. Despite the initial increase in toluene conversion, the degree of deactivation in 5 hours was not significantly affected by the increase in S/C ratio with final yield values being very close for the two conditions.

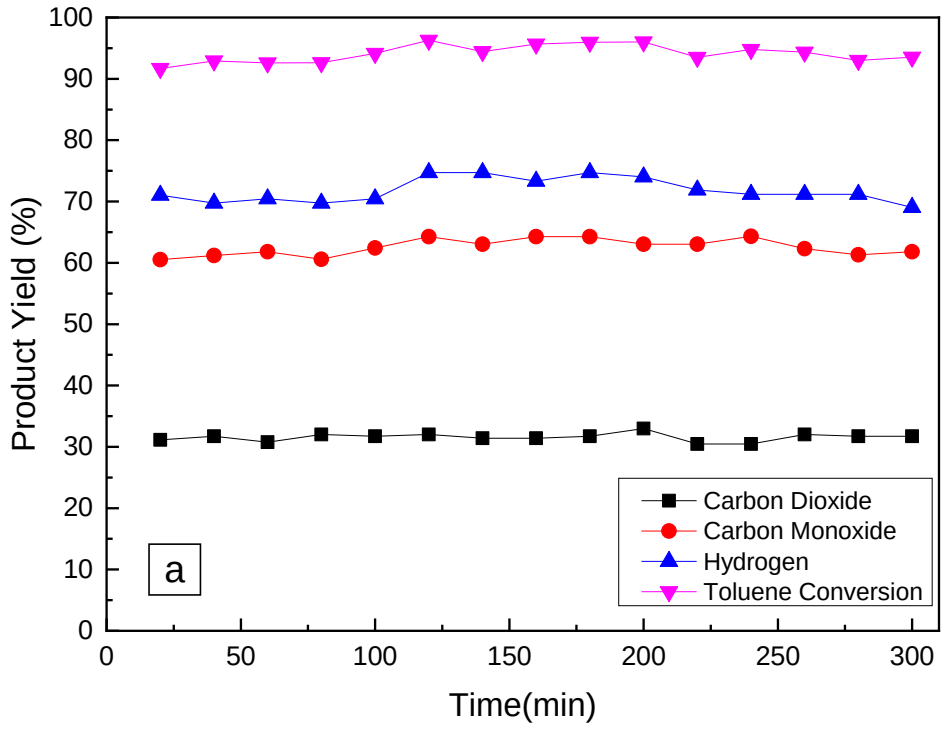

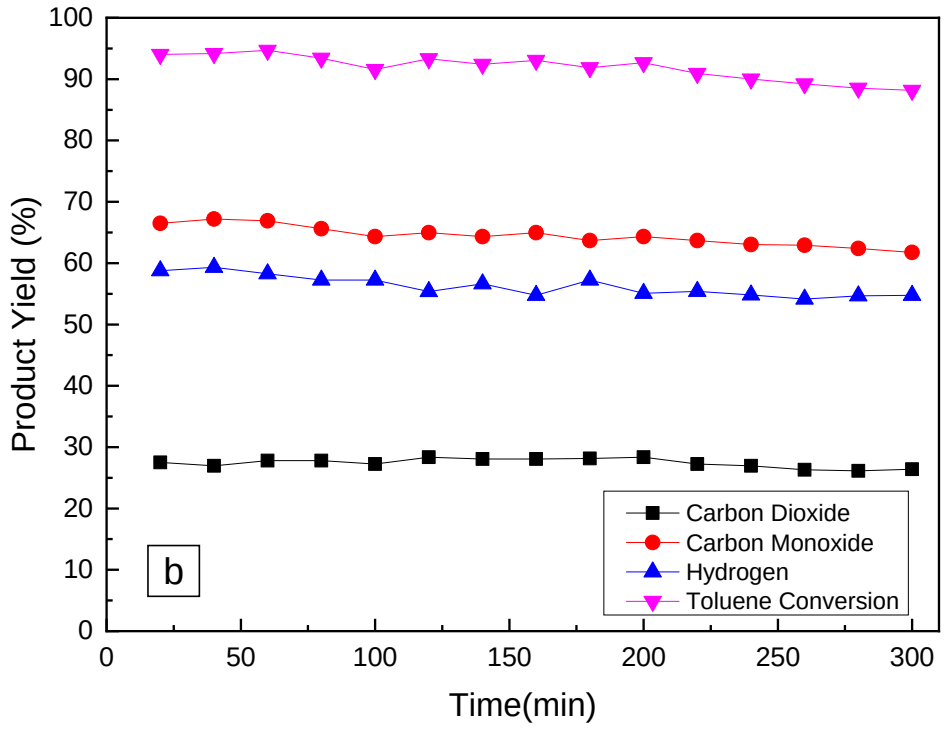
Product Yield (%)
Time(min)
b
Carbon Dioxide
Carbon Monoxide
Hydrogen
Toluene Conversion

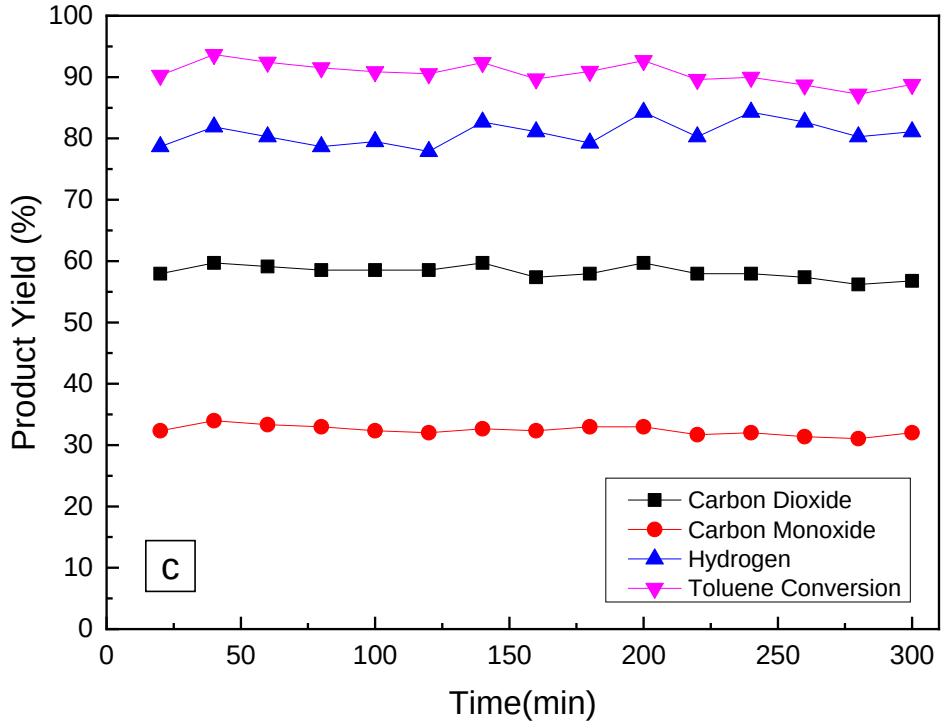
Product Yield (%)
Time(min)
c
Carbon Dioxide
Carbon Monoxide
Hydrogen
Toluene Conversion

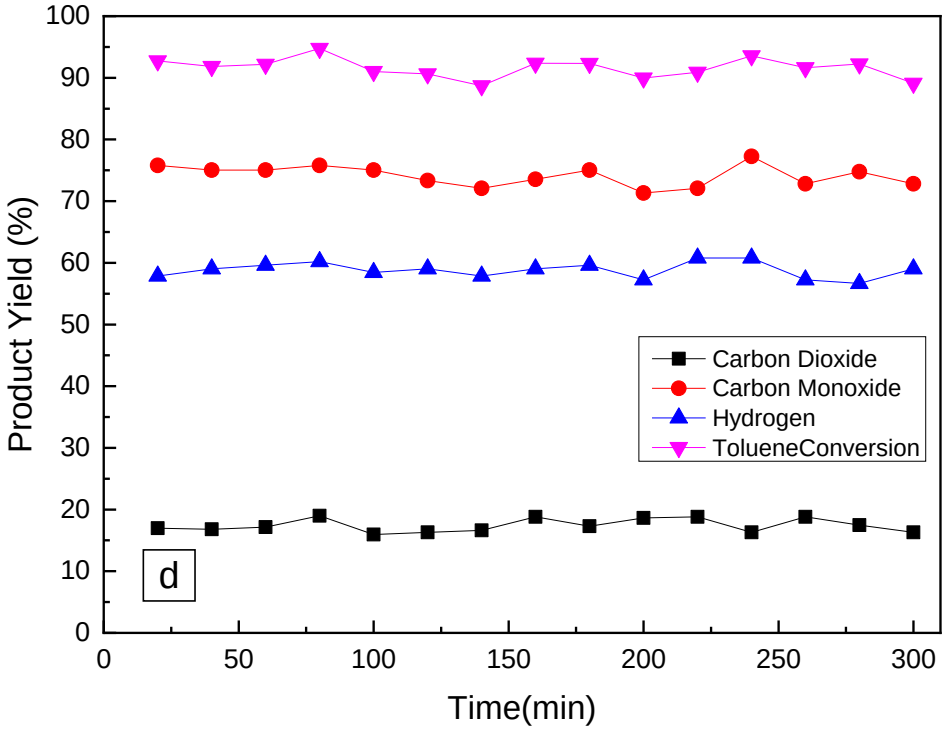
Product Yield (%)
Time(min)
Carbon Dioxide
Carbon Monoxide
Hydrogen
TolueneConversion
d

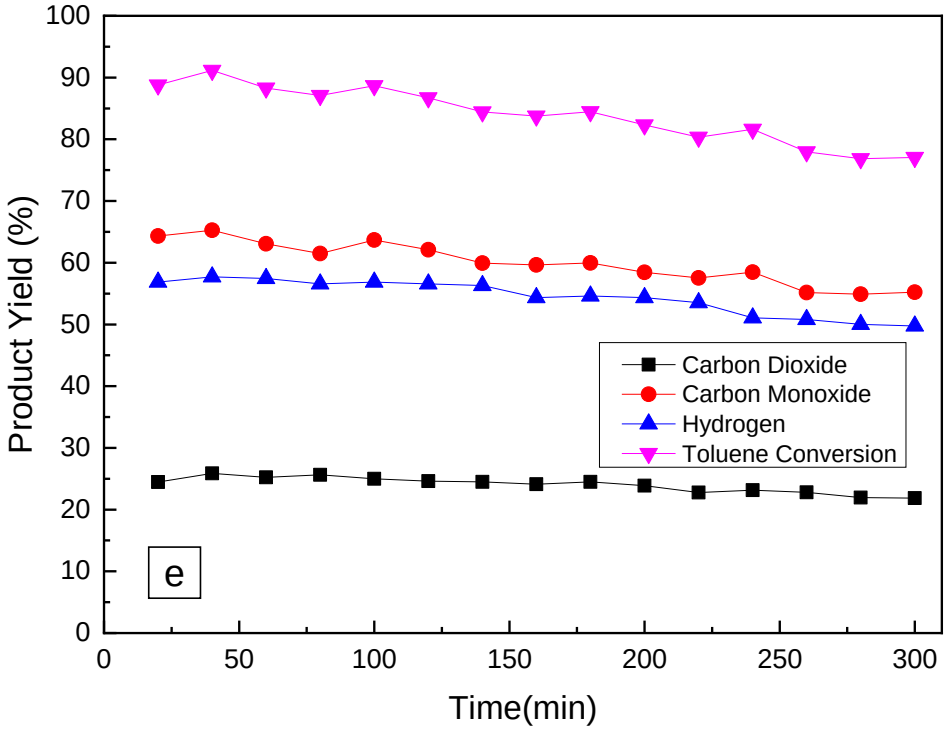
Product Yield (%)
Time(min)
Carbon Dioxide
Carbon Monoxide
Hydrogen
Toluene Conversion
e

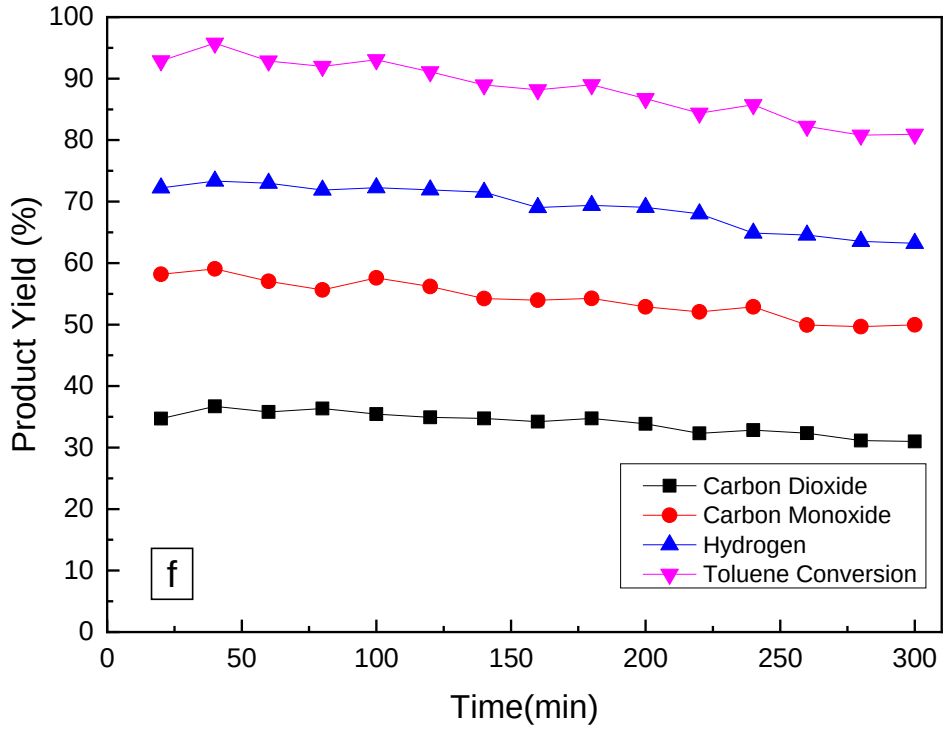

Figure 1. Gas product yield and toluene conversion as a function of time on stream in steam reforming tests carried out in (a) 100% N_2; (b) 30%H_2; (c) 30% CO; (d) 20% CO_2; (e) 3% CH_4 with $S/C_{Toluene}$: 3 (only C in toluene considered); (f) 3% CH_4. All atmospheres balanced in N_2. All experiments performed with a bed of Ni/Al_2O_3 catalyst at 800 °C and GHSV: 91,800 h^{-1}. S/C 3 for all runs except for (e) as indicated.

Figure 2 summarizes the CO and CO_2 yield and toluene conversion into C-containing gases under different gas atmospheres at the first and fifth hours of the catalytic tests and compares these values with equilibrium results. The equilibrium calculation showed that all these atmospheres reach 100% toluene conversion into gas, and CH_4 yield stayed lower than 0.01% in all the equilibrium results. The experimental results showed that toluene conversion to gas under 100% N_2, 30% CO in N_2, 20% CO_2 in N_2 atmosphere stayed over 90% throughout the 5-hour catalytic reforming tests, with very limited decreases in toluene conversion (< 2.5%) due to deactivation observed in these three atmospheres.

100% N_2 atmosphere presented the highest toluene conversion in the whole 5 hours on stream, while 30% CO in N_2, 20% CO_2 in N_2 and 30% H_2 in N_2 atmospheres showed lower toluene conversions in the 5-hour experiments. In particular, in the case of CO_2, it can be inferred that no significant extent of dry reforming was observed as toluene conversion did not exceed that obtained by steam reforming alone. This indicates that relatively high contents (>20%) of gasification gas products (CO, H_2, CO_2) can slightly inhibit the reforming reaction of toluene. The use of CH_4 did not show any obvious inhibition effects, probably due to its low concentration, presenting a similar initial toluene conversion to the 100% N_2 atmosphere. However, catalyst deactivation in the presence of CH_4 and toluene was large even though 3% CH_4 on its own (also included in Figure 2) did not deactivate the catalyst to any observable extent.

The injection of H_2, CO, CO_2 had a significant influence on gas product distribution both in experiments and equilibrium simulations. Equilibrium results confirmed that WGS reaction played an important role in CO/CO_2 selectivity and H_2 production. It can be observed in Figure 2 that CO_2 yield was typically lower than equilibrium calculations except for the CO_2 atmosphere experiment. The presence of CO in the carrier gas favored the WGSR reaction and more CO_2 was produced than in the N_2 atmosphere. On the other hand, feeding CO_2 would largely increase CO yield to ~75%, pushing the reverse WGS reaction. The experimental CH_4 yield in all tests was 0%. The absence of CH_4 under all atmospheres indicated that CH_4 had a total conversion over Ni/Al_2O_3 catalyst even when the deactivation of toluene reforming took place. The CH_4 atmosphere test experienced the largest decrement in toluene conversion during an experiment as it dropped from ~94% to 81% in 5 hours, as well as in CO and CO_2 yields, followed by H_2 atmosphere test. Considering that CH_4 only had a concentration of 3 vol% in carrier gas, it is clear that CH_4 plays a key role in reforming catalyst deactivation among syngas components.

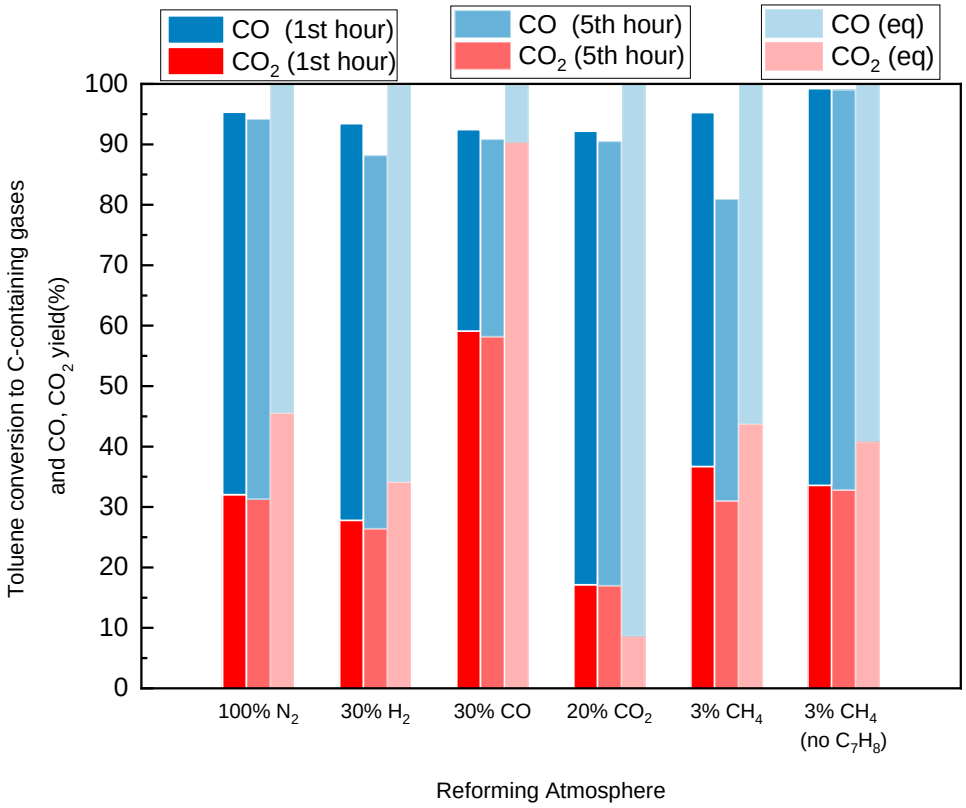

Figure 2. Toluene conversion to C-containing gases and CO/CO_2 yield at different single gas atmosphere (S/C ratio: 3, GHSV:91800 h^{-1}, reforming temperature 800 °C, all the gas atmospheres balanced with N_2).

Table 3 shows the gas product yields including CO, CO_2 and H_2 as mol/mol toluene at the first hour and the fifth hour under different atmospheres and compares with the respective equilibrium values. CO/CO_2 product ratios at different atmospheres also changed towards the equilibrium results. Experimental CO_2 selectivity under most atmospheres was lower than equilibrium predicted, indicating that toluene was reformed to CO first, which then underwent WGS reaction in the excess of steam to produce CO_2. The only exception was the 20% CO_2 atmosphere, which shifted the equilibrium towards a low CO_2 yield and made reverse WGSR predominant.

As a consequence of the WGSR equilibrium, the injection of CO promoted the production of H_2, while CO_2 inhibited H_2 yield. The addition of H_2 also reduced H_2 yield respect to the blank experiment in N_2 atmosphere but it was not enough to change the

predominant direction of the WGSR. 3% CH_4 in N_2 atmosphere test achieved the highest H_2 at 16.5 mol/mol toluene during the first hour due to the additional H_2 production. This run showed the highest decrement (by 16%) at the fifth hour. Meanwhile, H_2 yield of 30% H_2 in N_2 atmosphere test dropped by 7% from 11.2 to 10.4 mol/mol toluene in the 5-hour test. The ratio of CO/CO_2 stayed almost the same after 5-hour test in all the experiments, suggesting that both reforming and WGSR functions were deactivated to the same extent.

Table 3. Product yields for the gaseous products in the different reforming atmosphere (S/C ratio 3 GHSV:91800 h^{-1}, reforming temperature 800 °C, N_2: 100%N_2, H_2: 30% H_2 in N_2, CO: 30% CO in N_2, CO_2: 20% CO_2 in N_2, CH_4: 3% CH_4 in N_2).

Reforming Atmosphere	CO_2 (mol/mol toluene)	CO (mol/mol toluene)	H_2 (mol/mol toluene)	CO_2 selectivity
N_2 (1st hour)	2.2	4.5	13.0	33%
N_2 (5th hour)	2.2	4.4	13.0	33%
N_2 (Equilibrium)	(3.2)	(3.8)	(14.3)	(46%)
H_2 (1st hour)	1.9	4.6	11.2	29%
H_2 (5th hour)	1.8	4.3	10.4	30%
H_2 (Equilibrium)	(2.4)	(4.6)	(13.3)	(34%)
CO (1st hour)	4.1	2.3	14.7	64%
CO (5th hour)	4.0	2.3	14.5	63%

CO (Equilibrium)	(6.3)	(0.7)	(17.3)	(90%)
CO_2 (1st hour)	1.2	5.3	10.7	18%
CO_2 (5th hour)	1.2	5.1	10.6	19%
CO_2 (Equilibrium)	(0.6)	(6.4)	(11.6)	(9%)
CH_4 (1st hour)	3.0	4.8	16.5	38%
CH_4 (5th hour)	2.5	4.1	13.8	38%
CH_4 (Equilibrium)	(3.5)	(4.6)	(18.0)	(43%)

Table 4 shows the carbon conversion from toluene to coke and the fraction of coke on the catalyst under different reforming atmospheres determined by thermogravimetric analysis on the spent catalysts. In the CH_4 only (no C_7H_8) test, 2.35% of CH_4 converted into carbon deposition on the catalyst surface. The conversion to carbon deposits of 100% N_2, 30% CO in N_2 and 20% CO_2 in N_2 atmosphere was very close, which indicates that CO and CO_2 contents have very limited influence on carbon deposition on the catalyst, which remained stable during the tests. The presence of 30% H_2 increased the coke weight, which matched the slight deactivation observed in toluene conversion to C-containing gases and the drop in H_2 product yield. The presence of H_2 might prevent coke reaction with steam, and shift the equilibrium towards more

coke, an observation also made by Cao, Ren [41]. The mixed toluene-CH_4 atmosphere test led to the highest coke content and ratio, much higher than could be expected from the simple addition of effects observed with toluene and CH_4 separately. Catalyst deactivation was calculated from the H_2 yields (Y_{H_2}) initially and after 5 hours on stream (Equation 7).

$$Cat.Deac. = \frac{[Y_{H_2}]_{t=0} - [Y_{H_2}]_{t=5h}}{[Y_{H_2}]_{t=0}} \qquad \text{Eq. 7}$$

A reasonable correlation between amount of coke on the catalyst and catalyst deactivation was observed, where the latter does not take place significantly at coke to catalyst ratios below a threshold of around 20 wt% but increases markedly above that value.

Table 4. Toluene conversion to coke, fraction of coke deposited on the catalyst and catalyst deactivation at different reforming atmospheres (800 °C, S/C:3, GHSV:91800 h^{-1}, 5-hour test. N_2: 100%N_2, H_2: 30% H_2 in N_2, CO: 30% CO in N_2, CO_2: 20% CO_2 in N_2, CH_4: 3% CH_4 in N_2).

Reforming Atmosphere	N_2	H_2	CO	CO_2	CH_4	CH_4 (no C_7H_8)
Coke/C in toluene	0.68%	0.90%	0.61%	0.64%	1.54%	-
Coke/Catalyst (g_C/g_{cat})	0.184	0.245	0.165	0.173	0.417	0.112
Catalyst Deactivation (%)	0	7	1	1	16	0

3.2 Influence of multi-gas atmospheres on toluene steam reforming

While previous tests focused on the influence of single gas in N_2, this section presents the impact of syngas component mixtures on toluene steam reforming. First, a mixture of 30% H_2 and 30% CO balance N_2 is presented, followed by 3% CH_4 and 30% H_2 in N_2 and finally a full syngas mixture consisting of 3% CH_4, 30% H_2, 30% CO and 20% CO_2 in N_2, typical of a gasifier under normal operation conditions [45, 46]

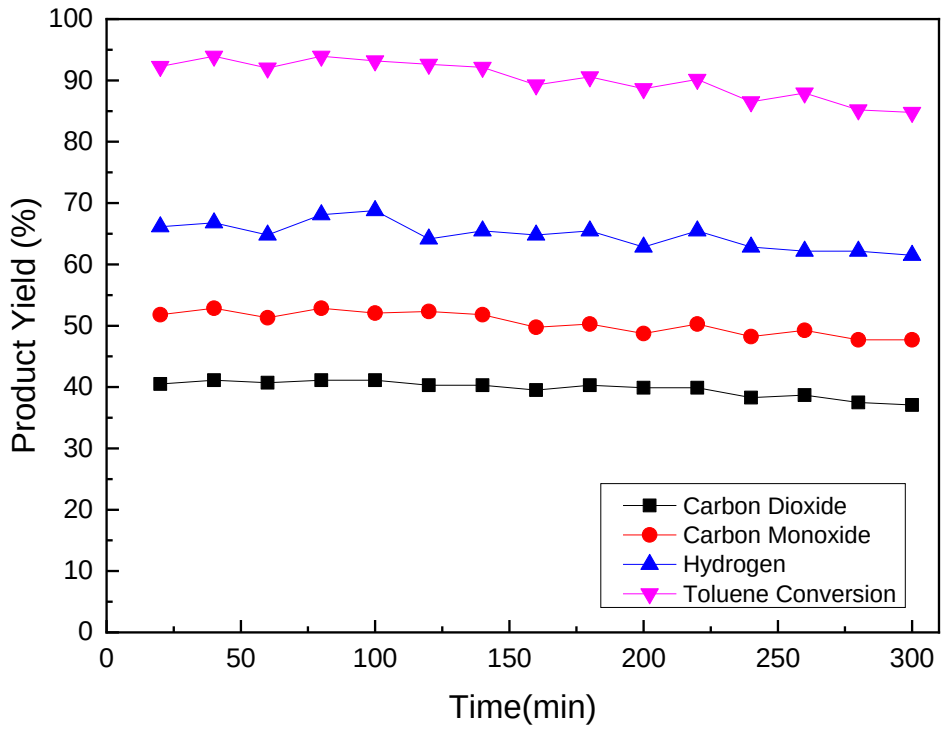

Figure 3. Product yield trend and conversion of toluene steam reforming test in 30% H_2 and 30% CO balanced N_2 atmosphere (5-hour test, Ni/Al_2O_3 catalyst, 800 °C, S/C ratio 3, GHSV: 91800 h^{-1})

Figure shows the gas product yield and conversion of toluene steam reforming 5-hour test in 30% H_2 and 30% CO balanced N_2 atmosphere. Product yields of CO and H_2 were very stable in the first 2.5 hours, and then started to drop slowly until the end of the tests. The overall conversion from toluene to gases also decreased below 90% at

160 mins to reach a final value of 84%, lower than achieved in CO and H_2 separately. **Error! Not a valid bookmark self-reference.** shows CO_2, CO and H_2 yields (in mol/mol toluene) declined by ~10% in the 5-hour test, but selectivity towards CO_2 was not affected by catalyst deactivation as discussed above.

Table 5. Product yields for the gaseous products in 30% H_2 and 30% CO balanced N_2 atmosphere (5-hour test, Ni/Al_2O_3 catalyst, 800 °C, S/C ratio 3, GHSV: 91800 h^{-1})

Atmosphere	CO_2 (mol/mol toluene)	CO (mol/mol toluene)	H_2 (mol/mol toluene)	CO_2 selectivity
H_2 & CO (1st hour)	2.8	3.7	11.9	43%
H_2 & CO (5th hour)	2.6	3.3	11.1	44%
(Equilibrium)	(4.3)	(2.7)	(15.3)	(61%)

Figure summarizes toluene conversion to C-containing gases and CO, CO_2 yields at H_2, CO and mixture gas atmosphere. CO content in the carrier gas had no obvious effect on catalyst deactivation in multi-gas mixture atmosphere. Instead, the decrease in toluene conversion was led by the presence of H_2, as the overall toluene conversion showed similar trends in 30% H_2 in N_2 and 30% CO, 30%H_2 in N_2 atmosphere tests. The equilibrium and experimental results both showed that CO had more significant influence on the selectivity of product CO/CO_2 than H_2. When equal concentrations of CO and H_2 were introduced to the reaction system, the equilibrium shifted to produce more CO_2 when comparing to inert N_2 atmosphere and the experimental results followed this behavior.

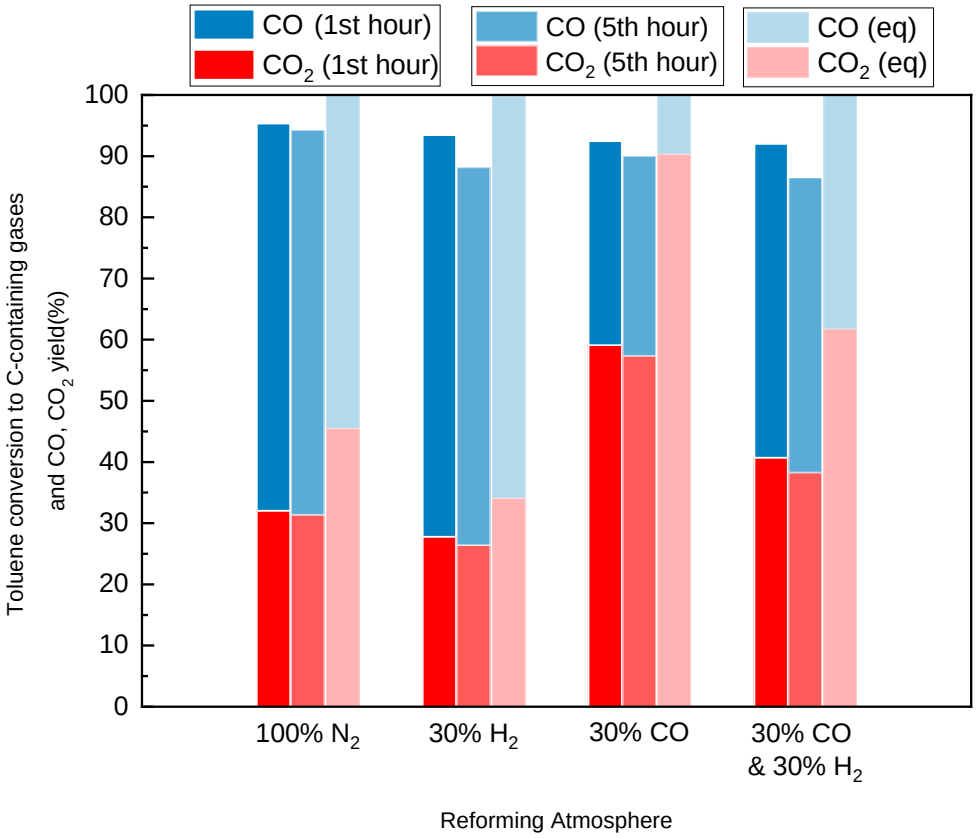

Figure 4. Toluene conversion to C-containing gases and CO, CO_2 yields at H_2, CO and mixture gas atmosphere (S/C ratio 3 GHSV:91800 h^{-1}, reforming temperature 800 °C, all the gas atmosphere balanced with N_2).

The results presented so far showed that CH_4 and H_2 atmosphere had relatively more influence on toluene conversion and carbon deposition than CO and CO_2. Next, the impact of CH_4 and H_2 mixture atmosphere on toluene steam reforming is discussed. To compare with the previous results, the reforming gas atmosphere was designed as 3% CH_4 and 30% H_2 in N_2 with a S/C ratio of 3, including CH_4.

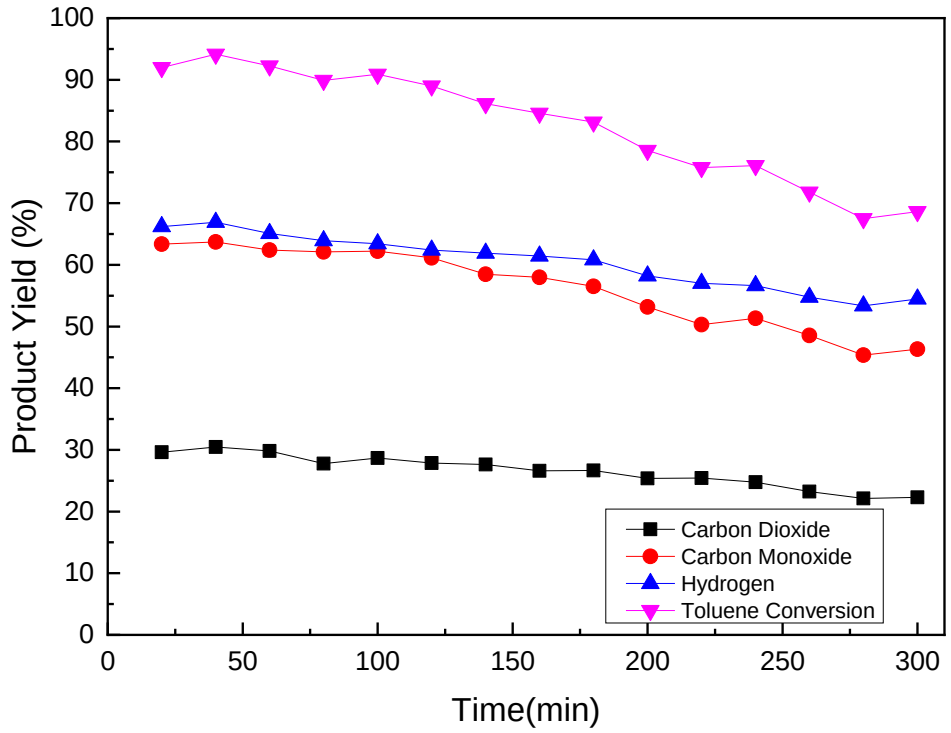

Figure 5. Product yield trend and toluene conversion of steam reforming test in 3% CH_4 and 30% H_2 balanced N_2 atmosphere (5-hour test, Ni/Al_2O_3 catalyst, 800 °C, S/C ratio 3, GHSV: 91800 h^{-1})

Table 6. Product yields for the gaseous products in 3% CH_4 and 30% H_2 balanced N_2 atmosphere (5-hour test, Ni/Al_2O_3 catalyst, 800 °C, S/C ratio 3, GHSV: 91800 h^{-1})

Atmosphere	CO_2 (mol/mol toluene)	CO (mol/mol toluene)	H_2 (mol/mol toluene)	CO_2 selectivity
H_2 & CH_4(1st hour)	2.5	5.2	15.1	32%
H_2 & CH_4 (5th hour)	1.8	3.8	10.9	32%
(Equilibrium)	(2.8)	(5.3)	(17.1)	35%

Error! Reference source not found. shows the gas product yield and toluene conversion into gases in 3% CH_4 and 30% H_2 balanced N_2 atmosphere. The toluene conversion and CO, CO_2 and H_2 yield started to decrease after 100 min and declined steadily until the end of the test. The conversion of toluene dropped markedly from 93% to 69%, while the CO, H_2 and CO_2 yields decreased from 64%, 66% and 29% to 46%, 54% and 22%, respectively. The CH_4 and H_2 combined atmosphere showed a more significant decrement in gas production from toluene steam reforming respect to the two gases separately.

Table 6 presents CO, CO_2 and H_2 production during the first and fifth hours on stream and compares them with equilibrium results. H_2 production yield decreased by 28%, from 15.1 to 10.9 mol/mol toluene, which was larger than expected based on the behavior of the individual gases. According to Table 3, the decreases in H_2 yield in 30% H_2 in N_2 atmosphere and 3% CH_4 in N_2 atmosphere were 7% and 16%, respectively. The presence of CH_4 and H_2 can deactivate the Ni/Al_2O_3 catalyst much more rapidly than CH_4 or H_2 single gas atmosphere (Figure 6).

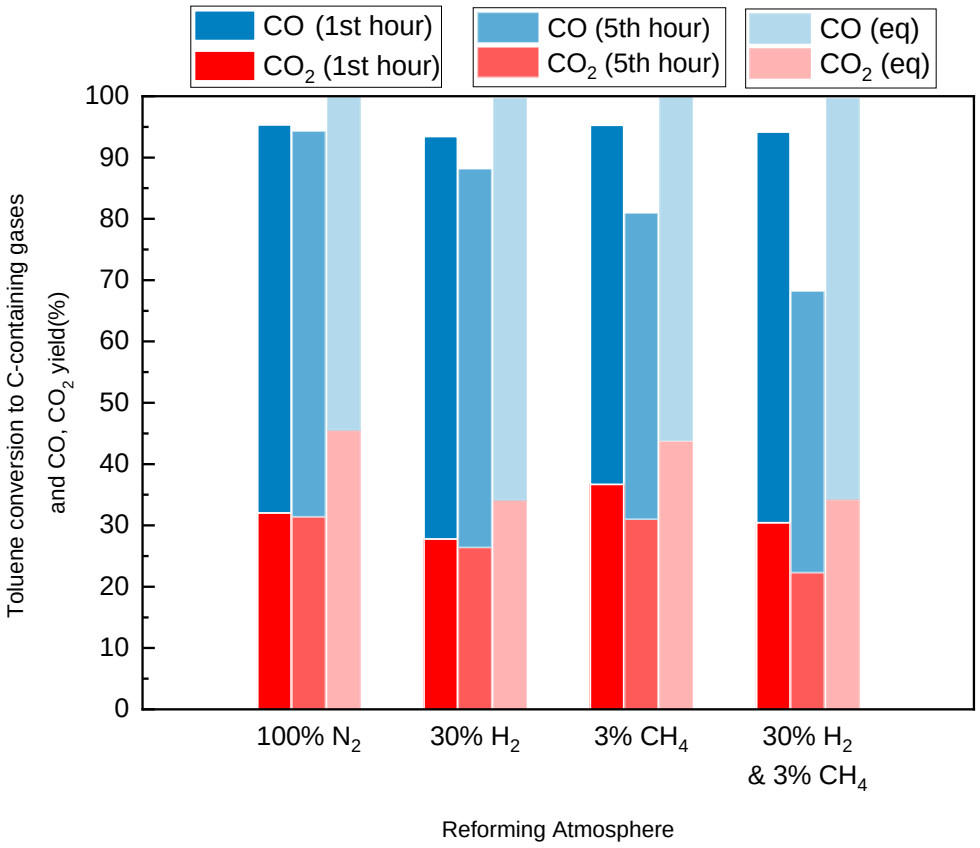

Figure 6. Toluene conversion to C-containing gases and CO, CO_2 yield at H_2, CH_4 and mixture gas atmosphere (S/C ratio 3, GHSV:91800 h^{-1}, reforming temperature 800 °C, all the gas atmosphere balanced with N_2).

Finally, a full gas mixture composed of 3% CH_4, 30% H_2, 30% CO and 20% CO_2 in N_2 was chosen to simulate a typical biomass gasification gas product. Figure 7.7 shows the gas product yield and toluene conversion in this simulated gasification atmosphere. Toluene conversion and gas yields started to decline slightly in the second hour, and

then decreased significantly in the rest 3 hours. The conversion of toluene dropped from 92% to 66% in the 5-hour test. The trend was similar to the test in 3% CH_4 and 30% H_2 atmosphere, which indicated that CO and CO_2 had limited influence on the deactivation of the catalyst.

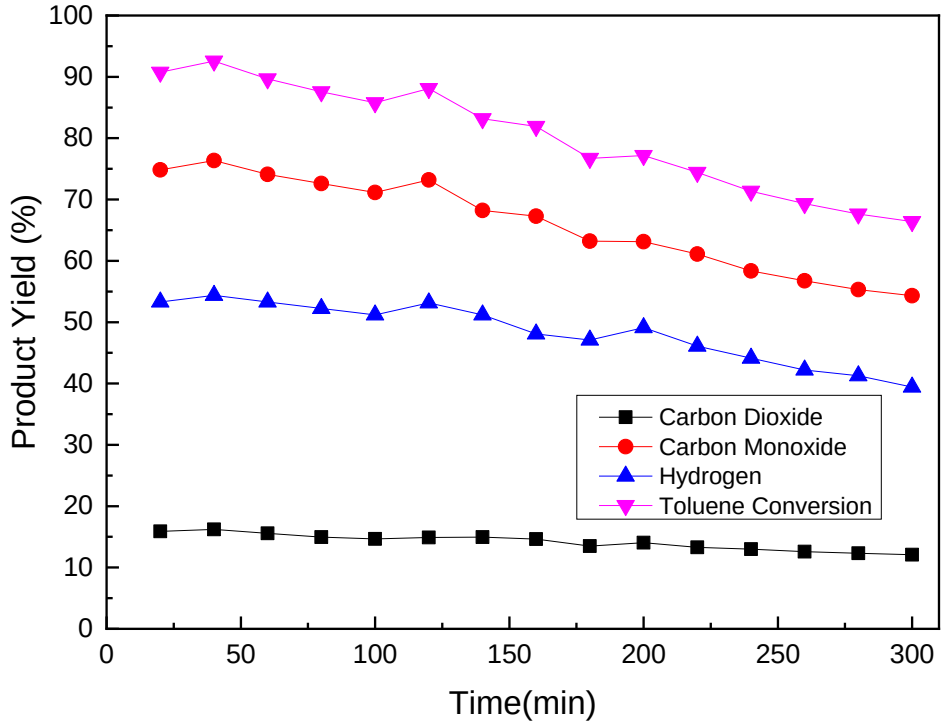

Figure 7. Product yield trend and conversion of toluene steam reforming test in 3% CH_4, 30% H_2, 30% CO and 20% CO_2 balanced N_2 atmosphere (Ni/Al_2O_3 catalyst, 800 °C, S/C ratio 3, GHSV: 91800 h^{-1})

Table 7 and Figure summarize the toluene conversion to C-containing gases and CO, CO_2 yields in all the CH_4–containing atmospheres and compares with the experiments in the N_2 atmosphere. Although the concentration of CH_4 in carrier gas was fixed at 3 vol%, which was much lower than the concentration of CO, CO_2 and H_2, CH_4 was the main reason for catalyst deactivation. The injected H_2 could largely decrease the toluene conversion to gases with the presence of a small amount of CH_4.

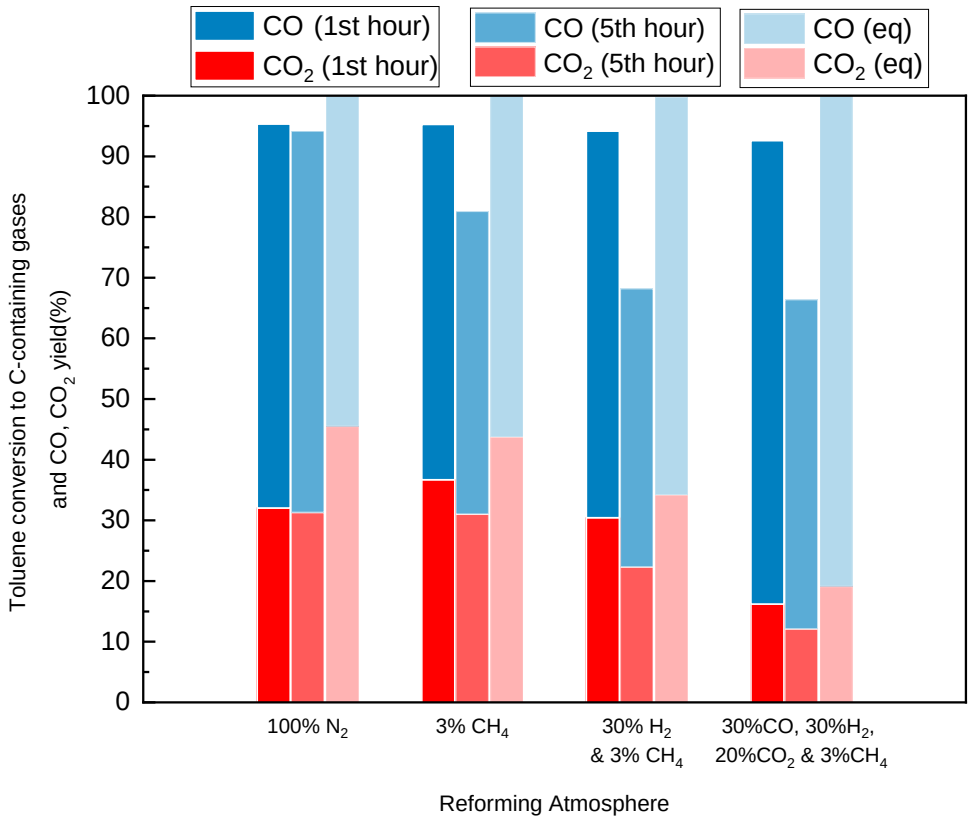

Figure 8. Toluene conversion to C-containing gases and CO, CO_2 yield at CO, CO_2, H_2, CH_4 and mixture gas atmosphere (S/C ratio 3 GHSV:91800 h^{-1}, reforming temperature 800 °C, all the gas atmosphere balanced with N_2).

Table 7. Product yields for the gaseous products in 3% CH_4, 30% H_2, 30% CO and 20%CO_2 balanced N_2 atmosphere (5-hour test, Ni/Al_2O_3 catalyst, 800 °C, S/C ratio 3, GHSV: 91800 h^{-1})

Atmosphere	CO_2 (mol/mol toluene)	CO (mol/mol toluene)	H_2 (mol/mol toluene)	CO_2 selectivity
All gas (1st hour)	1.3	6.2	12.0	17%
All gas (5th hour)	1.0	4.8	8.7	17%
(Equilibrium)	(1.6)	(6.5)	(15.5)	(20%)

As shown in Table 8, coke formation was favored by the complex gas atmosphere, in particular when a mixture containing H_2 and CH_4 was applied. The amount of coke over the Ni/Al_2O_3 catalyst when 3% CH_4 and 30% H_2 balanced N_2 were employed as well as with the full syngas atmosphere was much larger than observed in any single-gas composition. On the other hand, under 30% H_2 and 30% CO balanced N_2, the coke formation was nearly identical to that observed under H_2 only, reinforcing the role of CH_4 as a trigger in toluene conversion to coke. CO and CO_2 were observed to have no influence on coke formation, with the difference between the full syngas with the CH_4 and H_2 atmosphere being around 1%. The large coke formation in the atmospheres containing H_2 and CH_4 markedly deactivated the Ni/Al_2O_3 catalyst in the first 5 hours on stream (Table 8).

Table 8. Toluene conversion to coke, fraction of coke deposited on the catalyst and catalyst deactivation at different reforming atmosphere (800 °C, S/C:3, GHSV:91800 h^{-1}, 5-hour test. CO & H_2 in N_2: 30% H_2 and 30% CO balanced N_2, CH_4 & H_2 in N_2: 3% CH_4 and 30% H_2 balanced N_2, All gas mixtures: 3% CH_4, 30% H_2, 30% CO and 20%CO_2 balanced N_2).

Reforming Atmosphere	CO & H_2 in N_2	CH_4 & H_2 in N_2	All gas mixture
Coke/C in toluene	0.88%	2.53%	2.49%
Coke/Catalyst (g_C/g_{cat})	0.238	0.684	0.676
Catalyst Deactivation (%)	7	28	27

4. Conclusions

This analysis of the effect of reforming gas atmosphere on the catalytic steam reforming of tar using a conventional Ni/Al_2O_3 catalyst shows how the conversion of toluene is markedly affected by the presence of some syngas components, even at constant steam to carbon ratio and despite full equilibrium conversion being expected in all cases. These effects related to inhibition, observed as a drop in the initial toluene conversion respect to that in a N_2 atmosphere, and catalyst deactivation, evidenced by a decrease in toluene conversion with time on stream. While only slight inhibition and no significant deactivation can be concluded from the presence of CO and CO_2, H_2 and CH_4 have been found to have a significant adverse effect on the reforming of toluene in terms of catalyst deactivation. H_2 also showed a mild inhibitory effect, which interestingly was not observed when CH_4 only was used, albeit this may be due to the low concentration employed.

Strong interactions between gas components were observed, with the joint presence of toluene and CH_4 leading to greater carbon formation, which could not have been predicted from separate steam reforming experiments with each of them. Moreover, the simultaneous exposure of the toluene reforming system to H_2 and CH_4 causes a marked deactivation of the catalyst by carbon deposition with each gas potentiating the negative effects of the other. In view of these results, the importance of testing tar reforming catalysts with full syngas compositions to avoid misleading, typically too optimistic, outcomes cannot be overemphasized.

5. References

1. Tan, R.S., et al., *Catalytic steam reforming of tar for enhancing hydrogen production from biomass gasification: a review.* Frontiers in Energy, 2020: p. 1-25.
2. Xiao, Y., et al., *Biomass steam gasification for hydrogen-rich gas production in a decoupled dual loop gasification system.* Fuel Processing Technology, 2017. **165**: p. 54-61.
3. Ruiz, J.A., et al., *Biomass gasification for electricity generation: Review of current technology barriers.* Renewable and Sustainable Energy Reviews, 2013. **18**: p. 174-183.
4. Deonarine, B., et al., *Ultra-microporous membrane separation using toluene to simulate tar-containing gases.* Fuel Processing Technology, 2017. **161**: p. 259-264.
5. Ashok, J., et al., *Recent progress in the development of catalysts for steam reforming of biomass tar model reaction.* Fuel Processing Technology, 2020. **199**: p. 106252.
6. Dagle, V.L., et al., *Steam reforming of hydrocarbons from biomass-derived syngas over MgAl2O4-supported transition metals and bimetallic IrNi catalysts.* Applied Catalysis B: Environmental, 2016. **184**: p. 142-152.
7. Nunnally, T., et al., *Gliding arc plasma oxidative steam reforming of a simulated syngas containing naphthalene and toluene.* International Journal of Hydrogen Energy, 2014. **39**(23): p. 11976-11989.
8. Long, X., et al., *Emission of species of environmental and process concern during simulated oxy-fuel gasification.* Fuel, 2021. **299**: p. 120886.
9. Fidalgo, B., D. Van Niekerk, and M. Millan, *The effect of syngas on tar quality and quantity in pyrolysis of a typical South African inertinite-rich coal.* Fuel, 2014. **134**: p. 90-96.

10. Berrueco, C., et al., *Evolution of tar in coal pyrolysis in conditions relevant to moving bed gasification.* Energy & Fuels, 2014. **28**(8): p. 4870-4876.
11. Rabou, L.P., et al., *Tar in biomass producer gas, the Energy research Centre of the Netherlands (ECN) experience: an enduring challenge.* Energy & fuels, 2009. **23**(12): p. 6189-6198.
12. Gao, N., et al., *Modified nickel-based catalysts for improved steam reforming of biomass tar: A critical review.* Renewable and Sustainable Energy Reviews, 2021. **145**: p. 111023.
13. Guan, G., et al., *Catalytic steam reforming of biomass tar: Prospects and challenges.* Renewable and sustainable energy reviews, 2016. **58**: p. 450-461.
14. Li, C. and K. Suzuki, *Tar property, analysis, reforming mechanism and model for biomass gasification—An overview.* Renewable and Sustainable Energy Reviews, 2009. **13**(3): p. 594-604.
15. Yoon, S.J., Y.K. Kim, and J.G. Lee, *Catalytic oxidation of biomass tar over platinum and ruthenium catalysts.* Industrial & engineering chemistry research, 2011. **50**(4): p. 2445-2451.
16. Li, D., et al., *Production of renewable hydrogen by steam reforming of tar from biomass pyrolysis over supported Co catalysts.* International Journal of hydrogen energy, 2013. **38**(9): p. 3572-3581.
17. Chianese, S., et al., *Hydrogen from the high temperature water gas shift reaction with an industrial Fe/Cr catalyst using biomass gasification tar rich synthesis gas.* Fuel Processing Technology, 2015. **132**: p. 39-48.
18. Zuber, C., et al., *Investigation of sulfidation and regeneration of a ZnO-adsorbent used in a biomass tar removal process based on catalytic steam reforming.* Fuel, 2015. **153**: p. 143-153.
19. Li, W.-P., et al., *Interaction of Ce-char catalyst and partial oxidation on changes in biomass syngas composition.* Journal of Renewable and Sustainable Energy, 2019. **11**(2): p. 023101.
20. Shen, Y. and K. Yoshikawa, *Recent progresses in catalytic tar elimination during biomass gasification or pyrolysis—A review.* Renewable and Sustainable Energy Reviews, 2013. **21**: p. 371-392.
21. Miyazawa, T., et al., *Catalytic properties of Rh/CeO2/SiO2 for synthesis gas production from biomass by catalytic partial oxidation of tar.* Science and technology of Advanced Materials, 2005. **6**(6): p. 604-614.
22. Heo, D.H., et al., *The effect of addition of Ca, K and Mn over Ni-based catalyst on steam reforming of toluene as model tar compound.* Catalysis Today, 2016. **265**: p. 95-102.
23. Park, S.Y., et al., *Deactivation characteristics of Ni and Ru catalysts in tar steam reforming.* Renewable Energy, 2017. **105**: p. 76-83.
24. Baker, E.G. and L.K. Mudge, *Mechanisms of catalytic biomass gasification.* Journal of analytical and applied pyrolysis, 1984. **6**(3): p. 285-297.
25. Uchida, H. and M.R. Harada, *Hydrogen Energy Engineering Applications and Products*, in *Science and Engineering of Hydrogen-Based Energy Technologies*. 2019, Elsevier. p. 201-220.

26. Sehested, J., *Four challenges for nickel steam-reforming catalysts.* Catalysis Today, 2006. **111**(1-2): p. 103-110.
27. Dabai, F., et al., *Tar formation and destruction in a fixed-bed reactor simulating downdraft gasification: equipment development and characterization of tar-cracking products.* Energy & fuels, 2010. **24**(8): p. 4560-4570.
28. Dabai, F., et al., *Tar formation and destruction in a fixed bed reactor simulating downdraft gasification: effect of reaction conditions on tar cracking products.* Energy & fuels, 2014. **28**(3): p. 1970-1982.
29. Rios, M.L.V., et al., *Reduction of tar generated during biomass gasification: A review.* Biomass and bioenergy, 2018. **108**: p. 345-370.
30. Mermelstein, J., M. Millan, and N. Brandon, *The impact of carbon formation on Ni–YSZ anodes from biomass gasification model tars operating in dry conditions.* Chemical Engineering Science, 2009. **64**(3): p. 492-500.
31. Tian, Y., et al., *The influence of shell thickness on coke resistance of core-shell catalyst in CO2 catalytic reforming of biomass tar.* International Journal of Hydrogen Energy, 2022. **47**(29): p. 13838-13849.
32. Geis, M., et al., *Coupling SOFCs to biomass gasification-The influence of phenol on cell degradation in simulated bio-syngas. Part I: Electrochemical analysis.* International journal of hydrogen energy, 2018. **43**(45): p. 20417-20427.
33. Taira, K., K. Nakao, and K. Suzuki, *Steam reforming of 1-methylnaphthalene over pure CeO2 under model coke oven gas conditions containing high H2S concentrations.* International Journal of Hydrogen Energy, 2020. **45**(58): p. 33248-33259.
34. Long, X., et al., *Towards integrated gasification and fuel cell operation with carbon capture: Impact of fuel gas on anode materials.* Fuel, 2022. **318**: p. 123561.
35. Lorente, E., M. Millan, and N. Brandon, *Use of gasification syngas in SOFC: Impact of real tar on anode materials.* International Journal of Hydrogen Energy, 2012. **37**(8): p. 7271-7278.
36. Lorente, E., et al., *Effect of tar fractions from coal gasification on nickel–yttria stabilized zirconia and nickel–gadolinium doped ceria solid oxide fuel cell anode materials.* Journal of Power Sources, 2013. **242**: p. 824-831.
37. Boldrin, P., M. Millan-Agorio, and N.P. Brandon, *Effect of sulfur-and tar-contaminated syngas on solid oxide fuel cell anode materials.* Energy & Fuels, 2015. **29**(1): p. 442-446.
38. Huang, C.W., et al., *Optimal Fe/Ni/Ca‐Al catalyst for tar model steam reforming by using the Taguchi method.* International Journal of Energy Research, 2022. **46**(6): p. 7799-7815.
39. Gao, X., et al., *Steam reforming of toluene as model compound of biomass tar over Ni–Co/La2O3 nano-catalysts: Synergy of Ni and Co.* International Journal of Hydrogen Energy, 2021. **46**(60): p. 30926-30936.
40. Yahya, H.S.M., T. Abbas, and N.A.S. Amin, *Optimization of hydrogen production*

via toluene steam reforming over Ni–Co supported modified-activated carbon using ANN coupled GA and RSM. International Journal of Hydrogen Energy, 2021. **46**(48): p. 24632-24651.

41. Cao, J.-P., et al., *Effect of atmosphere on carbon deposition of Ni/Al2O3 and Ni-loaded on lignite char during reforming of toluene as a biomass tar model compound.* Fuel, 2018. **217**: p. 515-521.
42. Mermelstein, J., M. Millan, and N. Brandon, *The interaction of biomass gasification syngas components with tar in a solid oxide fuel cell and operational conditions to mitigate carbon deposition on nickel-gadolinium doped ceria anodes.* Journal of power sources, 2011. **196**(11): p. 5027-5034.
43. Bizkarra, K., et al., *Nickel based monometallic and bimetallic catalysts for synthetic and real bio-oil steam reforming.* International Journal of Hydrogen Energy, 2018. **43**(26): p. 11706-11718.
44. Zhu, H.L., L. Pastor-Pérez, and M. Millan, *Catalytic Steam Reforming of Toluene: Understanding the Influence of the Main Reaction Parameters over a Reference Catalyst.* Energies, 2020. **13**(4): p. 813.
45. Abu El-Rub, Z., E.A. Bramer, and G. Brem, *Review of catalysts for tar elimination in biomass gasification processes.* Industrial & engineering chemistry research, 2004. **43**(22): p. 6911-6919.
46. Sutton, D., B. Kelleher, and J.R.H. Ross, *Review of literature on catalysts for biomass gasification.* Fuel Processing Technology, 2001. **73**(3): p. 155-173.
47. Puron, H., et al., *Hydroprocessing of Maya vacuum residue using a NiMo catalyst supported on Cr-doped alumina.* Fuel, 2020. **263**: p. 116717.

How syngas composition affects catalytic steam reforming of tars: an analysis using toluene as model compound

Authors

HuaLun Zhu, Ziyin Chen, Laura Pastor-Perez, Xiangyi Long, Marcos Millan*

Department of Chemical Engineering, Imperial College, London SW7 2AZ

*Corresponding author

Marcos Millan

Mailing address: Department of Chemical Engineering, Imperial College

London SW7 2AZ, UK

Tel.: +44 (0)20 7594 1633

E-mail: marcos.millan@imperial.ac.uk

Abstract

Tar removal by catalytic steam reforming has an important role to play in gasification hot gas treatment. Despite the importance of understanding the influence gas atmosphere has on this reaction, the effect of a full syngas mixture has not been comprehensively investigated. This study aims to bridge that gap by analyzing the effect of each component as well as their combinations on steam reforming of toluene as biomass gasification tar model over a Ni/Al_2O_3 catalyst. It has been found that H_2, CO and CO_2 have minor inhibitory effects, slightly decreasing the initial toluene conversion. On the other hand, while CO and CO_2 do not lead to catalyst deactivation, H_2 and CH_4 deactivate Ni/Al_2O_3 by promoting coke deposition. Only 3 vol.% of CH_4 can significantly increase deactivation, despite being insignificant with toluene or CH_4 separately. The joint presence of CH_4 and H_2 causes further drops in conversion with time on stream.

Keywords

syngas, tar steam reforming, nickel catalyst, carbon deposition, catalyst deactivation.

1. Introduction

Biomass gasification can act as a source of renewable heat and power as well as chemicals. At the core of gasification-based processes is synthesis gas (syngas), a valuable mixture that can provide remarkable versatility in terms of products, including hydrogen, synthetic natural gas, liquid fuels through Fischer-Tropsch synthesis, methanol and others [1-3]. However, one of the major hindrances to technology development is the formation of tar, which consists of a complex mixture of high molecular weight organic material. Tar formed in the biomass gasification process will be present as an impurity in the syngas at high temperatures and could condense or react downstream of the gasifier, affecting power generation, as well as gas separation membranes [4] and catalysts [5], for example decreasing the conversion of methane by steam reforming [6, 7].

Methods studied for tar abatement include optimizing gasifier design and operating parameters to limit their formation [8-10], physical removal (eg. scrubbers, filters) [11], and thermal, plasma or catalytic conversion downstream from the gasifier [12]. Among these technologies, tar catalytic reforming is particularly appealing as the process can take place without cooling the syngas and convert tar into valuable gases, especially H_2, substantially reducing its concentration [1, 13].

Catalytic tar reforming can be applied in either in-situ or ex-situ gasification systems, to remove tar content as part of the treatment to the hot syngas downstream from the gasifier [13, 14]. Systems have been developed that can crack tars while enhancing H_2 production by CO_2 sorption simultaneous to the reforming reaction [15]. Various types of catalyst have been studied, including olivine, dolomite, zeolite, char, metal-based (eg. Fe, Co, Ni, Zn, Pt, Ce, Ru, Rh), and alkali-based (K and Ca) [16-20]. Ni-based catalysts are the most studied for tar removal, likely due to their widespread application in industrial steam reforming of natural gas and other hydrocarbons, representing a lower cost option to noble metals while still providing high activity [14,

21].

The major challenge for Ni-based catalysts is deactivation caused by carbon deposition and sintering [19, 22, 23], which shortens their life cycle [24]. Carbon deposition on the catalyst may encapsulate the active metal particles and prevent the contact between reactants and the metal active sites [12]. Carbon can quickly diffuse into or form on the Ni catalyst surface, cover or block the pores of the active nickel and decrease Ni catalytic activity [25, 26]. Carbonaceous deposits (coke) are found in three forms: polymer, whisker and pyrolytic [27]. Pyrolytic carbon is formed due to the cracking of hydrocarbons which encapsulate the nickel active site [25], and has a significant influence on catalyst deactivation. High temperature (>600 °C) and the acidity of the catalyst promote its formation [12].

The main syngas components are H_2, CO, CO_2 and CH_4. Tar concentrations in the syngas depend on the gasifier type and operating conditions. In moving beds, they can reach relatively high values (~100 g Nm^{-3}) in updraft gasifiers. Downdraft configurations, as they allow cracking to take place in the hot char bed [28, 29], can reach values as low as ~ 1 g Nm^{-3}. Fluidised beds present intermediate values, typically around 15 g Nm^{-3} [30].

Not only is tar quantity but also its composition affected by the gasifier operating conditions. An attempt to rationalize the broad range of chemical species has involved grouping them into primary, secondary and tertiary tars [31, 32]. Primary tars are formed directly from solid biomass and composed of highly oxygenated compounds, like levoglucosan derived from cellulose and methoxyphenols originated in lignin. Secondary (phenols and light olefins) and tertiary tars, consisting largely of monoaromatic and polyaromatic hydrocarbons, are the products of subsequent reactions in the gas phase. Tar composition changes from primary to tertiary as it is exposed to higher temperatures for longer times, losing oxygen functionalities and showing predominance of mono- and polyaromatic hydrocarbons in the process. Thus, updraft gasification tars are richer in primary species while downdraft gasification

tends to produce tertiary tars [33]. An example of this trend is the reported composition of wood gasification tars in a fluidized bed gasifier operating at 940 °C and 5 bar, in which 65 wt.% of the tar was benzene and its derivatives, mostly toluene, styrene and indene, 33 wt.% polyaromatic hydrocarbons and only below 1 wt.% was in molecules containing heteroatoms, mostly as dibenzofurane with a small amount of phenol [34]. This tar distribution is also consistent with the tendency to dealkylation reactions, for example of xylenes, reported in the literature [35] and shows that even relatively short times at such high temperature suffice to remove nearly all heteroatoms in the tar as the freeboard residence time was only 4 s. Reports from fluidized bed gasifiers operating at lower temperatures (up to 850 °C) do not deviate substantially from this trend, reporting concentrations of benzene, toluene and naphthalene as the main components and only 0.7 wt.% of phenol [36].

Work in the literature tends to make use of model compounds to compare the performance of different catalysts and assess their deactivation in catalytic reforming tests. These have included benzene [37], toluene [38], polyaromatic hydrocarbons [39], among others including phenol [40], although it is more typically used as a model compound for the catalytic steam reforming of pyrolysis oils [41, 42]. The use of monoaromatics as model compounds, in particular toluene, has been observed to represent a worst-case scenario for carbon formation on Ni materials in comparison with polyaromatics [37] and real tar samples [43, 44]. This was corroborated by a study showing that lighter tar fractions [45] led to greater carbon formation than heavier ones.

Toluene steam reforming is described by Reaction 1.

$$C_7H_8 + 7H_2O \leftrightarrow 7\,CO + 11\,H_2 \qquad \text{Reaction 1}$$

The water gas shift (WGS) reaction (Reaction 2) will affect the syngas composition as well as steam methane reforming (Reaction 3), which can happen simultaneously if methane is present. Methane addition has also been reported as a way to increase

117 syngas quality after reforming [46] as Reaction 3 enhances H_2 production.

118 $$CO + H_2O \leftrightarrow CO_2 + H_2$$ Reaction 2

119 $$CH_4 + H_2O \leftrightarrow CO + 3H_2$$ Reaction 3

120 Other relevant reactions in the presence of CO_2 or CO are toluene dry reforming
121 (Reaction 4) and the reverse Boudouard reaction (Reaction 5).

122 $$C_7H_8 + 7\,CO_2 \leftrightarrow 14\,CO + 4\,H_2$$ Reaction 4

123 $$2\,CO \leftrightarrow C + CO_2$$ Reaction 5

124 Most past and current research on catalytic steam reforming of tars has the aim of
125 developing new catalyst formulations that can suffer less from deactivation than
126 standard industrial catalysts [13, 45, 46, 47]. Despite the complex reaction system
127 given by Reactions 1-5, novel catalysts are more often than not tested in atmospheres
128 only containing tar (usually a model compound) or other contaminants, such as H_2S
129 [39, 48] and NH_3, and steam [49-51], in some cases with hydrogen added [52].
130 However, catalyst performance, in particular its activity and tendency to deactivation
131 by carbon deposition, can be very different when all components of the syngas mixture
132 are considered. A previous study has hinted at complex interactions between syngas
133 components, affecting formation of carbon on Ni materials used in solid oxide fuel cell
134 anodes [53], but the influence of syngas composition tends to be overlooked even in
135 comprehensive reviews on this topic [12, 13, 54].
136 Few research studies have focused on the effect of syngas composition on catalytic
137 tar reforming process, with most of them focusing on varying steam and H_2
138 concentrations [37, 52]. It is well-known that steam addition increases conversion and
139 decreases carbon deposition on the catalyst. An excess of steam over the reforming
140 stoichiometric amount is necessary to avoid widespread carbon formation and catalyst
141 deactivation. A steam to carbon (S/C) ratio of 1 has been shown to lead to the
142 thermodynamic prediction of no carbon on the catalyst [55], but in practice this

condition resulted in heavy coke formation. S/C ratios of 2 and above have been found suitable to operate the process without significant deactivation in steam/N_2 atmospheres [52, 56]. It has however been reported that S/C ratios of up to 20 keep producing an increase in toluene steam reforming [24].

H_2 has been found to produce a negative impact on the reforming reactions, a feature that may be expected as it is a product from this reversible reaction, with a decrease in tar conversion as well as greater carbon formation as its concentration increases [52]. However, this effect may also be dependent on temperature, as enhancement of benzene and toluene reforming with H_2 partial pressure has been observed in the low temperature treatment of these model compounds between 350-400 °C and S/C ratios from 0 to 1.25 [57].

The effect of CO_2 on tar reforming has been mostly studied as part of dry reforming research both in the presence [58] and absence [-59] of steam. Boudouard reaction was shown effective to lower carbon deposition even at the relatively low temperature of 650 °C and employing a CO_2 to carbon ratio just below one [60]. However, an increase in temperature to 800 °C and in CO_2 to carbon ratio to 4.5 nearly completely removed formation of deposits on various Ni/Palygorskites. In the presence of steam the extent of the Boudouard reaction seems to be small [61]. At lower temperatures, the Sabatier reaction to produce methane competes for the active sites, as observed on a Ni-CeO_2/Al_2O_3 catalyst, and therefore some inhibition of the tar model compound reactions has been observed [57].

A more complex syngas mixture containing CO, H_2, CO_2 and CH_4 was used in a methane steam reforming studies [62, 63] including a comparison at fixed syngas concentrations between Ni and Rh catalysts in the presence of phenanthrene [63]. Similarly, Claude et al. [64] analyzed the behavior of four Ni/γ-Al_2O_3 catalysts with Ni loadings varying between 10 and 50 wt.% in a syngas atmosphere containing relatively fixed amounts of H_2, CO, CO_2 and H_2O at 650 °C. Different scenarios involved injection of toluene only, CH_4 only, and both toluene and CH_4 with a focus to analyze Ni

171 reduction by toluene under these conditions.
172 Syngas composition was varied in a study related to air gasification [58], which
173 therefore employed relatively diluted syngas, in which it was found that CO inhibited
174 toluene conversion. It was also established that the reaction takes place mostly
175 through steam rather than dry reforming when both reforming agents are present.
176 Fe-containing silicates including ores and olivine as reference material were
177 investigated as benzene reforming catalysts in a full simulated syngas atmosphere
178 [65]. Variations in the syngas composition affected Fe redox chemistry, with increasing
179 concentrations of reducing agents (H_2 and CO) enhancing benzene conversions at
180 800 °C while more oxidative atmospheres had the opposite effect.
181 A recent study [61] focused on the simultaneous reforming of toluene, naphthalene,
182 methane and higher hydrocarbons at S/C ratio of 2 and in a full syngas atmosphere in
183 the context of sorbent enhanced gasification. This is a particular syngas composition,
184 markedly different from a straight gasifier output, as it contains relatively small
185 amounts of CO and CO_2 (9% and 6%, respectively were used in this study), but high
186 H_2 (70%) and CH_4 (13%) contents. It was concluded that there was a competition
187 between hydrocarbons for the Ni active sites that affected the conversion of tars in the
188 presence of non-condensable species and vice-versa.
189 The objective of this work is to gain an understanding of the influence of reforming gas
190 atmosphere on catalytic steam reforming by performing a systematic study where the
191 effects of major (H_2, CO) and minor (CO_2, CH_4) syngas components and their mixtures
192 of increasing complexity are analyzed. These effects have been investigated using
193 toluene as model compound over a standard Ni/Al_2O_3 catalyst. Toluene is deemed a
194 very suitable model for high-temperature gasification tars and its propensity to carbon
195 formation can be seen as a significant challenge to gasification followed by reforming
196 systems, as discussed above.

2. Experimental

2.1 Catalyst preparation

The Ni/Al_2O_3 catalyst used in the catalytic reforming tests was prepared by the wetness impregnation method, Nickel was impregnated onto an alumina support to produce 20 wt.% of NiO with the alumina support. To this effect $Ni(NO_3)_2{\cdot}6H_2O$ (≥97.0%, Sigma-Aldrich) was dissolved in acetone (≥99.8%, Sigma Aldrich); the support γ- Al_2O_3 (≥98.0% purity, Sasol) was added into the solution stirred for 2 h, then a rotating evaporator at 60 °C under vacuum was used to remove the acetone. The resulting solid was dried overnight at 110 °C and then calcined at 600 °C with a ramping rate of 2 °C·min^{-1} for 4 hours. Finally, it was sieved into particles ranging between 250 and 500 μm. The Ni content is 16.4 wt.% as fully reduced Ni. The catalyst specific surface area measured by BET was 153 m^2 g^{-1}. A full characterization of its textural properties was given in a previous study [56].

2.2 Catalytic toluene steam reforming tests

Toluene steam reforming tests were carried out in a fixed bed reactor used in previous bio-oil reforming studies [66]. A scheme of the system employed, and a detailed drawing of the reactor have been given elsewhere [56]. Briefly, the reactor consists of an Incoloy alloy 625 tube (12 mm i.d., 2 mm thick, 253 mm long), equipped with an inner quartz tube (9 mm i.d., 1 mm thick and 300 mm long) to avoid potential reaction between reactant gas stream and the Incoloy tube walls. Two copper electrodes controlled by a WEST 6100+ digital temperature controller were used to heat up the reactor by Joule effect. Two syringe pumps were installed at the top of the reactor to inject toluene and water into it.

Before each experiment, the reactor was purged with N_2 for 10 min to remove air. The catalyst was reduced under 50 mL·min^{-1} of H_2 at 800 °C for 1 hour. Following catalyst reduction, the carrier gas was switched to the experimental atmosphere gas

composition and allowed 10 min to stabilize. It was made sure the outlet gas pressure remained unchanged during this process as there are five different gas channels and slight pressure changes would affect the accuracy of the gas mixture. The injection of steam and toluene started when the reading of the analyzers stayed stable at desired input readings for at least 5 minutes. The liquid phase reactants were carried by the atmosphere gas and preheated at 200 °C in a bed of 1 g of SiC to vaporize them. Then, the reactant mixture gas entered a 500 mg of Ni/Al_2O_3 catalyst bed, which was held by wire mesh and quartz wool in the middle of the quartz tube. The bed temperature was continuously monitored by a K-type thermocouple.

The product gases passed through two condensers in series to collect any liquid product as well as unreacted toluene and water. Ice and dry ice were used as coolant in the first and second condenser, respectively. The products identified in the gas phase were H_2, CH_4, CO_2 and CO. Two on-line gas analyzers were used to determine product gas compositions: an MGA3000 (ADC, UK) Multi-Gas infrared analyzer for CO_2, CH_4 and CO, followed by a K1550 MLT (Eaton Electric Limited, UK) thermal conductivity H_2 analyzer. The software started to collect gas data (product gas concentrations) when the reactant injection started, and the gas concentrations were recorded continuously for 5 hours.

The reaction gas atmosphere was designed to simulate the syngas composition from biomass gasification processes. The main products include H_2, CO, CO_2 and CH_4. The typical composition ranges of H_2, CO, CO_2 and CH_4 in biomass gasification syngas are 20 – 50 vol%, 20 – 40 vol%, 10 – 30 vol% and 1 – 8 vol% respectively [21, 67, 68]. To investigate the influence of H_2, CO, CO_2 and CH_4 on catalytic toluene steam reforming, their inlet concentrations were fixed at 30, 30, 20 and 3 vol%, respectively, and balanced with N_2. Table 1 shows the detailed reforming atmosphere gas compositions of different toluene catalytic steam reforming tests.

Table 1. Toluene steam reforming atmospheres used in this work (on dry basis). A S/C ratio of 3 was applied in all experiments.

Experimental Condition	Component Concentration (%vol) [Flowrate (mmol h^{-1})]				
	H_2	CO	CO_2	CH_4	N_2
N_2	0	0	0	0	100% [536]
H_2	30% [161]	0	0	0	70% [375]
CO	0	30% [161]	0	0	70% [359]
CO_2	0	0	20% [107]	0	80% [429]
CH_4	0	0	0	3% [16]	97% [520]
H_2 & CO	30% [161]	30% [161]	0	0	40% [214]
H_2 & CH_4	30% [161]	0	0	3% [16]	67% [359]
Full gas mixture	30% [161]	30% [161]	20% [107]	3% [16]	17% [91]

The catalytic reforming test conditions applied in catalytic steam reforming test are shown in Table 2, which were found to be optimal in previous work [56]. S/C ratio is defined as in Equation 1, where *n* is the molar flowrate of each species. This definition takes into account the carbon contents of toluene and methane, and is used throughout this work unless otherwise stated.

$$S/C = \frac{n_{H_2O,in}}{7\, n_{C_7H_8,in} + n_{CH_4,in}} \qquad \text{Eq.1}$$

Table 2. Experimental conditions

Reforming parameters	Value
Temperature	800 °C
S/C ratio	3
GHSV	91800 h^{-1}
Carrier gas flow rate	200 mL min^{-1}
Toluene injection rate	1.38 mL h^{-1} (13 mmol h^{-1})
Toluene concentration	100 g m^{-3}
Catalyst	500 mg Ni/Al_2O_3

The performance of catalysts was evaluated by the toluene conversion ($X_{C_7H_8}$) into gaseous products (based on a carbon balance between the reactor inlet and outlet), according to Equation 2:

$$X_{C_7H_8}(\%) = \frac{(n_{CO,out} - n_{CO,in}) + (n_{CO_2,out} - n_{CO_2,in}) + (n_{CH_4,out} - n_{CH_4,in})}{7\, n_{C_7H_8,in}} * 100 \qquad \text{Eq.2}$$

CO, CO_2 and H_2 yield (*Y*) were defined as in Equations 3 to 5. In the case of H_2, a 100% yield was defined considering the WGS reaction was fully shifted to the right.

$$Y_{CO}(\%) = \frac{(n_{CO,out} - n_{CO,in})}{7\, n_{C_7H_8,in} + n_{CH_4,in}} * 100 \qquad \text{Eq. 3}$$

$$Y_{CO_2}(\%) = \frac{(n_{CO_2,out} - n_{CO_2,in})}{7\, n_{C_7H_8,in} + n_{CH_4,in}} * 100 \qquad \text{Eq. 4}$$

$$Y_{H_2}(\%) = \frac{(n_{H_2,out} - n_{H_2,in})}{18\, n_{C_7H_8,in} + 4\, n_{CH_4,in}} * 100 \qquad \text{Eq. 5}$$

CO_2 selectivity was also calculated to investigate the influence of different gas atmospheres on CO/CO_2 selectivity and assess the extent of WGS reaction. As methane had a total conversion in all the experiments, CO_2 selectivity is defined by the equation below where each term is in moles:

$$S_{CO_2}(\%) = \frac{(n_{CO_2,out} - n_{CO_2,in})}{(n_{CO_2,out} - n_{CO_2,in}) + (n_{CO,out} - n_{CO,in})} * 100 \qquad \text{Eq. 6}$$

The experimental error in toluene conversion, gas selectivity and yield is ± 2%.

Thermogravimetric analysis (TGA) was conducted to investigate the coke deposition on the spent catalyst using a Pyris 1 thermogravimetric analyzer from PerkinElmer. The samples were heated from room temperature to 900 °C at 10 °C·min^{-1} in air according to a procedure described elsewhere [69]. The derivative of the weight loss with time was calculated and normalized to compare regions of carbon burnout.

2.3 Thermodynamic equilibrium simulation

ASPEN V8.4 software was used to study the thermodynamic equilibrium of the toluene reforming reactions under different reaction atmospheres, using an ideal base property method and a RGIBBS reactor (based on Gibbs free energy minimization) to identify reforming products and yields. Material flows, reaction conditions (reforming temperature, pressure) are identical to those from the corresponding experiments.

3. Results and discussion

3.1 Influence of single syngas component atmosphere

A first group of experiments was conducted to understand the influence of single gas atmospheres on toluene steam reforming over a Ni/Al_2O_3 catalyst at the conditions

290 shown in Table 2. A baseline is provided by experiments with an inert atmosphere (100%
291 N_2). Figure 1 presents toluene conversion and product gas yields for H_2, CO and CO_2
292 as a function of time on stream during reforming test for each of the single syngas
293 component atmospheres (balanced in N_2) with a S/C ratio of 3. It was observed (Figure
294 1a) that toluene reforming in a N_2 atmosphere led to steady gas yields and a
295 conversion of nearly 95% over the 5-hour experiment. This experiment is used as the
296 baseline to determine the effect of the presence of each syngas component and their
297 mixtures. The effect of these gases can be related to inhibition of the reforming
298 reaction and/or catalyst deactivation. Inhibition is observed as a drop in the initial
299 activity of the fresh catalyst (at the very beginning of a run) when a given syngas
300 component is introduced respect to that obtained in N_2. Catalyst deactivation is
301 reflected by a decrease in toluene conversion with time on stream within a run.

302 During the 5-hour test in 30% H_2 atmosphere, shown in Figure 1b, the carbon
303 conversion from toluene to gas steadily decreased from 94% to 88%, as CO yield was
304 reduced from 67% to 62%, while a steady yield of 26 – 28 % was observed for CO_2
305 throughout the test. H_2 yield declined slightly from 59% to 55%. These trends point to
306 a certain deactivation of the catalyst taking place as a consequence of the presence
307 of H_2 in the gas.

308 On the other hand, no significant deactivation was observed in CO or CO_2
309 atmospheres. The toluene conversion into gas products observed in a 30% CO
310 atmosphere (Figure 1c) showed no significant change in 5 hours, and CO, CO_2 yield
311 remained stable at ~33% and ~58%, respectively, throughout the experiment. The
312 input of CO in the carrier gas shifted the WGS reaction to produce more H_2 and CO_2,
313 and H_2 yield stayed above 75% in the 5-hour test. In 20% CO_2, shown in Figure 1d,
314 the overall conversion of toluene stayed higher than 90% during the 5 hours, while
315 CO_2 yield ranged from 17% to 19% and CO yield ranged from 71% to 76%. H_2 yield
316 also remained stable at ~58%.

Two different conditions were tested with a 3% CH_4 concentration to gain a better understanding on the behavior of the system with toluene and methane mixtures. In one of them, the molar ratio between steam and carbon in toluene was 3 (carbon in CH_4 was not considered in the calculation, which is equivalent to S/C ratio of 2.55). In this case, the overall conversion from toluene to gases decreased from 90% to 79% after 5 hours, and H_2 yield declined from 58% to 49% (Figure 1e). CO and CO_2 yields decreased from 65% and 25% to 56% and 22%, respectively. CH_4 conversion stayed at 100% throughout the test.

In another experiment the steam feeding rate was increased to keep the S/C ratio at 3, as per the definition in Equation 1 (considering all carbon in toluene and CH_4). The product yield and total gas conversion trends are presented in Figure 1f. The toluene conversion into gases in first hour achieved 93% as a result of the increasing of S/C ratio from 2.55 to 3. Then the overall conversion decreased with time smoothly, and finally dropped to 79% during the fifth hour. H_2, CO and CO_2 yields decreased from 72%, 59% and 36% to 64%, 52% and 31%, respectively. H_2 yield also increased with the increasing of S/C ratio. Despite the initial increase in toluene conversion, the degree of deactivation in 5 hours was not significantly affected by the increase in S/C ratio with final yield values being very close for the two conditions.

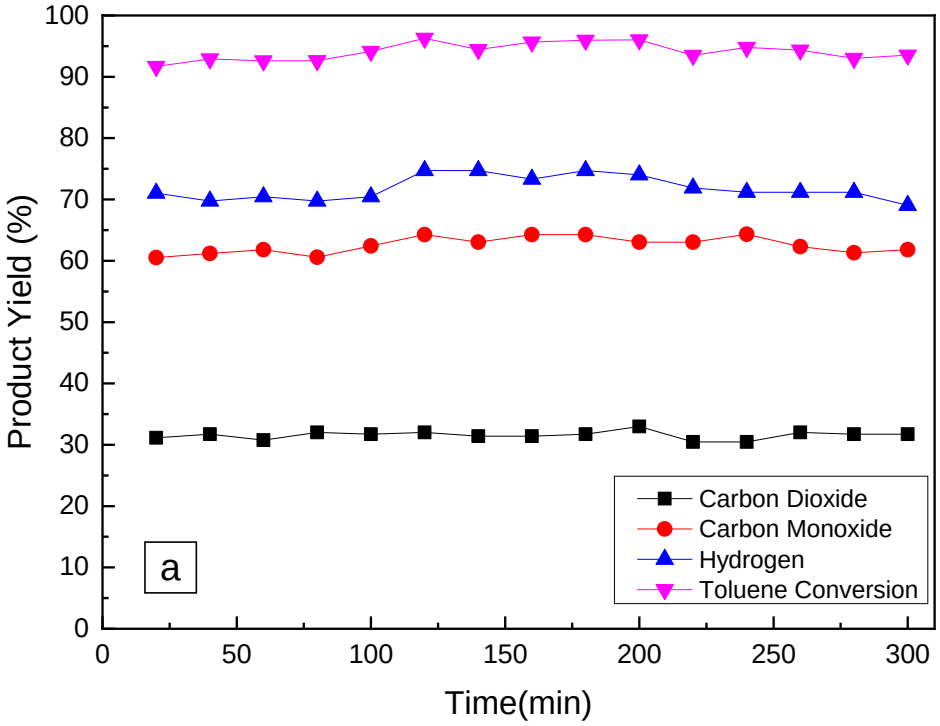
Product Yield (%)
Time(min)
Carbon Dioxide
Carbon Monoxide
Hydrogen
Toluene Conversion
a

335

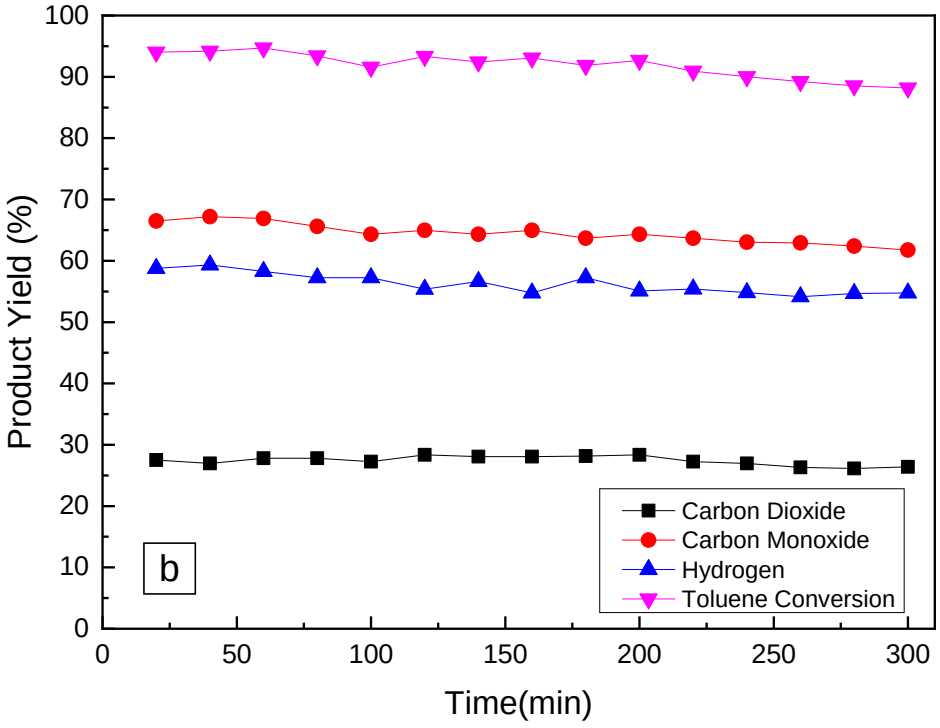
Product Yield (%)
Time(min)
Carbon Dioxide
Carbon Monoxide
Hydrogen
Toluene Conversion
b

336

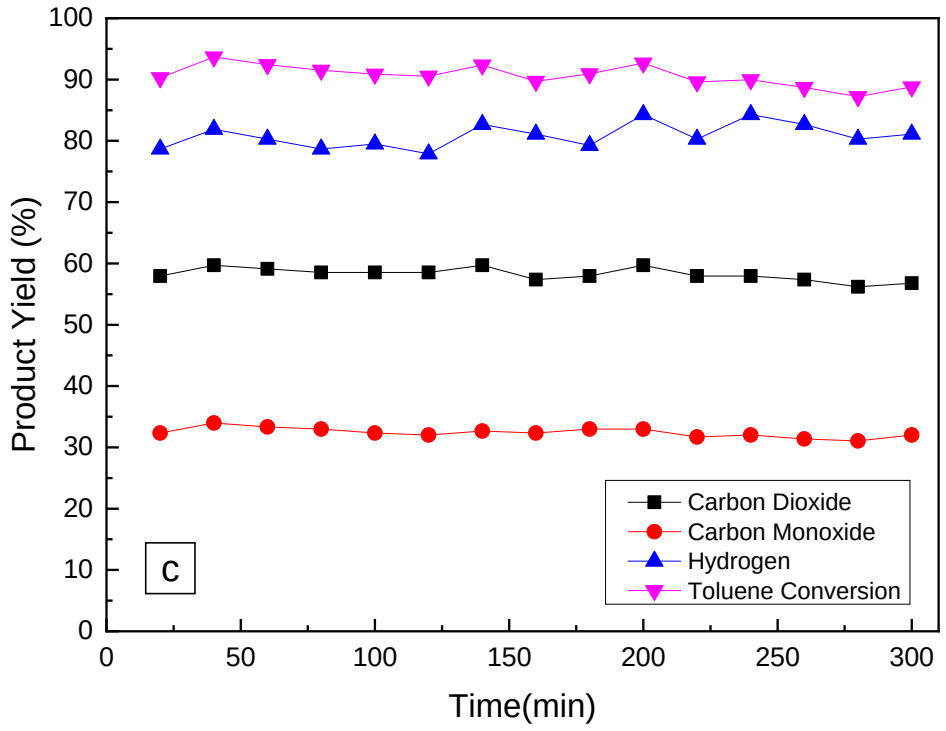
Product Yield (%)
Time(min)
Carbon Dioxide
Carbon Monoxide
Hydrogen
Toluene Conversion
c

337

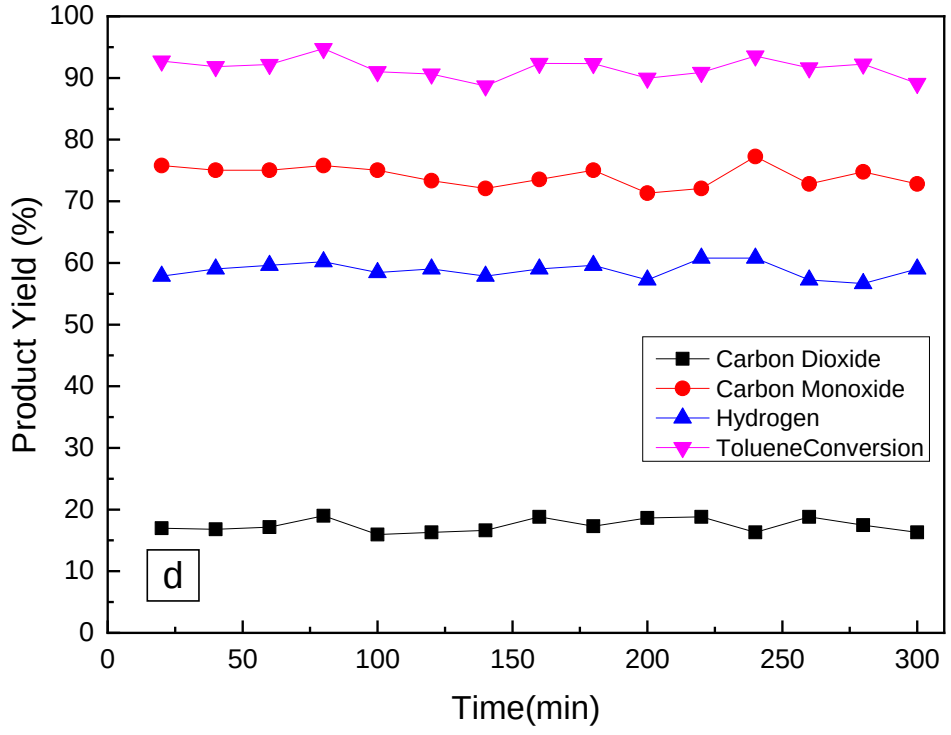
Product Yield (%)
Time(min)
Carbon Dioxide
Carbon Monoxide
Hydrogen
ToluneConversion
d

338

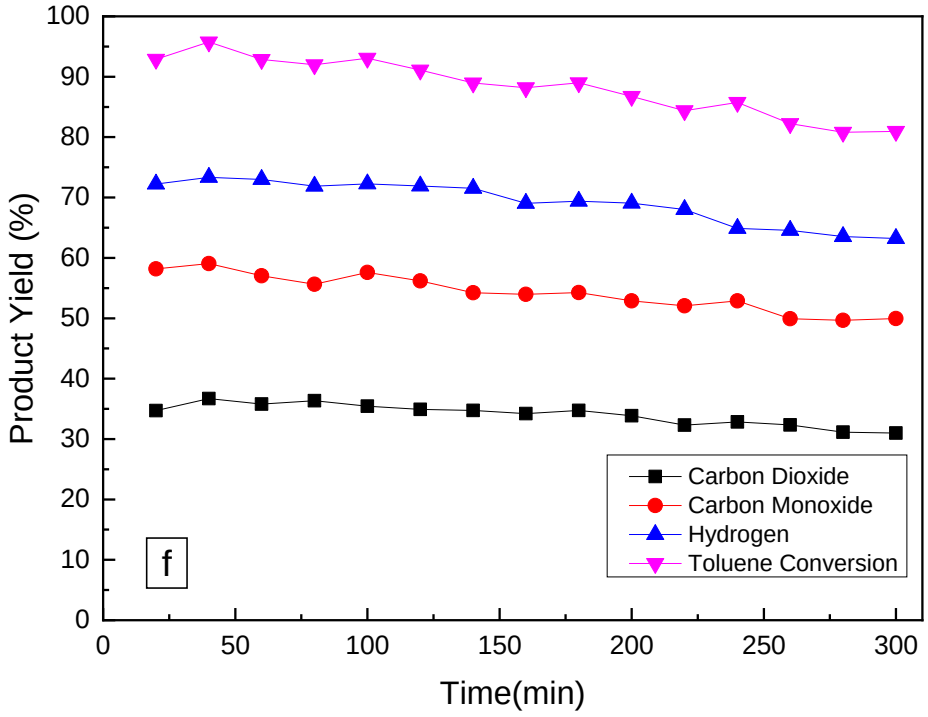

339

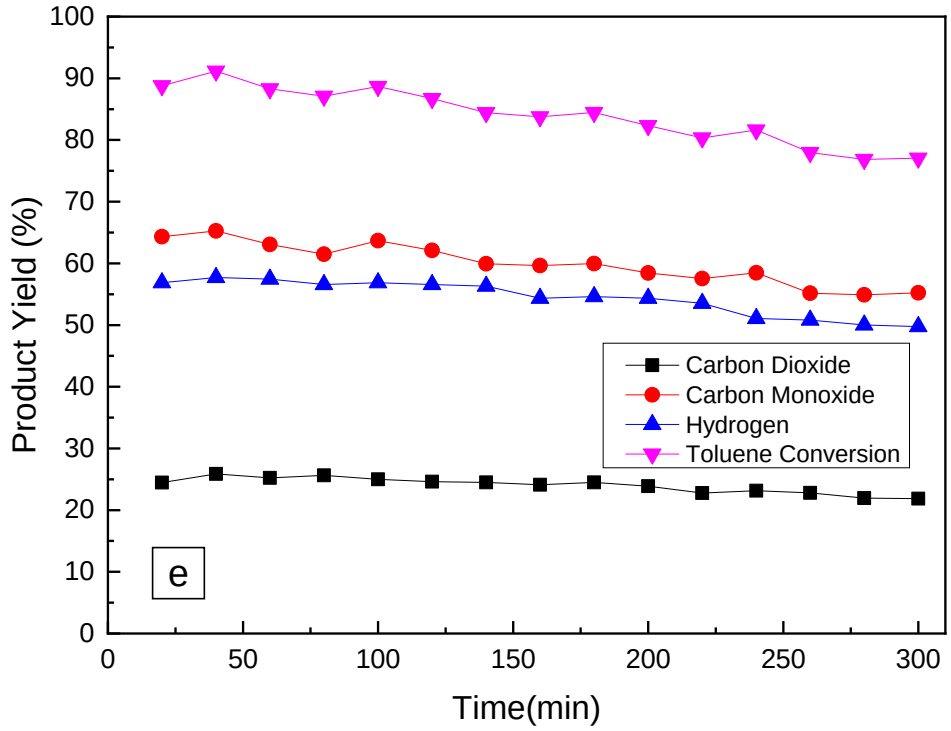

340

341 **Figure 1. Gas product yield and toluene conversion as a function of time on stream in**
342 **steam reforming tests carried out in (a) 100% N_2; (b) 30%H_2; (c) 30% CO; (d) 20% CO_2;**
343 **(e) 3% CH_4 with $S/C_{Toluene}$: 3 (only C in toluene considered); (f) 3% CH_4. All atmospheres**
344 **balanced in N_2. All experiments performed with a bed of Ni/Al_2O_3 catalyst at 800 °C and**

GHSV: 91,800 h^{-1}. S/C 3 for all runs except for (e) as indicated.

Figure 2 summarizes the CO and CO_2 yield and toluene conversion into C-containing gases under different gas atmospheres at the first and fifth hours of the catalytic tests and compares these values with equilibrium results. The equilibrium calculation showed that all these atmospheres reach 100% toluene conversion into gas, and CH_4 yield stayed lower than 0.01% in all the equilibrium results. The experimental results showed that toluene conversion to gas under 100% N_2, 30% CO in N_2, 20% CO_2 in N_2 atmosphere stayed over 90% throughout the 5-hour catalytic reforming tests, with very limited decreases in toluene conversion (< 2.5%) due to deactivation observed in these three atmospheres.

100% N_2 atmosphere presented the highest toluene conversion in the whole 5 hours on stream, while 30% CO in N_2, 20% CO_2 in N_2 and 30% H_2 in N_2 atmospheres showed lower toluene conversions in the 5-hour experiments. In particular, in the case of CO_2, it can be inferred that no significant extent of dry reforming was observed as toluene conversion did not exceed that obtained by steam reforming alone. This indicates that relatively high contents (>20%) of gasification syngas components (CO, H_2, CO_2) can slightly inhibit the reforming reaction of toluene. The use of CH_4 did not show any obvious inhibition effects, presenting a similar initial toluene conversion to the 100% N_2 atmosphere. However, catalyst deactivation in the presence of CH_4 and toluene was large even though 3% CH_4 on its own (also included in Figure 2) did not deactivate the catalyst to any observable extent. The experiment carried out with CH_4 but no toluene presented nearly complete carbon conversion. It led to the formation of 0.112 g of coke per g of catalyst, which represents around only 2.35% of the CH_4 injected. CH_4 was mostly steam reformed into CO, CO_2 and H_2, which is consistent with the fact that these experiments have been carried out a temperature much lower than the onset of CH_4 pyrolysis, which is the main route to ethane, ethylene and carbon formation [70].

The injection of H_2, CO, CO_2 had a significant influence on gas product distribution both in experiments and equilibrium simulations. Equilibrium results confirmed that the WGS reaction played an important role in CO/CO_2 selectivity and H_2 production. It can be observed in Figure 2 that CO_2 yield was typically lower than equilibrium calculations except for the CO_2 atmosphere experiment. The presence of CO in the carrier gas favored the WGS reaction and more CO_2 was produced than in the N_2 atmosphere. On the other hand, feeding CO_2 would largely increase CO yield to ~75%, pushing the reverse WGS reaction. The experimental CH_4 yield in all tests was 0%. The absence of CH_4 under all atmospheres indicated that CH_4 had a total conversion over Ni/Al_2O_3 catalyst even when the deactivation of toluene reforming took place. The CH_4 atmosphere test experienced the largest decrement in toluene conversion during an experiment as it dropped from ~94% to 81% in 5 hours, as well as in CO and CO_2 yields, followed by H_2 atmosphere test. Considering that CH_4 only had a concentration of 3 vol% in carrier gas, it is clear that CH_4 plays a key role in reforming catalyst deactivation among syngas components.

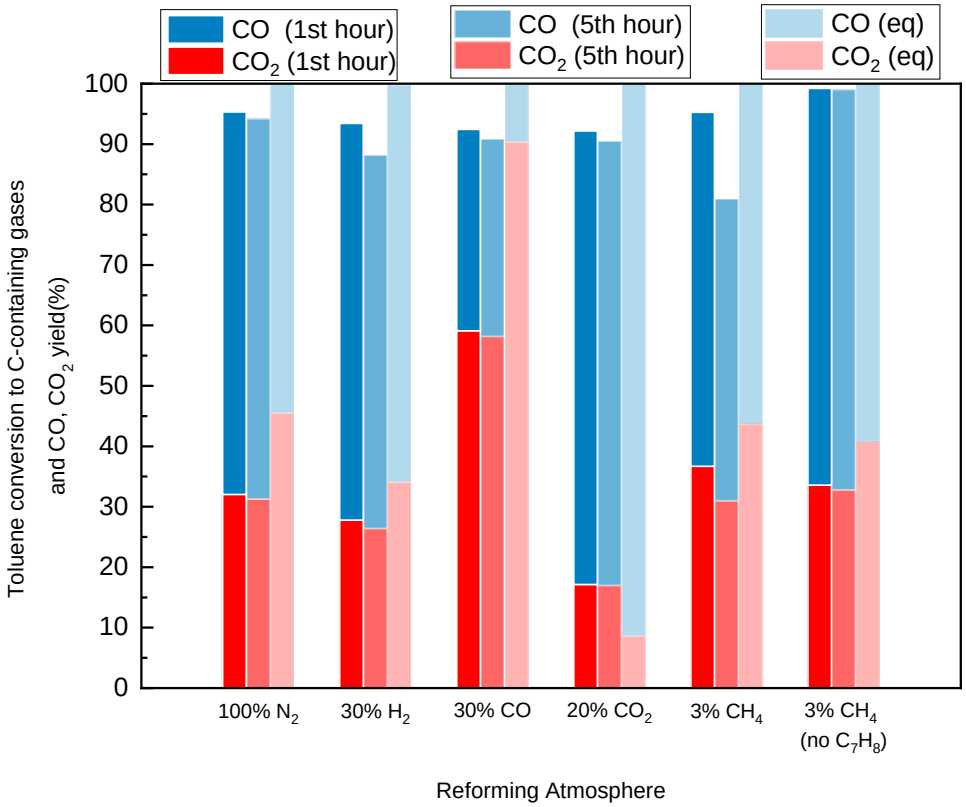

387

388 **Figure 2. Toluene conversion to C-containing gases and CO/CO_2 yield at different single**
389 **gas atmospheres (S/C ratio: 3, GHSV:91800 h^{-1}, reforming temperature 800 °C, all the**
390 **gas atmospheres balanced with N_2). Methane conversion is shown for the experiment**
391 **containing CH_4 but no toluene.**

392 Table 3 shows the gas product yields including CO, CO_2 and H_2 as mol/mol toluene at
393 the first hour and the fifth hour under different atmospheres and compares with the
394 respective equilibrium values. CO/CO_2 product ratios at different atmospheres also
395 changed towards the equilibrium results. Experimental CO_2 selectivity under most
396 atmospheres was lower than equilibrium predicted, indicating that toluene was
397 reformed to CO first, which then underwent WGS reaction in the excess of steam to
398 produce CO_2. The only exception was the 20% CO_2 atmosphere, which shifted the
399 equilibrium towards a low CO_2 yield and made reverse WGSR predominant.

400 As a consequence of the WGS reaction equilibrium, the injection of CO promoted the

401 production of H_2, while CO_2 inhibited H_2 yield. The addition of H_2 also reduced H_2 yield
402 respect to the blank experiment in N_2 atmosphere but it was not enough to change the
403 predominant direction of the WGS reaction. 3% CH_4 in N_2 atmosphere test achieved
404 the highest H_2 at 16.5 mol/mol toluene during the first hour due to the additional H_2
405 production. This run showed the highest decrement (by 16%) at the fifth hour.
406 Meanwhile, H_2 yield of 30% H_2 in N_2 atmosphere test dropped by 7% from 11.2 to 10.4
407 mol/mol toluene in the 5-hour test. The ratio of CO/CO_2 stayed almost the same after
408 5-hour test in all the experiments, suggesting that both reforming and WGS reaction
409 functions were deactivated to the same extent.

410 **Table 3. Product yields for the gaseous products in the different reforming atmosphere**
411 **(S/C ratio 3 GHSV:91800 h^{-1}, reforming temperature 800 °C, N_2: 100%N_2, H_2: 30% H_2 in**
412 **N_2, CO: 30% CO in N_2, CO_2: 20% CO_2 in N_2, CH_4: 3% CH_4 in N_2).**

Reforming Atmosphere	CO_2 (mol/mol toluene)	CO (mol/mol toluene)	H_2 (mol/mol toluene)	CO_2 selectivity
N_2 (1st hour)	2.2	4.5	13.0	33%
N_2 (5th hour)	2.2	4.4	13.0	33%
N_2 (Equilibrium)	(3.2)	(3.8)	(14.3)	(46%)
H_2 (1st hour)	1.9	4.6	11.2	29%
H_2 (5th hour)	1.8	4.3	10.4	30%
H_2 (Equilibrium)	(2.4)	(4.6)	(13.3)	(34%)
CO (1st hour)	4.1	2.3	14.7	64%

CO (5th hour)	4.0	2.3	14.5	63%
CO (Equilibrium)	(6.3)	(0.7)	(17.3)	(90%)
CO_2 (1st hour)	1.2	5.3	10.7	18%
CO_2 (5th hour)	1.2	5.1	10.6	19%
CO_2 (Equilibrium)	(0.6)	(6.4)	(11.6)	(9%)
CH_4 (1st hour)	3.0	4.8	16.5	38%
CH_4 (5th hour)	2.5	4.1	13.8	38%
CH_4 (Equilibrium)	(3.5)	(4.6)	(18.0)	(43%)

413

414 Table 4 shows the carbon conversion from toluene to coke and the fraction of coke on
415 the catalyst under different reforming atmospheres determined by thermogravimetric
416 analysis on the spent catalysts. In the CH_4 only (no C_7H_8) test, 2.35% of CH_4 was
417 converted into carbon deposits on the catalyst surface. The conversion to carbon
418 deposits of 100% N_2, 30% CO in N_2 and 20% CO_2 in N_2 atmosphere was very close,
419 which indicates that CO and CO_2 contents have very limited influence on carbon
420 deposition on the catalyst, which remained stable during the tests. The presence of
421 30% H_2 increased the coke weight, which matched the slight deactivation observed in
422 toluene conversion to C-containing gases and the drop in H_2 product yield. The

presence of H_2 might prevent coke reaction with steam, and shift the equilibrium towards more coke, an observation also made in the literature [52]. The mixed toluene-CH_4 atmosphere test led to the highest coke content and ratio, much higher than could be expected from the simple addition of effects observed with toluene and CH_4 separately. Catalyst deactivation was calculated from the H_2 yields (Y_{H_2}) initially and after 5 hours on stream (Equation 7).

$$Cat.Deac. = \frac{[Y_{H_2}]_{t=0} - [Y_{H_2}]_{t=5h}}{[Y_{H_2}]_{t=0}} \qquad \text{Eq. 7}$$

A reasonable correlation between amount of coke on the catalyst and catalyst deactivation was observed, where the latter does not take place significantly at coke to catalyst ratios below a threshold of around 20 wt.% but increases markedly above that value.

Table 4. Toluene conversion to coke, fraction of coke deposited on the catalyst and catalyst deactivation at different reforming atmospheres (800 °C, S/C:3, GHSV:91800 h^{-1}, 5-hour test. N_2: 100%N_2, H_2: 30% H_2 in N_2, CO: 30% CO in N_2, CO_2: 20% CO_2 in N_2, CH_4: 3% CH_4 in N_2).

Reforming Atmosphere	N_2	H_2	CO	CO_2	CH_4	CH_4 (no C_7H_8)
Coke/C in toluene	0.68%	0.90%	0.61%	0.64%	1.54%	-
Coke/Catalyst (g_C/g_{cat})	0.184	0.245	0.165	0.173	0.417	0.112
Catalyst Deactivation (%)	0	7	1	1	16	0

3.2 Influence of multi-gas atmospheres on toluene steam reforming

While previous tests focused on the influence of single gas in N_2, this section presents the impact of syngas component mixtures on toluene steam reforming. First, a mixture of 30% H_2 and 30% CO balance N_2 is presented, followed by 3% CH_4 and 30% H_2 in N_2 and finally a full syngas mixture consisting of 3% CH_4, 30% H_2, 30% CO and 20% CO_2 in N_2, typical of a gasifier under normal operation conditions [48, 49]

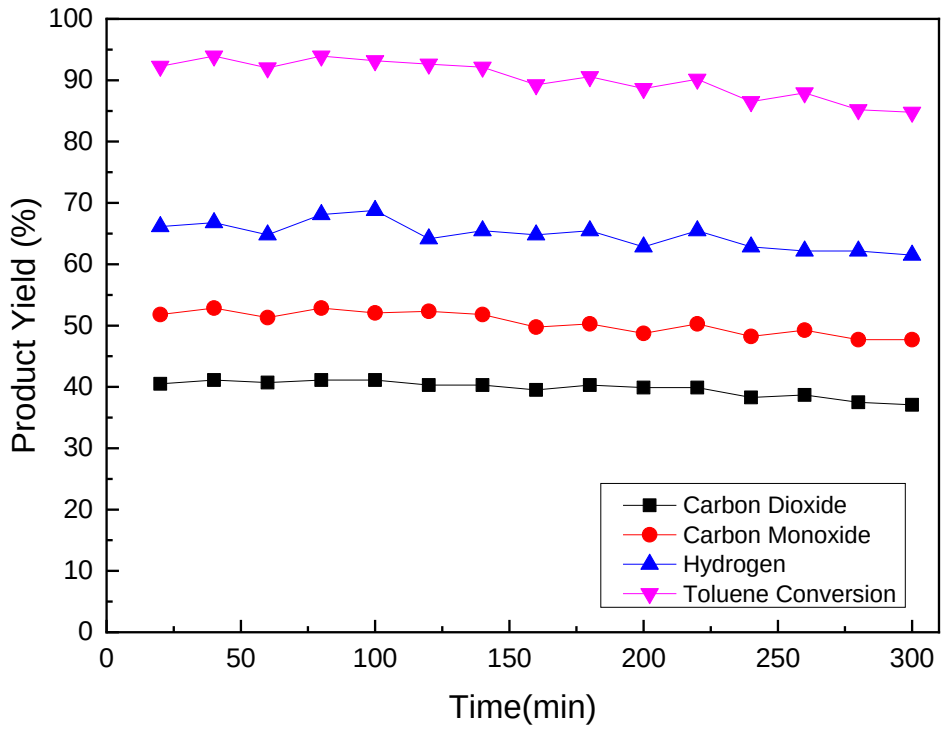

Figure 3. Product yield trend and conversion of toluene steam reforming test in 30% H_2 and 30% CO balanced N_2 atmosphere (5-hour test, Ni/Al_2O_3 catalyst, 800 °C, S/C ratio 3, GHSV: 91800 h^{-1}).

Figure 3 shows the gas product yield and conversion of toluene steam reforming 5-hour test in 30% H_2 and 30% CO balanced N_2 atmosphere. Product yields of CO and H_2 were very stable in the first 2.5 hours, and then started to drop slowly until the end of the tests. The overall conversion from toluene to gases also decreased below

90% at 160 mins to reach a final value of 84%, lower than achieved in CO and H_2 separately. Table 5 shows CO_2, CO and H_2 yields (in mol/mol toluene) declined by ~10% in the 5-hour test, but selectivity towards CO_2 was not affected by catalyst deactivation as discussed above.

Table 5. Product yields for the gaseous products in 30% H_2 and 30% CO balanced N_2 atmospheres (5-hour test, Ni/Al_2O_3 catalyst, 800 °C, S/C ratio 3, GHSV: 91800 h^{-1})

Atmosphere	CO_2 (mol/mol toluene)	CO (mol/mol toluene)	H_2 (mol/mol toluene)	CO_2 selectivity
H_2 & CO (1st hour)	2.8	3.7	11.9	43%
H_2 & CO (5th hour)	2.6	3.3	11.1	44%
(Equilibrium)	(4.3)	(2.7)	(15.3)	(61%)

Figure 4 summarizes toluene conversion to C-containing gases and CO, CO_2 yields at H_2, CO and mixture gas atmosphere. CO content in the carrier gas had no obvious effect on catalyst deactivation in multi-gas mixture atmosphere. Instead, the decrease in toluene conversion was led by the presence of H_2, as the overall toluene conversion showed similar trends in 30% H_2 in N_2 and 30% CO, 30%H_2 in N_2 atmosphere tests. The equilibrium and experimental results both showed that CO had more significant influence on the selectivity of product CO/CO_2 than H_2. When equal concentrations of CO and H_2 were introduced to the reaction system, the equilibrium shifted to produce more CO_2 when comparing to inert N_2 atmosphere and the experimental results followed this behavior.

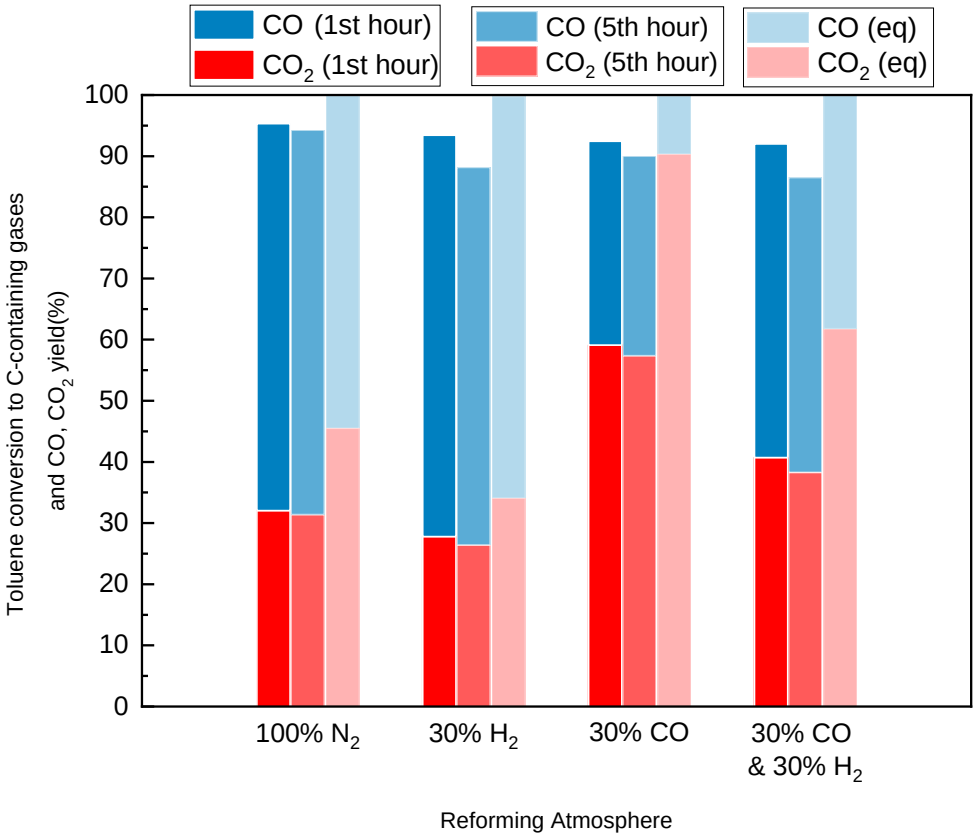

469

470 **Figure 4. Toluene conversion to C-containing gases and CO, CO_2 yields at H_2, CO and**
471 **mixture gas atmospheres (S/C ratio 3 GHSV:91800 h^{-1}, reforming temperature 800 °C,**
472 **all the gas atmosphere balanced with N_2).**

473 The results presented so far showed that CH_4 and H_2 atmosphere had relatively more
474 influence on toluene conversion and carbon deposition than CO and CO_2. Next, the
475 impact of CH_4 and H_2 mixture atmosphere on toluene steam reforming is discussed.
476 To compare with the previous results, the reforming gas atmosphere was designed as
477 3% CH_4 and 30% H_2 in N_2 with a S/C ratio of 3, including CH_4.

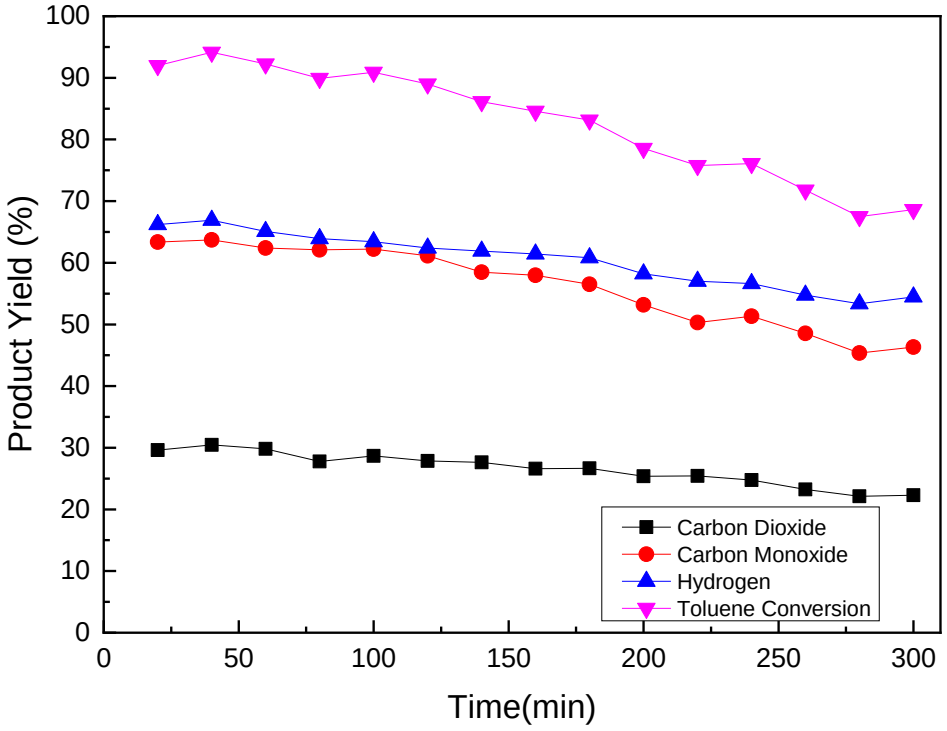

478

479 **Figure 5. Product yield trend and toluene conversion of steam reforming test in 3% CH_4**

480 **and 30% H_2 balanced N_2 atmosphere (5-hour test, Ni/Al_2O_3 catalyst, 800 °C, S/C ratio 3,**

481 **GHSV: 91800 h^{-1})**

482

Table 6. Product yields for the gaseous products in 3% CH_4 and 30% H_2 balanced N_2 atmosphere (5-hour test, Ni/Al_2O_3 catalyst, 800 °C, S/C ratio 3, GHSV: 91800 h^{-1})

Atmosphere	CO_2 (mol/mol toluene)	CO (mol/mol toluene)	H_2 (mol/mol toluene)	CO_2 selectivity
H_2 & CH_4(1st hour)	2.5	5.2	15.1	32%
H_2 & CH_4 (5th hour)	1.8	3.8	10.9	32%
(Equilibrium)	(2.8)	(5.3)	(17.1)	35%

Figure 5 shows the gas product yield and toluene conversion into gases in 3% CH_4 and 30% H_2 balanced N_2 atmosphere. The toluene conversion and CO, CO_2 and H_2 yield started to decrease after 100 min and declined steadily until the end of the test. The conversion of toluene dropped markedly from 93% to 69%, while the CO, H_2 and CO_2 yields decreased from 64%, 66% and 29% to 46%, 54% and 22%, respectively. The CH_4 and H_2 combined atmosphere showed a more significant decrement in gas production from toluene steam reforming respect to the two gases separately.

Table 6 presents CO, CO_2 and H_2 production during the first and fifth hours on stream and compares them with equilibrium results. H_2 production yield decreased by 28%, from 15.1 to 10.9 mol/mol toluene, which was larger than expected based on the behavior of the individual gases. According to Table 4, the decreases in H_2 yield in 30% H_2 in N_2 atmosphere and 3% CH_4 in N_2 atmosphere were 7% and 16%, respectively. The presence of CH_4 and H_2 can deactivate the Ni/Al_2O_3 catalyst much more rapidly than CH_4 or H_2 single gas atmosphere (Figure 6).

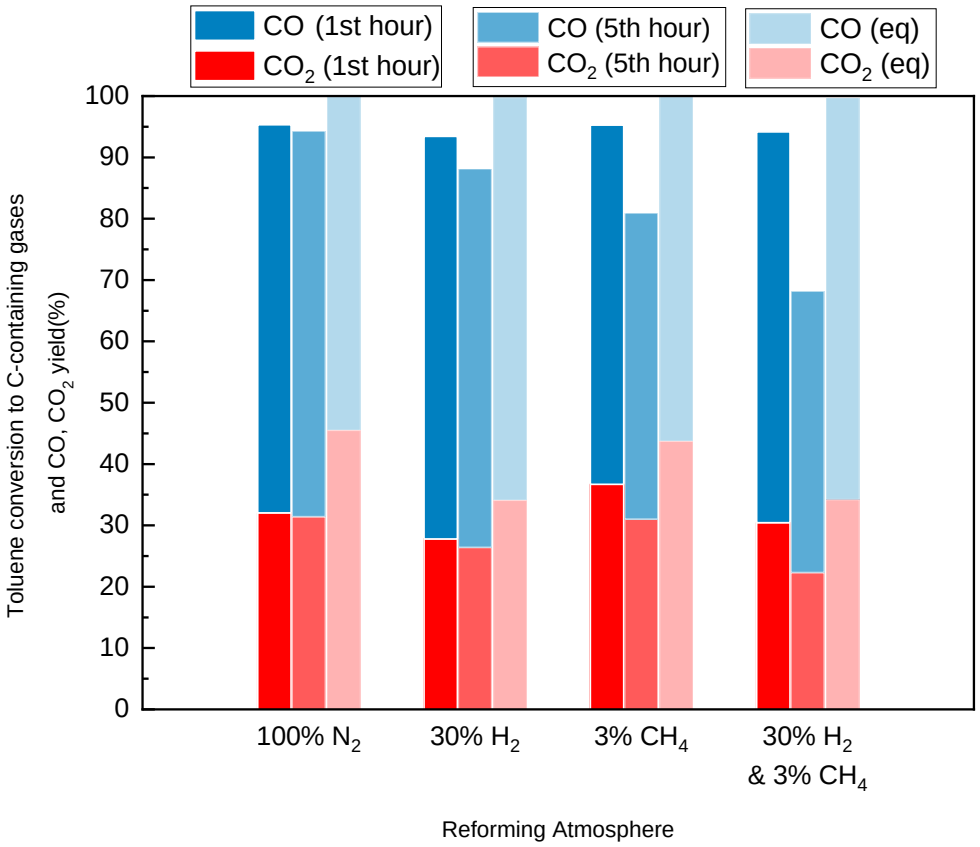

499

500 **Figure 6. Toluene conversion to C-containing gases and CO, CO_2 yield at H_2, CH_4 and**
501 **mixture gas atmosphere (S/C ratio 3, GHSV:91800 h^{-1}, reforming temperature 800 °C, all**
502 **the gas atmosphere balanced with N_2).**

503 Finally, a full gas mixture composed of 3% CH_4, 30% H_2, 30% CO and 20% CO_2 in N_2
504 was chosen to simulate a typical biomass gasification syngas. Figure 7.7 shows the
505 gas product yield and toluene conversion in this simulated gasification atmosphere.
506 Toluene conversion and gas yields started to decline slightly in the second hour, and
507 then decreased significantly in the rest 3 hours. The conversion of toluene dropped
508 from 92% to 66% in the 5-hour test. The trend was similar to the test in 3% CH_4 and
509 30% H_2 atmosphere, which indicated that CO and CO_2 had limited influence on the
510 deactivation of the catalyst.

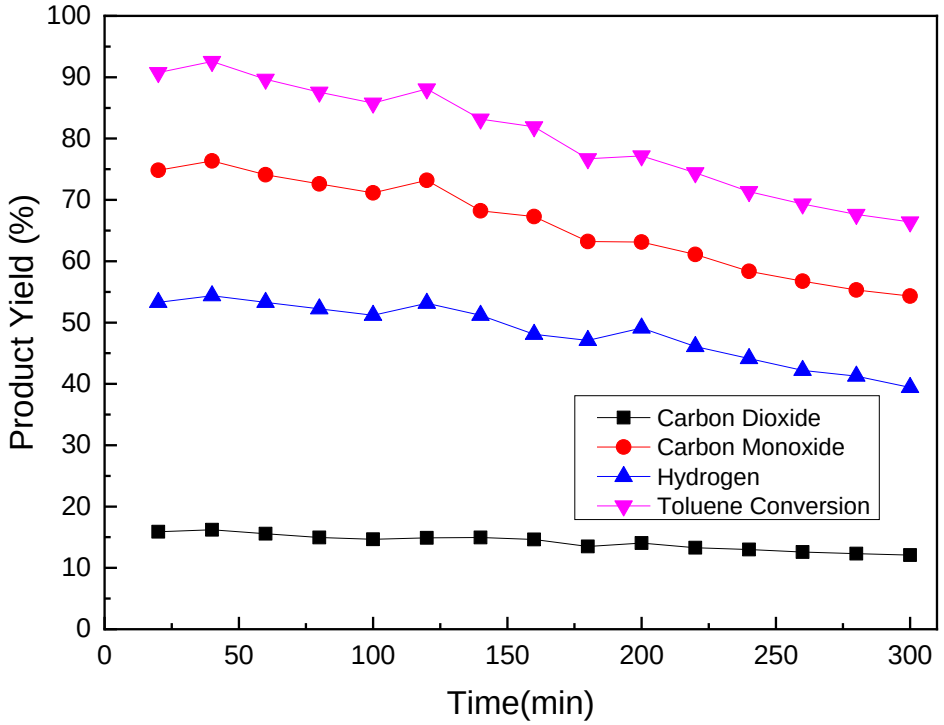

Figure 7. Product yield trend and conversion of toluene steam reforming test in 3% CH_4, 30% H_2, 30% CO and 20% CO_2 balanced N_2 atmosphere (Ni/Al_2O_3 catalyst, 800 °C, S/C ratio 3, GHSV: 91800 h^{-1})

Table 7 and Figure 8 summarize the toluene conversion to C-containing gases and CO, CO_2 yields in all the CH_4–containing atmospheres and compares with the experiments in the N_2 atmosphere. Although the concentration of CH_4 in carrier gas was fixed at 3 vol%, which was much lower than the concentration of CO, CO_2 and H_2, CH_4 was the main reason for catalyst deactivation. The injected H_2 could largely decrease the toluene conversion to gases with the presence of a small amount of CH_4.

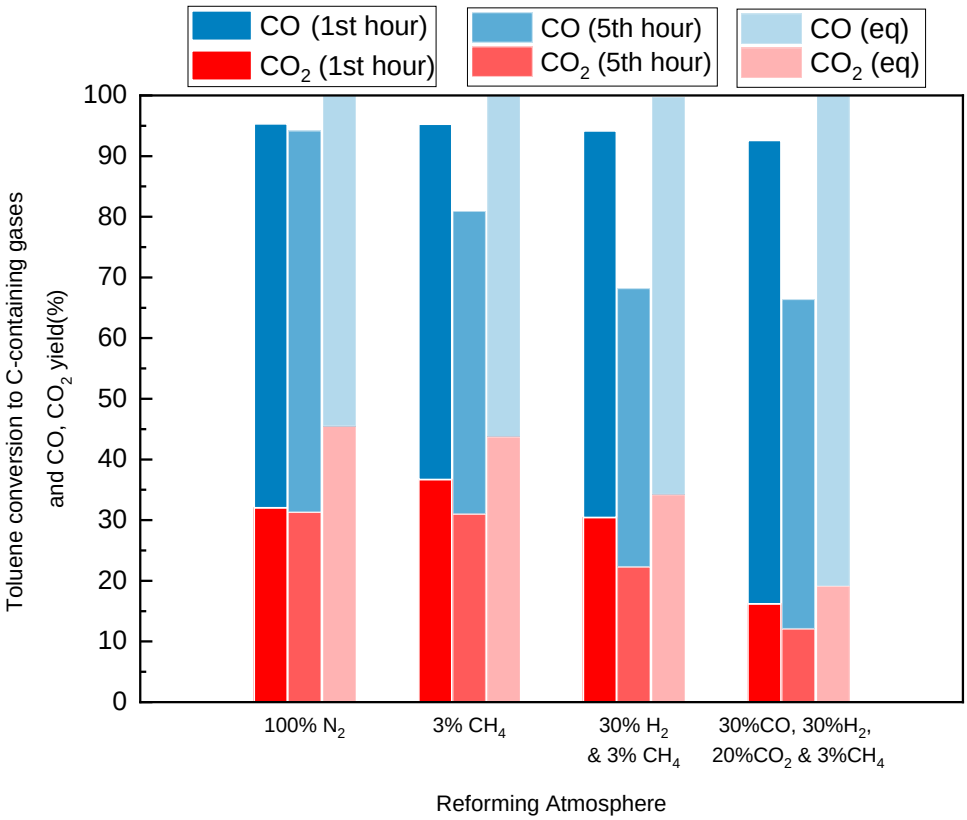

521

522 **Figure 8. Toluene conversion to C-containing gases and CO, CO_2 yield at CO, CO_2, H_2,**

523 **CH_4 and mixture gas atmosphere (S/C ratio 3 GHSV:91800 h^{-1}, reforming temperature**

524 **800 °C, all the gas atmosphere balanced with N_2).**

525

Table 7. Product yields for the gaseous products in 3% CH_4, 30% H_2, 30% CO and 20%CO_2 balanced N_2 atmosphere (5-hour test, Ni/Al_2O_3 catalyst, 800 °C, S/C ratio 3, GHSV: 91800 h^{-1})

Atmosphere	CO_2 (mol/mol toluene)	CO (mol/mol toluene)	H_2 (mol/mol toluene)	CO_2 selectivity
Full gas (1st hour)	1.3	6.2	12.0	17%
Full gas (5th hour)	1.0	4.8	8.7	17%
(Equilibrium)	(1.6)	(6.5)	(15.5)	(20%)

As shown in Table 8, coke formation was favored by the complex gas atmosphere, in particular when a mixture containing H_2 and CH_4 was applied. The amount of coke over the Ni/Al_2O_3 catalyst when 3% CH_4 and 30% H_2 balanced N_2 were employed as well as with the full syngas atmosphere was much larger than observed in any single-gas composition. On the other hand, under 30% H_2 and 30% CO balanced N_2, the coke formation was nearly identical to that observed under H_2 only, reinforcing the role of CH_4 as a trigger in toluene conversion to coke. CO and CO_2 were observed to have no influence on coke formation, with the difference between the full syngas with the CH_4 and H_2 atmosphere being around 1%. The large coke formation in the atmospheres containing H_2 and CH_4 markedly deactivated the Ni/Al_2O_3 catalyst in the first 5 hours on stream (Table 8).

Table 8. Toluene conversion to coke, fraction of coke deposited on the catalyst and catalyst deactivation at different reforming atmosphere (800 °C, S/C:3, GHSV:91800 h^{-1}, 5-hour test. CO & H_2 in N_2: 30% H_2 and 30% CO balanced N_2, CH_4 & H_2 in N_2: 3% CH_4 and 30% H_2 balanced N_2, Full gas mixtures: 3% CH_4, 30% H_2, 30% CO and 20%CO_2 balanced N_2).

Reforming Atmosphere	CO & H_2 in N_2	CH_4 & H_2 in N_2	Full gas mixture
Coke/C in toluene	0.88%	2.53%	2.49%
Coke/Catalyst (g_C/g_{cat})	0.238	0.684	0.676
Catalyst Deactivation (%)	7	28	27

3.3 Discussion of potential pathways for influence of syngas composition on the balance between syngas and carbon formation

A further insight on the type of carbon formed on the catalyst was obtained by analyzing the derivative thermogravimetric profiles obtained during temperature programmed oxidation (DTG-TPO) of the spent catalysts. These are shown in Figure 9, where each profile was normalized to the maximum peak to facilitate comparison. No low-temperature DTG-TPO peak corresponding to gum carbon formation are observed in any of the spent catalysts. This is expected given the high temperature of the reforming experiments, well above the range (typically reported as up to 450 °C [12]) in which gum formation is favored. Two DTG-TPO peaks are visible in most of the spent catalysts, the one at lower temperature corresponding to pyrolytic carbon and the other related to whisker structures. The threshold between both has been estimated to be around 650 °C in the literature [46, 71], which is consistent with the temperature of the shoulder observed in these DTG-TPO curves. It can be seen that

pyrolytic carbon is predominant in all atmospheres, although there is still a significant contribution from whisker carbon.

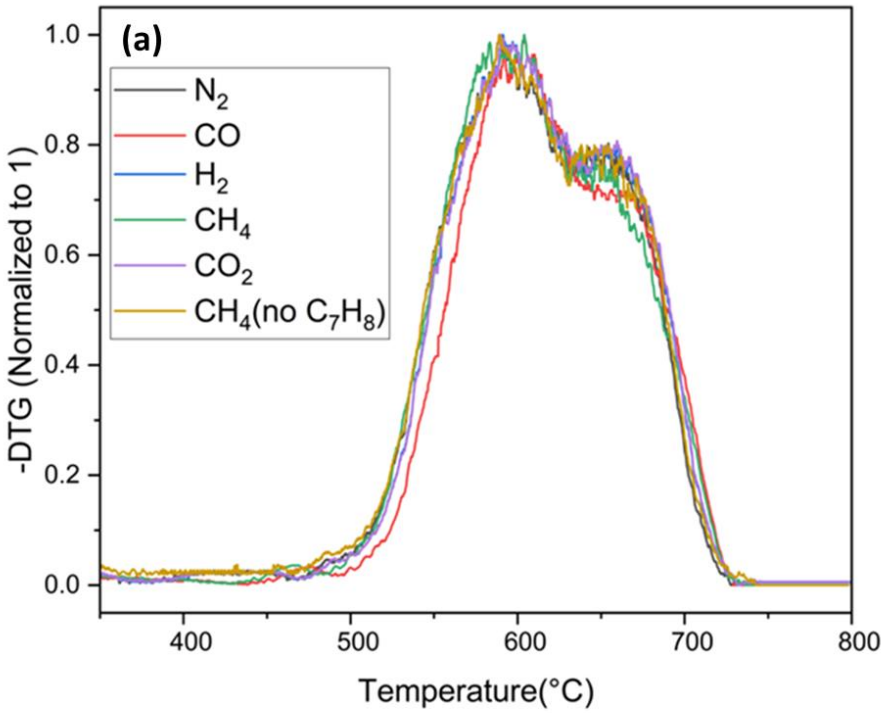

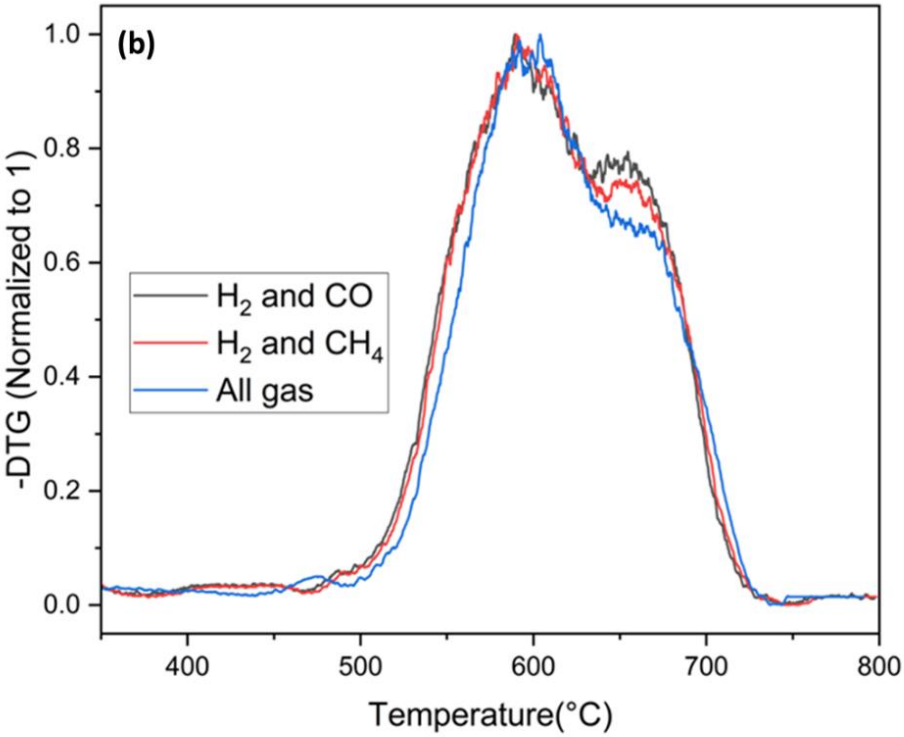

564

565 **Figure 9. DTG-TPO analysis for the spent catalysts at different reforming atmospheres**
566 **(800 °C, S/C:3, GHSV:91800 h^{-1}, 5-hour test). (a) N_2: 100%N_2, H_2: 30% H_2 in N_2, CO: 30%**
567 **CO in N_2, CO_2: 30% CO_2 in N_2, CH_4: 3% CH_4 in N_2 with and without toluene). (b) CO & H_2**
568 **in N_2: 30% H_2 and 30% CO balanced N_2, CH_4 & H_2 in N_2: 3% CH_4 and 30% H_2 balanced N_2,**
569 **All gas mixture: 3% CH_4, 30% H_2, 30% CO and 20%CO_2 balanced N_2. Each trace has**
570 **been normalized.**

571 As differences in carbon formation between different atmospheres appear to be
572 quantitative rather than qualitative, an attempt can be made to rationalize them based
573 on a common reaction pathway. The simplified steam reforming reaction scheme
574 shown in Figure 10 has been proposed [72]. Following adsorption on the catalyst the
575 hydrocarbons undergo hydrocracking to produce adsorbed C and H. These carbon
576 species can then either react with adsorbed OH from the dissociation of water, to
577 produce CO, which can be desorbed into the gas phase or further react to CO_2 with
578 adsorbed OH, or associate with other adsorbed C to form carbon deposits. The latter
579 may involve migration through the Ni particle in the case of whisker carbon. Adsorbed

H species can recombine and undergo desorption to produce H_2 in the gas phase. This scheme can be linked to the observations in this work to explain the effect of syngas components.

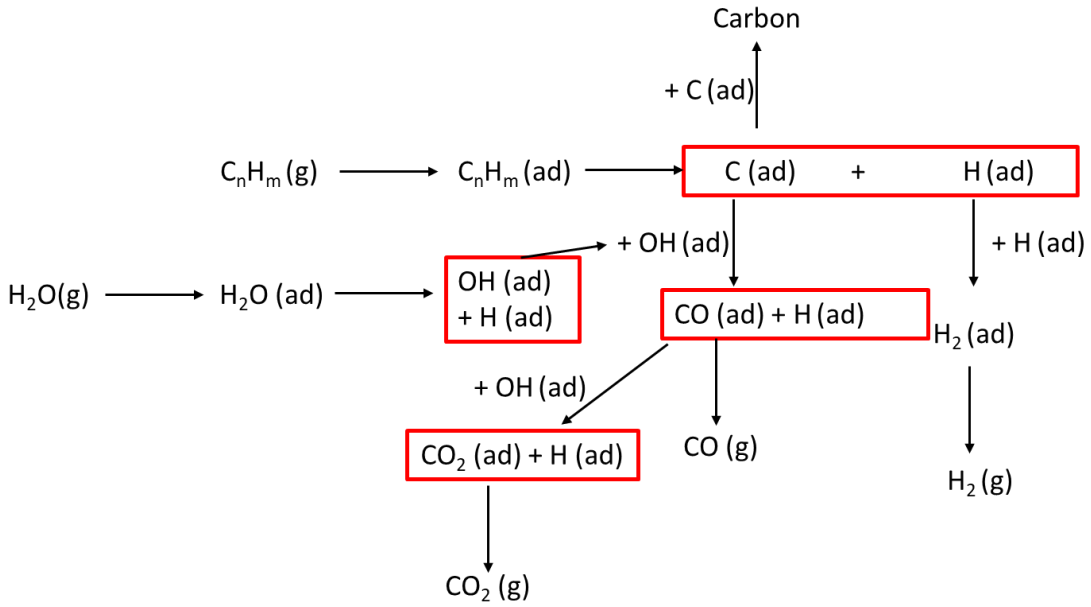

Figure 10. Simplified scheme for the steam reforming reaction of hydrocarbons on a Ni catalyst based on [72].

Taking the experiment in N_2 as the baseline, it was observed that H_2 led to inhibition and a moderate increase in carbon formation. Higher partial pressures of H_2 would tend to counteract the dissociation of the hydrocarbon on the catalyst active site and therefore cause the inhibition detected in the experiments. At the same time, the higher hydrogen pressure would decrease the concentration of surface OH, favoring the competing pathway towards carbon formation.

CO and CO_2 led to very slight inhibition and a decrease in carbon formation. Both could be the result of competition with toluene for adsorption on the catalyst, the very first step on the scheme. As the potential for carbon formation of both gases is low, in the case of CO because the high temperature does not favor reverse Boudouard reaction (Reaction 5), a small substitution of toluene by CO and CO_2 would lead to

597 slightly lower carbon formation as well as diminished toluene conversion. On the other
598 hand, CH_4 leads to more adsorbed carbon (C(ad)) on the catalyst through
599 hydrocracking, enhancing the potential for carbon formation.

600 A more detailed reaction mechanism specific for toluene steam reforming has been
601 developed in a study [5] using density functional theory combined with in-situ infrared
602 measurements. It showed that the preferential hydrocracking mechanism would
603 involve full dehydrogenation of the methyl group first to produce a radical C_6H_5-$C^{\cdot}$
604 adsorbed on the catalyst. This structure subsequently losses an aromatic H atom from
605 one of the β C atoms, which then leads to ring opening by cleavage of the aryl carbon
606 bond resulting in a seven-carbon linear chain. Subsequent C-C dissociation leads to
607 shorter chains with three- and four-carbon linear structures being the more
608 energetically favorable. These structures undergo oxidation with O produced from
609 steam dissociation and subsequent C-H bond scissions to finally produce CO and CO_2
610 through aldehyde intermediates. Again, the availability of extra H would tend to reverse
611 the C-H bond scissions, causing a degree of inhibition while hindering conversion of
612 the linear structures into aldehydes and increasing the chances of repolymerization to
613 carbon. In this scheme it is also clear that extra carbon species originated in CH_4 would
614 potentiate the pathways leading to carbon formation over the formation of the aldehyde
615 intermediate.

616 4. Conclusions

617 This analysis of the effect of reforming gas atmosphere on the catalytic steam
618 reforming of tar using a conventional Ni/Al_2O_3 catalyst shows how the conversion of
619 toluene is markedly affected by the presence of some syngas components, even at
620 constant steam to carbon ratio and despite full equilibrium conversion being expected
621 in all cases. While only slight inhibition and no significant deactivation can be
622 concluded from the presence of CO and CO_2, H_2 and CH_4 have been found to have a

significant adverse effect on the reforming of toluene in terms of catalyst deactivation. H_2 also showed a mild inhibitory effect, which interestingly was not observed when CH_4 only was used, albeit this may be due to the low concentration employed. Strong interactions between gas components were observed, with the joint presence of toluene and CH_4 leading to greater carbon formation, which could not have been predicted from separate steam reforming experiments with each of them. Moreover, the simultaneous exposure of the toluene reforming system to H_2 and CH_4 causes a marked deactivation of the catalyst by carbon deposition with each gas potentiating the negative effects of the other. In view of these results, the importance of testing tar reforming catalysts with full syngas compositions to avoid misleading, typically too optimistic, outcomes cannot be overemphasized.

References

1. Tan, R.S., et al., *Catalytic steam reforming of tar for enhancing hydrogen production from biomass gasification: a review.* Frontiers in Energy, 2020: 1-25.
2. Xiao, Y., et al., *Biomass steam gasification for hydrogen-rich gas production in a decoupled dual loop gasification system.* Fuel Processing Technology, 2017. **165**: 54-61.
3. Ruiz, J.A., et al., *Biomass gasification for electricity generation: Review of current technology barriers.* Renewable and Sustainable Energy Reviews, 2013. **18**: 174-183.
4. Deonarine, B., et al., *Ultra-microporous membrane separation using toluene to simulate tar-containing gases.* Fuel Processing Technology, 2017. **161**: 259-264.
5. Ashok, J., et al., *Recent progress in the development of catalysts for steam reforming of biomass tar model reaction.* Fuel Processing Technology, 2020. **199**: 106252.
6. Dagle, V.L., et al., *Steam reforming of hydrocarbons from biomass-derived syngas over MgAl2O4-supported transition metals and bimetallic IrNi catalysts.* Applied Catalysis B: Environmental, 2016. **184**: 142-152.
7. Nunnally, T., et al., *Gliding arc plasma oxidative steam reforming of a simulated syngas containing naphthalene and toluene.* International Journal of Hydrogen Energy, 2014. **39**(23): 11976-11989.

8. Long, X., et al., *Emission of species of environmental and process concern during simulated oxy-fuel gasification.* Fuel, 2021. **299**: 120886.
9. Fidalgo, B., D. Van Niekerk, and M. Millan, *The effect of syngas on tar quality and quantity in pyrolysis of a typical South African inertinite-rich coal.* Fuel, 2014. **134**: 90-96.
10. Berrueco, C., et al., *Evolution of tar in coal pyrolysis in conditions relevant to moving bed gasification.* Energy & Fuels, 2014. **28**(8): 4870-4876.
11. Rabou, L.P., et al., *Tar in biomass producer gas, the Energy research Centre of the Netherlands (ECN) experience: an enduring challenge.* Energy & fuels, 2009. **23**(12): 6189-6198.
12. Gao, N., et al., *Modified nickel-based catalysts for improved steam reforming of biomass tar: A critical review.* Renewable and Sustainable Energy Reviews, 2021. **145**: 111023.
13. Guan, G., et al., *Catalytic steam reforming of biomass tar: Prospects and challenges.* Renewable and sustainable energy reviews, 2016. **58**: 450-461.
14. Li, C. and K. Suzuki, *Tar property, analysis, reforming mechanism and model for biomass gasification—An overview.* Renewable and Sustainable Energy Reviews, 2009. **13**(3): 594-604.
15. Wang, Y., Zaki Memon, M., Ali Seelro, M., Fu, W., Gao, Y., Dong, Y., Ji G., *A review of CO_2 sorbents for promoting hydrogen production in the sorption-enhanced steam reforming process.* International Journal of Hydrogen Energy, **46** (2021), 23358-23379.
16. Yoon, S.J., Y.K. Kim, and J.G. Lee, *Catalytic oxidation of biomass tar over platinum and ruthenium catalysts.* Industrial & engineering chemistry research, 2011. **50**(4): 2445-2451.
17. Li, D., et al., *Production of renewable hydrogen by steam reforming of tar from biomass pyrolysis over supported Co catalysts.* International Journal of hydrogen energy, 2013. **38**(9): 3572-3581.
18. Chianese, S., et al., *Hydrogen from the high temperature water gas shift reaction with an industrial Fe/Cr catalyst using biomass gasification tar rich synthesis gas.* Fuel Processing Technology, 2015. **132**: 39-48.
19. Zuber, C., et al., *Investigation of sulfidation and regeneration of a ZnO-adsorbent used in a biomass tar removal process based on catalytic steam reforming.* Fuel, 2015. **153**: 143-153.
20. Li, W.-P., et al., *Interaction of Ce-char catalyst and partial oxidation on changes in biomass syngas composition.* Journal of Renewable and Sustainable Energy, 2019. **11**(2): 023101.
21. Shen, Y. and K. Yoshikawa, *Recent progresses in catalytic tar elimination during biomass gasification or pyrolysis—A review.* Renewable and Sustainable Energy Reviews, 2013. **21**: 371-392.
22. Miyazawa, T., et al., *Catalytic properties of Rh/CeO2/SiO2 for synthesis gas production from biomass by catalytic partial oxidation of tar.* Science and

technology of Advanced Materials, 2005. **6**(6): 604-614.
23. Heo, D.H., et al., *The effect of addition of Ca, K and Mn over Ni-based catalyst on steam reforming of toluene as model tar compound.* Catalysis Today, 2016. **265**: 95-102.
24. Park, S.Y., et al., *Deactivation characteristics of Ni and Ru catalysts in tar steam reforming.* Renewable Energy, 2017. **105**: 76-83.
25. Baker, E.G. and L.K. Mudge, *Mechanisms of catalytic biomass gasification.* Journal of analytical and applied pyrolysis, 1984. **6**(3): 285-297.
26. Uchida, H. and M.R. Harada, *Hydrogen Energy Engineering Applications and Products*, in *Science and Engineering of Hydrogen-Based Energy Technologies*. 2019, Elsevier. p. 201-220.
27. Sehested, J., *Four challenges for nickel steam-reforming catalysts.* Catalysis Today, 2006. **111**(1-2): 103-110.
28. Dabai, F., et al., *Tar formation and destruction in a fixed-bed reactor simulating downdraft gasification: equipment development and characterization of tar-cracking products.* Energy & fuels, 2010. **24**(8): 4560-4570.
29. Dabai, F., et al., *Tar formation and destruction in a fixed bed reactor simulating downdraft gasification: effect of reaction conditions on tar cracking products.* Energy & fuels, 2014. **28**(3): 1970-1982.
30. Rios, M.L.V., et al., *Reduction of tar generated during biomass gasification: A review.* Biomass and bioenergy, 2018. **108**: 345-370.
31. Evans, R.J., Milne, T.A., *Molecular characterization of the pyrolysis of biomass. 1. Fundamentals.* Energy & Fuels 1987, **1**(2), 123-137.
32. Evans, R.J., Milne, T.A., *Molecular characterization of the pyrolysis of biomass. 2. Applications.* Energy & Fuels 1987, **1**(4), 311-319.
33. Milne, T.A., Evans, R.J., Abatzoglou, N., *Biomass gasifier "tars": their nature, formation, and conversion.* NREL/TP-570-25357; National Renewable Energy Lab (US DoE): 1998, available at https://www.nrel.gov/docs/fy99osti/25357.pdf. Accessed 18 August 2022.
34. Simell, P., Kurkela, E., Ståhlberg, P., *Formation and catalytic decomposition of tars from fludized-bed gasification.* in Bridgwater, A.V., editor. Advances in thermochemical biomass conversion Vol. 1, Chapman and Hall 1993, p 265-279.
35. Sarioglan, A., *Tar removal on dolomite and steam reforming catalyst: benzene, toluene and xylene reforming.* International Journal of Hydrogen Energy, **37** (2012), 8133-8142.
36. Di Carlo, A., Borello, D., Sisinni, M., Savuto, E., Venturini, P., Bocci, E., Kuramoto, K., R*eforming of tar contained in a raw fuel gas from biomass gasification using nickel-mayenite catalyst.* International Journal of Hydrogen Energy, **40** (2015), 9088-9095.
37. Mermelstein, J., M. Millan, and N. Brandon, *The impact of carbon formation on Ni–YSZ anodes from biomass gasification model tars operating in dry*

conditions. Chemical Engineering Science, 2009. **64**(3): 492-500.
38. Tian, Y., et al., *The influence of shell thickness on coke resistance of core-shell catalyst in CO2 catalytic reforming of biomass tar.* International Journal of Hydrogen Energy, 2022. **47**(29): 13838-13849.
39. Taira, K., K. Nakao, and K. Suzuki, *Steam reforming of 1-methylnaphthalene over pure CeO2 under model coke oven gas conditions containing high H2S concentrations.* International Journal of Hydrogen Energy, 2020. **45**(58): 33248-33259.
40. Geis, M., et al., *Coupling SOFCs to biomass gasification-The influence of phenol on cell degradation in simulated bio-syngas. Part I: Electrochemical analysis.* International journal of hydrogen energy, 2018. **43**(45): 20417-20427.
41. Wang, S., et al., *Catalytic steam reforming of bio-oil model compunds for hydrogen production over coal ash supported Ni catalyst.* International journal of hydrogen energy 39 (2014) 2018-2025,
42. Wang, S., et al., *Hydrogen production via catalytic reforming of the bio-oil model compunds: acetic acid, phenol and hydroxyacetone.* International journal of hydrogen energy 39 (2014) 18675-18687
43. Long, X., et al., *Towards integrated gasification and fuel cell operation with carbon capture: Impact of fuel gas on anode materials.* Fuel, 2022. **318**: 123561.
42. Lorente, E., M. Millan, and N. Brandon, *Use of gasification syngas in SOFC: Impact of real tar on anode materials.* International Journal of Hydrogen Energy, 2012. **37**(8): 7271-7278.
43. Lorente, E., et al., *Effect of tar fractions from coal gasification on nickel–yttria stabilized zirconia and nickel–gadolinium doped ceria solid oxide fuel cell anode materials.* Journal of Power Sources, 2013. **242**: 824-831.
44. Shen, Y., Liu, Y., Yu, H., *Enhancement of the quality of syngas from catalytic steam gasification of biomass by the addition of methane/model biogas.* International Journal of Hydrogen Energy, **43** (2018), 20428-20437.
45. Zhang, Z. et al., *Preparation, modification and development of Ni-based catalysts for caatalytic reforming of tar produced from biomass gasification*. Renewable and Sustainable Energy Reviews, 94, 2018, 1086-1109,
46. Wangen, E.S., Osatiashtiani, A., Blekkan, E.A., *Reforming of syngas from biomass gasification: deactivation by tar and potassium species*. Topics in Catalysis 2011, *54* (13-15) , 960-966.
47. Wang, L. et al. *Catalytic performance and characterization of Ni–Co catalysts for the steam reforming of biomass tar to synthesis gas*. Fuel 112 (2013) 654-661
48. Boldrin, P., M. Millan-Agorio, and N.P. Brandon, *Effect of sulfur-and tar-contaminated syngas on solid oxide fuel cell anode materials.* Energy & Fuels, 2015. **29**(1): 442-446.
49. Huang, C.W., et al., *Optimal Fe/Ni/Ca -Al catalyst for tar model steam reforming*

by using the Taguchi method. International Journal of Energy Research, 2022. **46**(6): 7799-7815.
50. Gao, X., et al., *Steam reforming of toluene as model compound of biomass tar over Ni–Co/La2O3 nano-catalysts: Synergy of Ni and Co.* International Journal of Hydrogen Energy, 2021. **46**(60): 30926-30936.
51. Yahya, H.S.M., T. Abbas, and N.A.S. Amin, *Optimization of hydrogen production via toluene steam reforming over Ni–Co supported modified-activated carbon using ANN coupled GA and RSM.* International Journal of Hydrogen Energy, 2021. **46**(48): 24632-24651.
52. Cao, J.-P., et al., *Effect of atmosphere on carbon deposition of Ni/Al2O3 and Ni-loaded on lignite char during reforming of toluene as a biomass tar model compound.* Fuel, 2018. **217**: 515-521.
53. Mermelstein, J., M. Millan, and N. Brandon, *The interaction of biomass gasification syngas components with tar in a solid oxide fuel cell and operational conditions to mitigate carbon deposition on nickel-gadolinium doped ceria anodes.* Journal of power sources, 2011. **196**(11): 5027-5034.
54. Ren, J., Cao, J-P., Yang, F-L., Liu, Y-L., Tang W., Zhao X-Y., *Understandings of catalyst deactivation and regeneration during biomass tar reforming: A crucial review*. ACS Sustainable Chemistry & Engineering 2021, 9, 17186-17206.
55. Mermelstein, J., Brandon, N.P., Millan, M., *The impact of steam on the interaction between biomass gasification tars and nickel based Solid Oxide Fuel Cell anode materials.* Energy & Fuels, 2009, 23, 10, 5042-5048.
56. Zhu, H.L., Pastor-Pérez, L., Millan, M., *Catalytic Steam Reforming of Toluene: Understanding the Influence of the Main Reaction Parameters over a Reference Catalyst.* Energies, 2020. **13**(4): 813.
57. Namioka et al. *Low-temperature trace light-tar reforming in biomass syngas by atmospheric hydrogenation and hydrogenolysis.* Fuel Processing Technology 181 (2018) 304-310.
58. Simell, P.A., Hepola, J.O., Krause, A.O.I., *Effects of gasification gas components on tar and ammonia decomposition over hot gas cleanup catalysts.* Fuel 1997, 76(12), 1117 - 1127.
59. Kong, M., et al., *Influence of supports on catalytic behaviour of nickel catalysts in carbon dioxide refrorming of toluene as a model compound of tar from biomass gasification.* Bioresource Technology 102 (2), 2011, 2004-2008
60. Chen et al., *CO_2 reforming of toluene as model compound of biomass tar on Ni/Palygorskite*. Fuel 107 (2013) 699-705.
61. Kertthong, T., et al., *Influence of gas atmosphere and role of tar on catalytic reforming of methane and tar model compounds: Special focus on syngas produced by sorption enhanced gasification*. Fuel 317 (2022) 123502.
62. Pinto F. et al., *Methane reforming of syngas produced by co-gasification of coal and wastes. Effect of catalysts and of experimental conditions.* Fuel 90 (4), 2011, 1645-1654.

63. Laprune, D., *Effects of H_2S and phenanthrene on the activity of Ni and Rh-based catalysts for the reforming of a simulated biomass-derived producer gas.*Applied Catalysis B: Environmental 221, 2018, 206-214.
64. Claude. V., et al., *Ni-doped γ-Al_2O_3 as secondary catalyst for bio-syngas purification: influence of Ni loading, catalyst preparation and gas composition on catalytic activity*. Materials Today Chemistry 13, 2019, 98-109.
65. Sarvaramini, A., Larachi, F., *Catalytic oxygenless steam cracking of syngas-containing benzene model tar compound over natural Fe-bearing silicate minerals*. Fuel 97 (2012) 741-750.
66. Bizkarra, K., et al., *Nickel based monometallic and bimetallic catalysts for synthetic and real bio-oil steam reforming.* International Journal of Hydrogen Energy, 2018. **43**(26): 11706-11718.
67. Abu El-Rub, Z., E.A. Bramer, and G. Brem, *Review of catalysts for tar elimination in biomass gasification processes.* Industrial & engineering chemistry research, 2004. **43**(22): 6911-6919.
68. Sutton, D., B. Kelleher, and J.R.H. Ross, *Review of literature on catalysts for biomass gasification.* Fuel Processing Technology, 2001. **73**(3): 155-173.
69. Puron, H., et al., *Hydroprocessing of Maya vacuum residue using a NiMo catalyst supported on Cr-doped alumina.* Fuel, 2020. **263**: 116717.
70. Hiblot, H., Ziegler-Devin, I., Fournet, R., Glaude, P.A., *Steam reforming of methane in a synthesis gas from biomass gasification*. International Journal of Hydrogen Energy, **41** (2016), 18329-18338.
71. Ashok, J., Kawi, S., *Nickel-Iron Alloy Supported over Iron-Alumina Catalysts for Steam Reforming of Biomass Tar Model Compound.* ACS Catalysis 2014, 4, 289-301.
72. Rostrup-Nielsen, J., Christiansen, L.J., *Concepts in Syngas Manufacture*. Catalytic Science Series Vol. 10, Imperial College Press, 2011.

Declaration of interests

☒ The authors declare that they have no known competing financial interests or personal relationships that could have appeared to influence the work reported in this paper.

☐The authors declare the following financial interests/personal relationships which may be considered as potential competing interests: